FLAME RETARDANT NANOCOATINGS FOR THE PROTECTION OF POLYURETHANE FOAM

A Dissertation

by

KEVIN MICHAEL HOLDER

Submitted to the Office of Graduate and Professional Studies of
Texas A&M University
in partial fulfillment of the requirements for the degree of

DOCTOR OF PHILOSOPHY

Chair of Committee,	Jaime Grunlan
Committee Members,	Abraham Clearfield
	Terry Creasy
	Micah Green
Head of Department,	Ibrahim Karaman

December 2016

Major Subject: Materials Science and Engineering

ABSTRACT

Layer-by-layer (LbL) assembly is a simple technique capable of building multi-functional thin films on a variety of surfaces from dilute aqueous solutions. LbL coatings on polyurethane foam have been successful in reducing the flammability through environmentally friendly means. This technology provides a potential avenue for replacing halogenated flame retardants which are successfully used on foams, but present a toxic threat to health and the environment.

A thin film nano-brick wall structure composed of chitosan and vermiculite clay was combined with an all-polymer film of chitosan and ammonium polyphosphate to form a stacked coating on polyurethane foam to reduce flammability. Individually, the coatings were able to reduce flammability of the foam, however the all-polymer coating was unable to prevent total degradation of the polyurethane due to inability to form char prior to the collapse of the foam. The nano-brick wall provided the necessary structure to allow the all-polymer coating to act and form an expanded insulating char layer that prevents flame spread across the surface of the polyurethane as well as reduce the peak heat release rate of the foam significantly.

Incorporating carbon nanotubes into a LbL assembly allowed further reductions in polyurethane foam flammability. Only a few layers of nanotube-containing polymer layers were able to completely prevent flame propagation in both horizontal and vertical flame tests. Cone calorimetry revealed significant reductions in peak heat release rate as well as total smoke release. Reduction in heat release rates and smoke release are important factors towards extending escape time in a fire scenario.

Barrier fabrics are commonly used to protect flammable materials. A polyelectrolyte complex was used to coat cotton fabric and prevented flame spread and igni-

tion of underlying polyurethane foam. This study also highlights the importance of testing combined fabric and foam assemblies as pertaining to upholstered furniture. Cone calorimetry is a useful instrument to ascertain interactions between varying fabric and foam compositions and potentially will highlight an appropriate method for flame retarding the combination.

DEDICATION

To my wife, Gabrielle, for supporting me and always reminding me that I can do anything I set my mind to, no matter the difficulty.

To my parents, David and Barbara, for raising me to be a caring and driven individual.

To my brother, Cody, for being a great friend and always encouraging me to doing something great with my life.

ACKNOWLEDGEMENTS

I would like to thank my committee chair, Dr. Jaime Grunlan for his guidance and providing a means for financial support throughout the course of this research. I would also like to thank Dr. Abraham Clearfield, Dr. Terry Creasy, and Dr. Micah Green for their time to serve on my committee.

I would like to thank Dr. Morgan Priolo for his guidance and wisdom during my years leading up to graduate school. Thanks also go to all of the present and former members of the polymer nanocomposites lab that I have had the pleasure to work with for their support and assistance, particularly Dr. Galina Laufer, Dr. Amanda Cain, Dr. David Hagen, Dr. Bart Stevens, Dr. Ping Tzeng, Dr. Fangming Xiang, Dr. Tyler Guin, Dr. Chungyeon Cho, Dr. Marcus Leistner, Dr. Debabrata Patra, Yixuan Song, Ryan Smith, Merid Haile, Shuang Qin, Alyssa John, and Morgan Plummer. I would also like to thank the many undergraduate assistants who helped me produce much of the data presented in this dissertation: Molly Huff, Mario Cosio, Emily Brown, Kyle Howard, Sofia Ruiz, Samuel Terrill, and Wyatt Hahn.

I would like to thank a few of my classmates, Blake Teipel, Brandon Sweeney, and Luke Johnson, for their friendship and for being awesome study partners.

I would also like to thank my friends, Jason, Ryan, Bryan, Chris, Mauricio, Jordyn, Vanessa, and Julisa for being my lifelines away from school.

Thanks also go to the many faculty and staff that I have had the pleasure of interacting with for making my time at Texas A&M University enjoyable and productive.

NOMENCLATURE

AL	Alginate
APP	Ammonium polyphosphate
APTES	3-aminopropyltriethoxysilane
ATH	Alumina trihydroxide
BL	Bilayer
BMT	Boehmite
CH	Chitosan
CNF	Carbon nanofibers
CNT	Carbon nanotubes
DNA	Deoxyribonucleic acid
DPAA	N-(5,5-dimethyl-1,3,2-dioxaphosphinyl-2-yl)-acrylamide
DPEPA	N-2-(5,5-dimethyl-1,3,2-dioxaphosphinyl-2-ylamino)-ethylacetamide-2-propenyl acid
F − POSS	Fluorinated-decyl polyhedral oligomeric silsquioxane
FNR	β-FeOOH nanorods
FR	Flame retardant
GO	Graphene oxide
HFT	Horizontal flame test
LbL	Layer-by-layer
LDH	Layered double hydroxide
LOI	Limiting oxygen index
MCC	Microcombustion calorimetry
MF	Melamine foam

MMT	Montmorillonite
MWNT	Multiwalled carbon nanotubes
NiA	Nickel alginate
NP	Nanoparticle
PA	Phytic acid
PAA	Poly(acrylic acid)
PAm	Polyamide
PAHDP	Poly(allylamine diphosphonate)
PC	Polycarbonate
PCFC	Pyrolysis-combustion flow calorimetry
PDDA	Polydiallyldimethylammonium chloride
PE	Polyethylene
PECO	Polyester-cotton
PEI	Polyethylenimine
PEI – Py	Pyrene-modified polyethylenimine
PET	Polyester
PHMGP	Polyhexamethylene guanidine phosphate
pkHRR	Peak heat release rate
PLA	Polylactide
POSS	Polyhedral oligomeric silsquioxane
PPA	Polyphosphoric acid
PS	Polystyrene
PSP	Sodium hexametaphosphate or poly(sodium phosphate)
PU	Polyurethane
PVPA	Poly(vinylphosphonic acid)

PVS	Poly(vinyl sulfonic acid sodium salt)
QL	Quadlayer
SEM	Scanning electron microscopy
SiN	Nitrogen-modified silane
TGA	Thermogravimetric analysis
THR	Total heat release
TL	Trilayer
TNT	Titanate nanotubes
TSR	Total smoke release
TTI	Time to ignition
VFT	Vertical flame test
VMT	Vermiculite

TABLE OF CONTENTS

Page

LIST OF FIGURES

FIGURE Page

LIST OF TABLES

TABLE Page

1. INTRODUCTION*

1.1 Background

An average of seven people died each day in United States home fires, from 2009 to 2013, according to the National Fire Protection Association [2]. Nearly 50% of these fires began in family rooms or bedrooms that contain the majority of household furniture. With ever increasing amounts of flammable polymeric materials in households (e.g., cushions for chairs, drapery for windows, mattresses, etc.), there is a tremendous need for sustainable and cost-effective flame retarding treatments [3]. The majority of upholstered furniture contains open-celled polyurethane (PU) foam that tends to smolder, flow, and pyrolyze under fire conditions due to its insulating behavior, low thermal inertia, and open structure [4]. A common technique for retarding the flammability of PUF is to introduce bromine-based molecules that scavenge (H• and OH•) radicals in the gas phase [5, 6], but these halogenated additives are undergoing worldwide scrutiny for the toxic smoke they release and their potential to leach into the environment [7, 8, 9].

Nanoparticle fillers including clays and carbon nanotubes have been shown to successfully reduced polymer flammability [6]. Thin films assembled using layer-by-layer (LbL) deposition are a good alternative to these filled nanocomposites with high tailorability and limited impact on the bulk polymer properties [10]. Along with superior flame retardant properties [11, 12, 13, 14], these films have also been prepared for gas barriers [15, 16], superhydrophobic [17, 18], antimicrobial [19, 20], and electrically conductive [21, 22] applications. The versatility of LbL is due to the wide range of components supported by the technology [23, 24, 25]. In addition to the

*Parts of this section are reprinted with permission from Reference [1]. Copyright 2014, Springer Science+Business Media New York

limitless combinations of components, film properties can be adjusted by changing parameters such as solution pH [26, 27], buffer content [28, 29], ionic strength [30], and temperature [27, 31].

The simplicity of layer-by-layer assemblies allows for production of complex assemblies without difficult processing. This is even possible on complex substrates such as fabric and foam making LbL a good solution for applying flame retardant coatings on polymer surfaces. Applying a coating to the surface where the combustion cycle takes place allows direct interaction with and obstruction of the fire. The LbL process has been used to create successful flame retardant coatings through the use of all-polymer and/or polymer-nanoparticle thin films [32, 33, 11, 34]. The water-based nature of the LbL process allows for tailorable chemistries to be deposited to suit the targeted substrate while limiting the negative effects on the physical properties [35, 36, 12].

The focus of this dissertation is on reducing the flammability of polyurethane foam because of its prominent use in upholstered furniture that is found in homes, automobiles and airplanes. Polyurethane is highly flammable and significantly increases the fire threat when present. Current flame retardants used for polyurethanes, specifically halogenated chemicals, are being banned for their danger to both personal and environmental health. Flame retardant thin films comprised of polymers and nanoparticles were developed on polyurethane (or cotton as a barrier fabric for polyurethane) to interfere with the combustion cycle and reduce flammability of the foam. The objective of this research was to create coatings that have to potential to reduce flammability of polyurethane and also completely prevent ignition of the foam, or fabric and foam combination.

1.2 Objectives and Dissertation Outline

Section 2 briefly discusses polymer combustion and flame retardants in general. An in depth review of existing literature focused on the development of layer-by-layer flame retardant thin films on a range of substrates. This overview of the technique discusses the progress of this technique and puts the contributions made by this body of work into perspective.

Section 3 focuses on the ability to combine two different layer-by-layer coatings into one and the improved effects they have on flame retarding foam. This stacked coating is composed of chitosan (CH), vermiculite (VMT), and ammonium polyphosphate (APP) [1]. Growth and layer structure were characterized using transmission electron microscopy (TEM). Thin films were deposited separately and as a stacked coating on flexible polyurethane foam and the flammability was assessed using a bench-top butane torch test and cone calorimetry.

Section 4 examines the effects of carbon nanotubes on flammability of PU [37]. Multiwall carbon nanotubes (MWNT) were suspended in pyrene-modified branched polyethylenimine (PEI-Py) and/or poly(acrylic acid) (PAA) and then deposited onto polyurethane using LbL assembly. Growth and composition were measured using profilometry, quartz crystal microbalance (QCM), and thermogravimetric analysis (TGA). Horizontal and vertical flame tests were used in conjunction with cone calorimetry to investigate the flame retardant behavior.

Section 5 investigates an alternate approach to designing flame retardants for polyurethane specifically related to upholstered foams. Cone calorimetry was used along with multiple fabric and foam combinations to analyze various behaviors caused by different chemical compositions. It highlights the ability of cone calorimetry to highlight important differences and trends relating to specific fabric or foam com-

positions and could provide a better understanding of how to flame retard these varying combinations. It is also shown that a simple polyelectrolyte complex can be deposited on cotton to create a lightweight barrier fabric for foam.

Section 6 provides conclusions pertaining to completed research and offers paths of future research. This dissertation studies the ability of nanocoatings to flame retard polyurethane foam through condensed phase mechanisms. It is evident that nanocoatings, given the correct composition, are able to reduce flammability and completely prevent ignition and flame spread.

Carbon nanotubes and titanate nanotubes show promise in LbL FR coatings on polyurethane foam. Halloysite nanotubes have also been shown to successfully deposit in layer-by-layer films [38]. Studies have shown halloysite can be effective as a flame retardant additive [39, 40]. Halloysite nanotubes offer a clay-based environmentally benign method of achieving similar reductions in flammability on polyurethane as other nanotube-based coatings. In a related study, halloysite has been filled with flame retardant molecules to act as both a thermally stable barrier former and a transport for other char forming moieties [41]. Utilizing the ability to fill these nanoparticles and incorporate them into a LbL coating provides a unique opportunity to further reduce polyurethane flammability.

Boron nitride comes in nanotubes and platelets that have high thermal stability similar to other nanoparticles discussed in this dissertation. Hexagonal boron nitride is also known to gain mass through oxidation when exposed to high temperatures which could lead to improved thermal barrier formation. Developing a coating utilizing boron nitride might prove to have significant reductions in flammability while also potentially providing good gas barrier properties.

An important aspect to consider for any application oriented research is scalability. LbL flame retardant technology has existed for many years and many suc-

cessful coatings have been developed. In order to transition this technology into a marketable product, scaling the technology on complex three dimension such as polyurethane foam needs to be studied. Most of this work has been completed through dipping in aqueous solutions, however that might not be viable on a large scale for something as large as a couch cushion. Assessing the viability of spray coating these films onto the outermost surface of foam is one potential avenue of scaling this technology. It will be important to assess the coating penetration depth and the uniformity of this deposition method given the complex structure of foam. The coatings will need to provide sufficient protection in the limited coated areas and would act as a barrier layer to protect any polyurethane in the bulk of the sample that does not get coated.

2. LITERATURE REVIEW

2.1 Polymer Flammability Threat

Plastics, textiles and foams play an important role in everyday life. These materials are primarily organic polymers which, due to their flammable nature, present a fire risk. Flame retardants have been developed for decades to reduce fire damage by either inhibiting ignition or reducing flame spread in the event that ignition does occur. Fire is a gas phase oxidative process that requires oxygen from the atmosphere and combustible compounds that act as fuel. In order to ignite, a polymeric material must first undergo some form of degradation. As they thermally decompose, polymers break down into constituent parts and free radicals, which enter the vapor phase and combust with atmospheric oxygen as long as the temperature is above the ignition temperature or a suitable ignition source is present (i.e., a spark). Combustion is exothermic, recycling thermal energy back into the underlying material, resulting in more material decomposition feeding the combustion zone with fuel [42]. This process is represented schematically in Figure 2.1. The key region is the interface between the flame and the solid polymer. It is in this region that the temperature is high enough to start the degradation reactions of the polymer that will affect both the polymer and any additives that may be present. At this point, volatile species formed will escape into the flame and heavier degradation products will remain to further degrade either into more volatiles or into solid char.

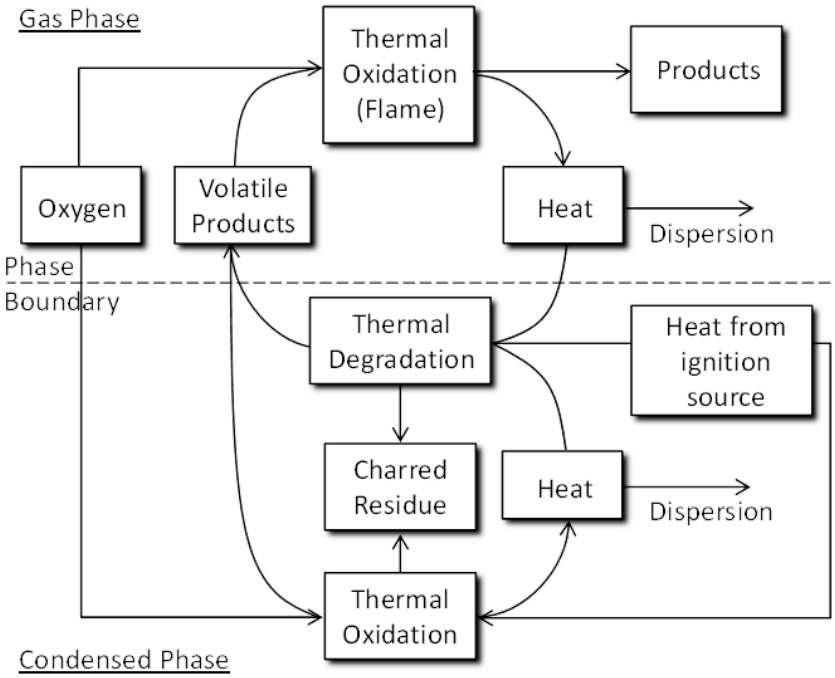

Figure 2.1: Scheme representing the polymer combustion process. Reproduced with permission from Reference [42]. Copyright 1991, Elsevier Science Publishers Ltd, England.

Interrupting the degradation at the flame-to-polymer interface is the primary goal of flame retardants (FR). Various flame retardants act in different ways depending on the burning characteristics of the base material. For example, thermoplastics typically melt when exposed to the heat of fire, whereas cellulose will simply combust, decomposing into combustible gases, smoke, and char. Improving char formation, suffocating the flame by removing reactive radical species, or reducing the heat available for further degradation are all methods employed by current flame retardants.

The increase use of plastics and other flammable materials over the past several decades has resulted in a significantly increased threat to human life as well as increased cost to repair damage resulting from fires every year. It was discovered that

as of 2013, the United States has double the reported deaths per million population compared to Great Britain [43]. A majority of these fatalities occur in residential settings. Furniture is one of the major fuel sources because it is generally composed completely of flammable materials (wood, textiles, foam, etc.). Regulations are supposed to help limit the risk associated with these flammable materials, but recent developments, including the removal of open flame test requirements in Californias Technical Bulletin 117, which is related to furniture flammability, may be reducing fire safety. This change was made based on growing environmental and health concerns related to halogenated flame retardants which are some of the most effective for diminishing flaming ignition. New technologies are being developed to provide more effective and environmentally-friendly flame retardant alternatives to pass even the most rigorous flammability tests. This review will focus on one technology in particular, layer-by-layer (LbL) assembly, and the past decade of tremendous progress and development made towards flame retarding polymeric materials using otherwise benign chemistries and particles.

2.2 Flame Retardant Mechanisms

In the past century, with advances in technology and the ability to better understand and study chemical reactions, the increase in flammable materials has been accompanied by a thorough understanding and development of fire retardants. In order for a material to become flame retardant, the flame cycle must be interrupted in one or more of the stages (Figure 2.1). The first option is to interrupt the degradation of the fuel source by providing an insulating shield that will act by preventing further thermal degradation of the material, as well as prevent some of the flammable degradation products from escaping into the flame zone. A flame starved of fuel will eventually extinguish. This is a condensed phase flame retardant process since it

interacts with the solid material, limiting the release of combustible components into the gas phase. Gas phase flame retardants are most commonly composed of free radical scavengers. As gas phase flame retardants decompose along with the fuel source, the radicals (most commonly halides) will scavenge the hydrogen and hydroxyl radicals that are combusting with the volatiles being released from the degradation of the solid phase. The fire will extinguish because the radical scavengers are starving the flame zone of combustion, reducing the amount of heat available to further degrade the polymer. Another way of interrupting the fire cycle is by reducing the amount of heat in the system through endothermic reactions, thereby limiting the degradation of the flammable material and starving the flame of fuel. This is done by incorporating materials that will release non-flammable gases such as water or carbon dioxide that will dilute the fuel, cooling the polymer and limiting further degradation. A brief overview of commonly used flame retardants is provided here.

2.2.1 Halogenated Flame Retardants

Halogenated molecules comprise the most diverse class of flame retardants [44]. These molecules function by releasing halogen radicals or hydrogen halides at or below the decomposition temperature of the polymer being protected [45, 46]. The most effective and commonly used materials are those containing chlorine or bromine. These are very suitable for a range of engineering plastics and epoxy resins [47]. Halogenated flame retardants function primarily in the gas phase through release of halogen radicals during a fire and immediately abstract hydrogen from nearby sources. At this point, the hydrogen halides volatilize and enter the flame where they react with either hydrogen or hydroxyl radicals to form hydrogen gas or water and regenerate the halogen. The renewed radical halogen can react with other hydrocarbons in the gas phase to regenerate hydrogen halides and continue scavenging

free hydrogen and hydroxyl radicals from the flame zone. Hydrogen halides can reduce the mass concentration of combustible gases as well as the temperature, which limits and eventually halts propagation of the fire [48]. There are other theories that suggest halogens also act in the condensed phase, encouraging char formation as the halogen abstracts hydrogen from the polymer and results in the formation of double bonds, which are known to be precursors to char [49, 50].

2.2.2 Phosporus-Containing Flame Retardants

Phosphorus-containing flame retardants are increasing in popularity due to growing global concern over health and environmental risks associated with halogenated materials. Phosphorous flame retardants exist in four primary categories: elemental red phosphorus, inorganic phosphates, organic phosphorus-based materials, and chlororganophosphates [51]. Phosphorus is most effective in materials containing oxygen or nitrogen because it acts in the condensed-phase and is directly involved in char formation [52]. Cellulose and other polymers containing hydroxyl groups work well with phosphorus [53]. The acids formed from the decomposition of phosphate salts or phosphate esters react with the hydroxyl groups of cellulose to catalyze char formation [54]. Nitrogen can sometimes accelerate the phosphorylation of cellulose through the formation of a P-N intermediate thereby synergizing the phosphorus flame retardant [55] Molecules such as pentaerythritol or melamine can be used in conjunction with phosphorus to promote phosphorylation and encourage char formation when this cannot occur with the polymer directly. These are called intumescent systems because they form a viscous swollen char. This char is insulating and slows the diffusion of volatile combustible products to the flame. Studies have shown the use of intumescent systems in various polymers and have studied the chemistry of formation of the intumescent chars in detail [56]. It is also possible that phosphorus-

based flame retardants can act in the gas phase via radical scavenging.

2.2.3 Inorganic Hydroxide Flame Retardants

Acting to cool the flame zone, inorganic hydroxides have been successfully used as flame retardants in many types of polymers. The primary benefit of inorganic hydroxides, such as aluminum or magnesium, is that they release water at elevated temperatures. This is an endothermic process, removing heat from the flame zone as well as diluting the combustible gases [57]. It is also possible that in addition to the endothermic release of water, anhydrous aluminum has a catalytic effect that helps acid-catalyzed dehydration of certain polymers that improves charring [53]. Inorganic hydroxides at high loadings tend to have negative influence on polymer physical properties, so methods of reducing loading by combining with other flame retardant chemistries or improving dispersion are often explored.

2.2.4 Other Common Flame Retardants

Other flame retardants act in similar ways to those mentioned above because they all serve to interrupt the fire cycle. Melamine-based flame retardants have high nitrogen content and a relatively high thermal stability. Melamine is commonly used in flexible polyurethane foams in conjunction with chloroalkyl phosphates and in intumescent coatings with ammonium polyphosphate and pentaerythritol. Melamine is beneficial because it does not melt, but rather sublimes near 350C, absorbing a significant amount of energy. At high enough temperatures, melamine can also decompose through an endothermic process into cyanamid [55]. A competing reaction involves melamine undergoing condensation, evolving ammonia and forming stable condensates [58]. This action dilutes the gas phase with non-combustibles and increases material in the condensed phase char layer. Melamine salts specifically tend to favor progressive condensation. Borates such as sodium borate and boric acid

have been used as flame retardants for cellulosic materials, whereas more thermally stable zinc borates have been used in thermoplastics. In the case of sodium borate and boric acid, it is believed they act very similarly to phosphorus by promoting char formation [59]. Zinc borate has the ability to release significant amounts of water due to extensive hydration of the borate. Borate dehydration is endothermic and dilutes the gas phase [60]. Silicon-based flame retardants include a wide variety of materials such as fumed silica, clays, and other particles. Many silicates act as heat dispersants and are also good at reinforcing char due to generally high thermal stability.

In most cases, the flame retardant chemistries mentioned above are included as additives to foam and bulk polymers. These fillers often have a negative impact on polymer physical properties due to high loading requirements. In the case of thermoplastics, dispersion of flame retardant fillers is also a major issue. Textiles, unlike bulk polymers and foams, do not typically support flame retardant fillers and generally require a difficult curing process, such as the required pass through an ammonia reactor to apply Proban to cotton or the application and cure of a back-coat in the form of a bonding resin to reduce total fabric flammability. In all cases, the current technologies are quite mature, dating back decades, and are simply reformulated for the development of new polymer products to meet application specific flammability requirements. In order to reduce the difficulties of processing and retaining inherent polymer physical properties, new flame retardant technologies must be created. Layer-by-layer deposition of flame retardant nanocoatings is one such opportunity to overcome the challenges associated with current treatment options.

2.3 Layer-by-Layer Assembly

2.3.1 Introduction to Layer-by-Layer Assembly

Layer-by-layer assembly is a simple and environmentally benign technique, most commonly performed with water-based solutions. LbL deposition was first demonstrated through the deposition of oppositely charged particles onto a substrate in 1966 [61]. Since that time, the technique has gained increasing popularity as researchers explore endless combinations of ingredients and their respective functionalities [62, 63, 64]. The typical preparation of LbL deposited coatings starts by appropriately preparing a surface, commonly involving a surface charge. The substrate is then exposed to aqueous solutions containing polymers or nanoparticles (NP), with tailored affinities to one another for periods of time ranging from seconds to minutes. Each deposition step is optionally followed by rinsing and drying steps to remove any loosely adhered material. This leaves a single layer deposited on a surface that has also reversed the effective surface interactions allowing a complimentary material to be deposited. This procedure forms one bilayer (BL) and can be repeated as many times as needed to achieve the desired thickness or properties. A two-component LbL process is shown schematically in Figure 2.2. Layer-by-layer deposition is not reliant on electrostatic interactions, as any complimentary interactions, such as hydrogen bonding, can be used for deposition of multilayer thin films [65]. In addition to bilayers, repeating sequences of trilayers (TL), quadlayers (QL), etc. (or even as stacked multilayers of varying composition) have been deposited to incorporate all the functionality required to achieve the desired final thin film properties [66, 67, 68, 69, 70, 71].

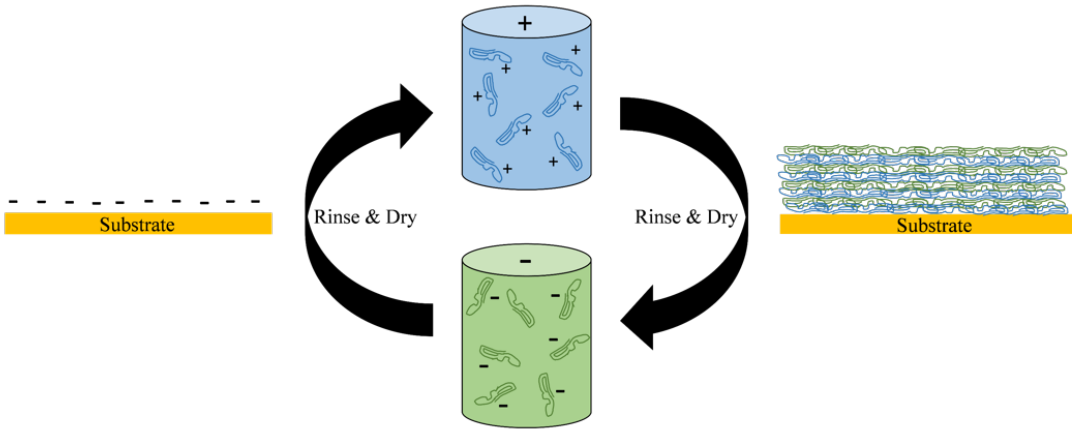

Figure 2.2: Schematic of layer-by-layer assembly of polyelectrolytes onto a charged surface.

2.3.2 Versatility of Layer-by-Layer Assembly

These multilayered thin films have a wide variety of tunable properties. Thickness can be adjusted by changing parameters such as solution pH [26, 27], buffer content [28, 29], ionic strength [30], and temperature [27, 31]. Polymers can also be layered with nanoparticles to impart properties such as superhydrophobicity [72, 73], UV absorption [74], high strength [75], gas barrier [69, 15], and energy generation [76]. Recently, a review was dedicated to the development of gas barrier coatings developed with this technique [15]. LbL deposition of polymer and clay results in highly aligned platelets that form a tortuous pathway for gas molecules to traverse, thereby dramatically improving the barrier properties.

2.4 Flame Retardant Layer-by-Layer Nanocoatings

A study investigating the combustion of layered silicate (i.e. clay) nanocomposites showed a diagram representing the believed combustion mechanism and ablative reassembly of a silicate nanocomposite [77]. Figure 2.3 shows how as the composite

undergoes combustion, the silicate filler migrates towards the surface, forming an ordered structure that very closely resembles the film structure created with polymer/clay LbL assembly, which is also shown for comparison. It was this concept that inspired the first use of clay-based LbL deposited nanocoatings for flame retardant [33]. Nanocoatings are a great option for adding flame retardant coatings to polymer surfaces since the material surface is the most important area to stop fire. Polymer chemistry, particles, and small molecules all have a role to play in the development of layer-by-layer nanocoatings for flame retarding various flammable polymeric substrates. Textiles, foams, bulk polymers and even fibrous materials have benefited from LbL flame retardant coatings. In less than ten years, the technology has been adapted to a large variety of substrates (and numerous chemistries) and the pace of development continues to grow. As will be shown in the subsequent section, this is not limited to nanoparticles. Many other flame retardant chemistries can be adapted into water-based environmentally friendly coatings. This review will discuss the significant body of work developed over the past decade that have focused on formulating flame retardant coatings for textiles, foam, bulk polymers and other unique flame retardant applications.

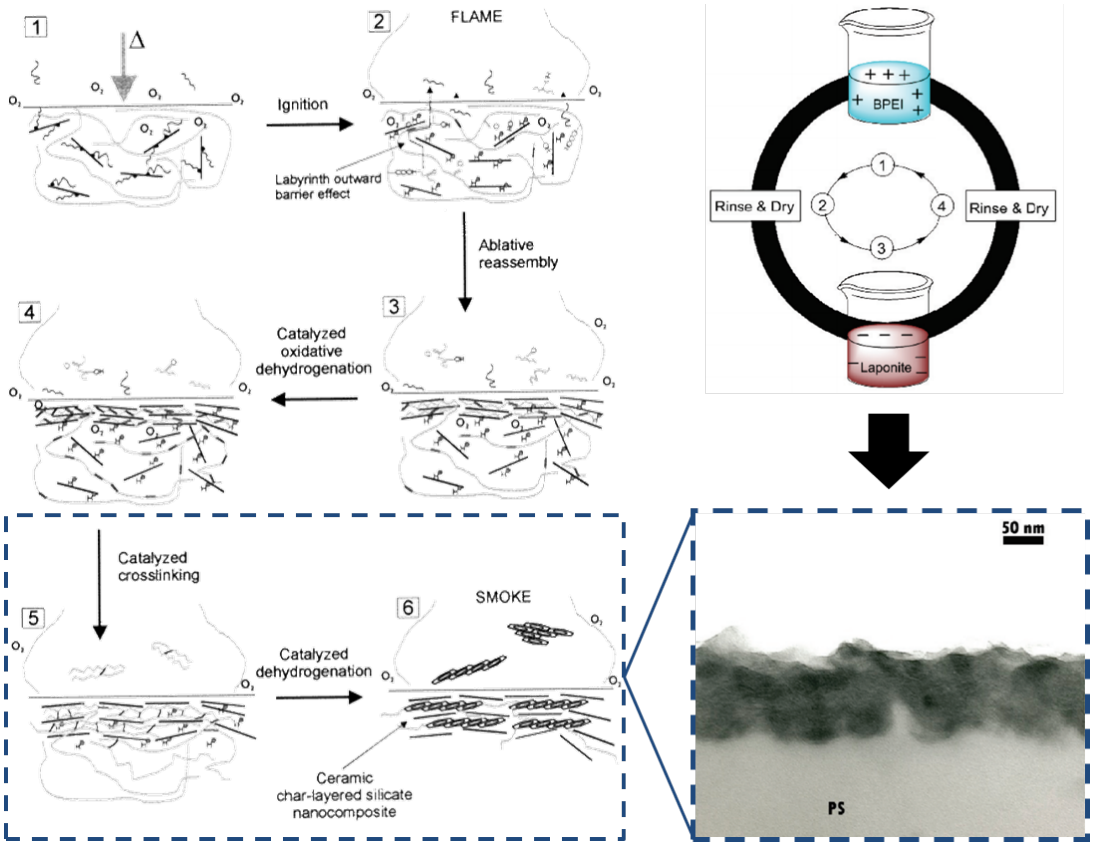

Figure 2.3: Schematic representation of the combustion mechanism and ablative reassembly of silicate-based nanocomposites (left). Reproduced with permission from Reference [77]. Copyright 2002, American Chemical Society. Layer-by-layer assembly of a clay-based bilayer gas barrier coating (upper right) with a cross-sectional TEM image (lower right) resembling the structure shown on the left. Reproduced with permission from Reference [33]. Copyright 2009, American Chemical Society.

2.4.1 Layer-by-Layer Flame Retardant Coatings on Textiles

2.4.1.1 Coatings on Natural Fibers

With regards to layer-by-layer flame retardants, textiles, and more specifically natural fiber based textiles, are by far the most studied materials. Due to the generally cellulosic nature of natural fibers, the primary focus has been on solid phase

chemistries that will form char barriers on the fabric. This has been done by adapting bulk intumescent and charring chemistry concepts and/or incorporating inorganic materials with high thermal stability. These coatings have the ability to create insulating char layers on the surface of the fibers that reduce heat and mass transfer. Due to the high volume of studies, the following section will be separated based on coating type, namely char forming/intumescent or nanoparticle-based coatings. Each section will then be discussed chronologically to show the growth of the field and how coatings have improved over the past decade.

In 2006, Srikulkit, et al., deposited chitosan (CH) and polyphosphoric acid (PPA) on silk to create the first flame retardant layer-by-layer coating [78]. The goal of this study was to capitalize on the known synergy between nitrogen and phosphorous to create a condensed phase char forming coating on the outside of the individual silk fibers. Evidence of improved thermal resistance was measured using thermogravimetric analysis (TGA) which showed that 60 layers (30 bilayers) retained 40 wt% at 600 °C compared to neat silk which had already completely decomposed. In 2011, Li, et al., developed a layer-by-layer intumescent coating using poly(allyl amine) (PAH) and sodium hexametaphosphate (PSP) as the LbL components to create a char-forming coating that swells as it decomposes, allowing the cotton to self-extinguish during vertical flame test (VFT), shown in Figure 2.4 [11]. This coating set a standard for LbL flame retardants as it is still one of the most successful LbL FR coatings to be presented in terms of heat release rate improvement and self-extinguishing behavior.

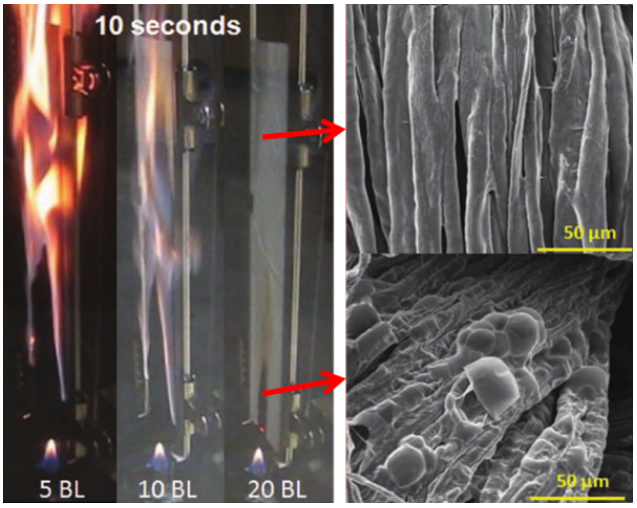

Figure 2.4: Left shows cotton self-extinguishing behavior of 20BL coating with red arrows directing to undamaged coated cotton (top) and charred fibers showing intumescent behavior (bottom). Reproduced with permission from Reference [11]. Copyright 2011, WILEY-VCH Verlag GmbH & Co. KgaA, Weinheim.

Translating bulk intumescent chemistry into nanocoatings seemed to be very effective and has since become one of the primary focuses of many LbL FR studies. Laufer, et al., prepared an intumescent coating on cotton using chitosan as an environmentally benign and renewable polyelectrolyte along with renewable phytic acid (PA) [79]. This coating exhibited self-extinguishing behavior during vertical flame testing. Microcombustion calorimetry (MCC) also exhibited significant reductions in peak heat release rate (pkHRR) and total heat release (THR) by up to 60% and 76% respectively. The bubble formation witnessed in this and the previous study is the char expansion commonly observed in macro-scale intumescent flame retardants. The expanded char increases the distance between the substrate and the flame/heat, improving the insulation and barrier effects of the char layer. Intumescent coatings were also shown to be successful on ramie fabric by Zhang, et al., when they

deposited polyethylenimine (PEI) with ammonium polyphosphate (APP) [80]. Self-extinguishing behavior was exhibited during vertical flame tests and swollen, bubbly char was observed under scanning electron microscopy (SEM).

In the spirit of creating environmentally benign flame retardants out of renewable resources, Carosio, et al., took advantage of deoxyribonucleic acid (DNA) due to its inherently intumescent nature [81]. DNA contains a phosphoric acid precursor, a char source, and the potential to release inert gases to act as a blowing agent. Pairing DNA with chitosan increases the available char forming agents. The coating reduced the pkHRR by 40% and the THR by 30%. These results are good and the idea of incorporating fully renewable resources is promising; however these results are still not as good as the first intumescent coating on cotton which reduced pkHRR by 64% and THR by 68% for the same number of bilayers and similar weight addition to the fabric [11]. Another attempt to show improved reduction in flammability on cotton using similarly renewable resources, chitosan and phosphorylated cellulose, was made by Pan, et al [82]. This study successfully improved the results on cotton showing self-extinguishing behavior in VFT and reducing the pkHRR by 70% and the THR by 81% with 20 BL. SEM revealed similar bubbled char as seen previously, indicating a successful intumescent coating that expanded during degradation, creating an effective insulating char barrier on the surface of the cotton.

A phosphonate containing coating was developed by Negrell-Guirao, et al., in which oligoallylamine was paired with synthesized phosphonated oligoallylamine [83]. This study showed that combining the two oligoallylamines improved the thermal and thermo-oxidative stability when compared to the individual components. A follow up study of this coating on cotton fabric was completed by Carosio, et al., which assessed the effect of molecular weight on the coating flame retardant properties [84]. The results showed that increasing the molecular weight from 4,500 g/mol to 20,000

g/mol and adjusting pH conditions of the solutions affect the coating results. As of this study, the results were not significant; however, this would be an interesting coating for further development. Based on after burn imaging, significant evidence of bubbling and swelling suggest that tailoring the phosphorous content could very well produce a coating that rivals previous intumescent systems.

Pan,et al., continued work on phosphorylating polymers to continue the improvement of intumescent materials from renewable resources, using chitin as the derivative for both LbL components [85]. In this study, chitin was phosphorylated and paired with chitosan to produce a successful flame retardant coating for cotton fabric. Both layering materials have the ability to be good char formers much like the underlying cellulose. The coating reduced the pkHRR by 74% and THR by 86% and self-extinguished in vertical flame tests with 20 BL. The phosphorous-containing coating promoted thermal degradation of the cotton fabric at lower temperatures creating a phosphorus-rich char barrier that reduced the amount of volatilized combustible products. Fang, et al., coated cotton with 20 BL of CH/APP [86]. This system reduced pkHRR and THR by 80% and 82% respectively. The improvement over previous coatings is likely due to the increased phosphorus content in the coating.

Wang, et al., prepared nitrogen-modified silane hybrids (SiN) and paired them with phytic acid to create an intumescent system that allowed cotton fabric to self-extinguish in vertical flame testing with only 15 BL [87]. This is a significant result for the VFT, but unfortunately heat release data was not as good as previous studies, reducing pkHRR by 31% and THR by 38%. There appeared to be a steady decrease in pkHRR as a function of bilayers so it is possible that with more layers, the reduction in these values could rival previous studies, especially since the swelling of this system during degradation is significant at 15 BL. It is possible that the silicate char formed from the silane during degradation is not as efficient of an insulating

layer as one based on a more significant amount of carbon. Much more significant reductions have been seen in coatings with chitosan as the alternate polyelectrolyte with the phosphorus containing material, while this coating appears to achieve the pronounced swelling behavior in fewer bilayers. A hybrid coating containing the modified silane and a carbon-based char former such as chitosan with the phytic acid might be able to further improve the heat release results.

Layer-by-layer is obviously capable of applying a variety of chemistries to a surface and to this point, has shown great success in developing flame retardant coatings on natural textiles, but LbL is not limited to incorporating a single property to the substrate. Chen, et al., presented an interesting study that combined an LbL FR coating with a hydrophobic functionality [88]. PEI was paired with APP particles in a single bilayer on cotton fabric with an additional layer of fluorinated-decyl polyhedral oligomeric silsesquioxane (F-POSS). The deposition time was significantly longer for each solution compared to a majority of studies, using 20 min to deposit PEI and 1 hr to deposit the APP layer. The increased deposition times allowed a significant amount of both materials to uniformly deposit onto the surface and after the addition of F-POSS from an ethanol solution forming a trilayer, the fabrics self-extinguished during vertical flame tests. This is a very significant result for only three deposited layers. Investigation into the coating revealed that the coating deposited a significant amount of weight to the fabric (approximately 1 wt% PEI, 19 wt% APP and 13 wt% F-POSS). The extremely high concentration of APP in the coating is likely the source of the self-extinguishing behavior as the increased phosphorus content increases the ability to catalyze char formation of the cotton. Even more impressive and something that is not frequently seen tested, the samples underwent abrasion testing and maintained self-extinguishing behavior. Fang, et al., produced a bi-functional LbL coating on cotton fabric that improved flame resistance and also acted

as an antimicrobial surface using polyhexamethylene guanidine phosphate (PHMGP) and ammonium polyphosphate [86]. The coating did not self-extinguish even with 20 BL deposited, though a swollen char similar to other intumescent coatings was observed. Regardless of the FR properties, this study shows an important step towards creating truly functional LbL coatings for marketable areas such as hospital fabrics where both fire and bacteria are of concern.

While multi-functional coatings are beneficial for broadening applications, using affordable and sustainable materials is useful for reducing cost. Carosio, et al., found that with only 4 BL of a starch-based coating, adding 7 wt% to the cotton, could reduce the pkHRR up to 40% [89]. Self-extinguishing behavior was also noted on horizontal flame spread tests (HFT). The use of starch which is a highly renewable resource provides a possible path to sustainable FR coatings much like chitosan does. Pan, et al., produced a coating with chitosan and phosphorylated poly(vinyl alcohol) which successfully self-extinguished in VFT with 30 BL [90]. This coating is not as efficient as previous coatings and serves more as an iterative step that solidifies the evidence that combining phosphorus-containing layers with char forming layers on natural fiber based fabrics is an effective flame retardant method.

Borates, much like phosphorus-containing materials, have been shown to have good flame retarding effects on cellulosic materials[91] and more recently have been shown to interact beneficially with P-N based FR materials[92, 93] to form multi-cellular graphitized char. This is due to the fact that borates can form a glassy insulating layer when melted, forming a good barrier to heat and oxygen [94]. Fang, et al., has produced the most recent LbL FR coating on cotton as of the writing of this review where the concept of including borate in intumescent systems to further improve the FR behavior was focused on by combining sodium polyborate with PHMGP [14]. The PHMGP provides the basic intumescent components and the

polyborate significantly improves the performance. These coatings were tested at 5, 10 and 20 BL (3.6 wt%, 7.5 wt% and 12.9 wt% gain respectively) using VFT, HFT, MCC and limiting oxygen index (LOI). VFT showed self-extinguishing behavior with 10 and 20 BL coatings and HFT self-extinguished in each case, with almost no flame spread at 20 BL. MCC revealed pkHRR reductions of 78% for 5 BL up to 88% with 20BL. THR was reduced between 66% and 70%. These results are very significant even at only 5 BL. LOI, which has rarely been analyzed for LbL coatings on fabric, was also analyzed and revealed an increase from 18.5% LOI of uncoated cotton to 41% LOI of the 20 BL sample. This is a tremendous improvement in the LOI and represents a very significant reduction in the overall flammability of the cotton. It was determined that the success of this coating weighed heavily on the ability of both the evolved phosphates and borate to rapidly catalyze the char formation of the cotton fabric.

Intumescent, char forming coatings are by far the most successful LbL FR treatments for natural fabrics, however many studies also focused on the incorporation of nanoparticles and all inorganic materials in an effort to deposit pre-formed insulating layers. LbL FR nanocoatings incorporating inorganic particles began in 2009 by Li, et al., who used clay nanoparticles to create a protective barrier around cotton fibers [33]. This coating prevented the complete decomposition of the cotton fabric after a vertical flame test and this was further improved using larger clay particles in 2010 which showed increased fabric retention with increased clay content (see Figure 2.5) [95]. The high thermal stability and insulating behavior of many inorganic particles led to several studies focusing on incorporating particles into LbL films on fabric. Li, et al., later created an all organo-silicon coating which prevented total decomposition of the cotton after VFT and showed minor improvements to MCC results [96]. The silicon based coating formed a hollow ceramic tube around the fibers after burning

which acted as a barrier once formed. Laufer, et al., created a similar coating using silica nanoparticles (8 and 27 nm) with polyethylenimine [97]. This coating saw very similar results to the organo-silicon coating. Uur, et al., tried a similar coating on cotton, but focused on the use of alumina nanoparticles instead of silica [98]. Only minor increases to the limiting oxygen index were observed for this coating (from LOI of 18% for the cotton to 22% in the best case coating). It is likely that this system would have performed similarly to the silica-based coatings in calorimetry and open flame tests.

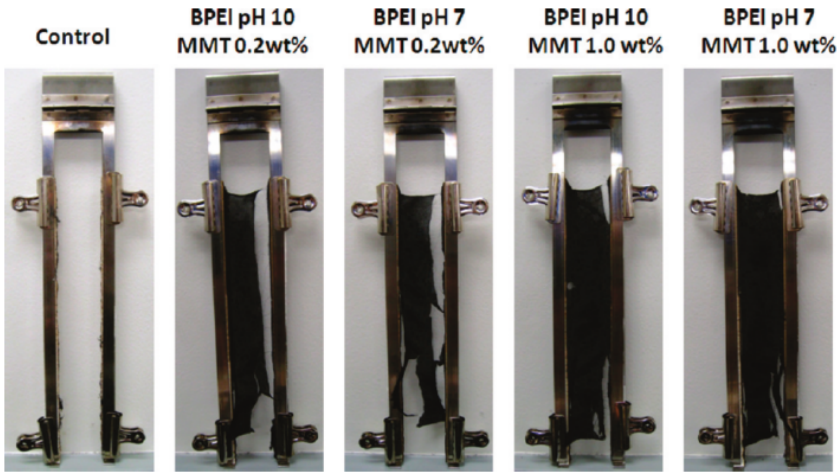

Figure 2.5: Images of uncoated and 20 BL-coated fabrics following the vertical flame test. Reproduced with permission from Reference [95]. Copyright 2010, American Chemical Society

Huang, et al., polymerized flame retardant polymers and combined them with clay platelets (and later, graphene oxide (GO) sheets) in attempt to benefit from the barrier effects of the impermeable particles and also the proven performance of char-forming polymer systems [99, 100]. The first study focused on pairing flame re-

tardant poly(acrylic acid) (PAA), which was modified with N-2-(5,5-dimethyl-1,3,2-dioxaphosphinyl-2-ylamino)-ethylacetamide-2-propenyl acid (DPEPA), with montmorillonite (MMT) clay [99]. Modifying the PAA with DPEPA in increasing amounts showed increased thermal stability using TGA. Coupled with the clay, these coatings formed a uniform and continuous char over the surface of the cotton fabrics, reducing the pkHRR and THR as well as increasing time to ignition (TTI). This coating is certainly acting in the solid phase and combines both char-forming chemistries as well as inorganic platelets, forming an expanded barrier to heat and volatiles, limiting flammability. The concept of combining platelets with charring chemistries was continued by Huang, et al., through the use of graphene oxide and modified polyacrylamide [100]. Acrylamide was polymerized with N-(5,5-dimethyl-1,3,2-dioxaphosphinyl-2-yl)-acrylamide (DPAA) to create an phosphorus-based charring polymer. This was paired with graphene oxide to form another platelet/char-forming coating combination. This coating successfully reduced the pkHRR and TTI by creating a continuous char. Based on the performance of previous inorganic particle containing coatings on natural fibers, these coatings might benefit from replacing the platelets (MMT or GO) with complimentary polymers. Using that layer to incorporate more phosphorus- or nitrogen-based materials for example could improve the intumescent effect and create a more powerful flame retardant.

Cheng, et al., used silver nanparticles paired with polydiallyldimethylammonium chloride (PDDA) to improve the thermal stability of cotton fabric [101]. TGA and VFT were used to assess the flame retardant properties of this coating. Thermal stability of the coated samples were higher, shifting the degradation temperature nearly 30°C and there was increased residue remaining (20%) after vertical flame testing. This study had similar results to those with silica particles and other spherical particles because the insulating properties that were assumed to be beneficial

are somewhat underutilized given the spherical nature of the particles, leaving many gaps and voids. Also, up to this point, all particle-based coatings tested in open-flame tests have not shown the ability to self-extinguish, but only reduce the amount of fabric lost.

Silmiar to the use of particles, Wang, et al., doped coatings on ramie fabric with metal ions, zinc and copper, in order to improve the flame retardant properties through reported synergy with phosphorous-based chemistries [102]. Reports have shown that metal ions can promote the release of phosphoric acid from phosphorous-containing compounds at lower temperatures, potentially initiating the flame retardant activity earlier [103, 104, 105]. Unfortunately this study did not compare the metal-containing coatings with just PEI and poly(vinylphosphonic acid) (PVPA) coating on ramie fabric so it is difficult to tell if there was significant benefit to including the metal ions, though it did appear that copper was more effective in reducing the pkHRR during MCC over zinc.

Zhang, et al., assembled amino-functionalized multiwalled carbon nanotubes with ammonium polyphosphate onto ramie fabric, utilizing the MWNT as somewhat of a char precursor and the APP as a char catalyzer [106]. The addition of MWNT produced results very similar to previous nanoparticles since the MWNT is effectively a char precursor and acts to reduce heat and mass transfer between the flame and the fibers. Increased performance was seen when the concentration of the APP was increased, however even at 20 BL with the higher concentration, only 4 wt% was added to the fabric, suggesting minimal growth of the LbL system. It is possible that optimizing the growth and increasing the weight gain while maximizing the phosphorous content would show significant improvements to the results of this system. Similar to using MWNT, Pan, et al., incorporated titanate nanotubes (TNT) into a LbL coating with chitosan to create a thermally stable network on the surface of

the cotton fabric [107]. This coating however, much like previous particle coatings, provided little benefit to the flammability of the cotton. The samples completely burned in vertical flame tests and it is evident through calorimetry and TGA that the coating does not interact with the cotton during degradation, limiting the flame retardant ability compared to coatings that have the ability to shift the degradation temperature of the cotton and encourage char formation. The latest work on cotton fabric using nanoparticles to impart flame retardant properties did not prevent the sample from burning, however Chen, et al., did show that multifunctionality could be imparted to the fabrics using antimicrobial and conductive componenets [108]. It is evident that for natural, cellulosic fiber based textiles, the current most successful route towards decreasing flammability via LbL is to add chemistries that directly interact with the fabric, altering the degradation pathway while also forming a solid insulating char barrier, creating significant separation between remaining fabric and the flame zone.

2.4.1.2 Coatings on Natural and Synthetic Fiber Blends

Natural fibers, primarily cotton, have been blended with synthetic fibers to achieve various physical properties. Unfortunately, synthetic fibers such as polyesters and polyamides worsen the flammability in many cases because they melt and have high heat release rates. Due to the high success on cotton, similar LbL coatings have been prepared on polyester-cotton (PECO) blends. Algoni, et al., was the first to try LbL on PECO blends using a combination of an intumescent coating and inorganic silica nanoparticles [66]. There were minimal improvements to the heat release, but the coating did allow some of the PECO to remain intact after vertical flame testing. This study focused on chitosan and ammonium polyphosphate bilayers, silica/silica bilayers, combinations of CH/APP + silica/silica bilayers, and

silica/silica/CH/APP quadlayers. A very similar study by Carosio, et al., focused on CH/APP bilayers compared to silica/APP bilayers [109]. The CH/APP coatings performed very similarly to the previous study on PECO with CH/APP layers and it was found that the silica/APP bilayers did not perform as well, which is understandable since phosphorus-based materials are known to interact with hydroxyl groups (i.e., chitosan) to promote charring. In both cases, the afterglow phenomena typically witnessed in the burning of cotton and PECO was suppressed. A follow up study was performed by the same group using APP with poly(diallydimethyl ammonium chloride) and poly(acrylic acid) [110]. This study compared the results of this quadlayer coating on cotton, PECO and pure polyester fabric. APP and PAA were considered the char forming agents, and while no open flame tests were performed, TGA analysis showed an increase in residue remaining after high temperature exposure and fabric textures were maintained to an extent. The same coating was used on the same substrates in a following study which incorporated open flame tests and heat release studies and found that the coating did improve substrate stability in open flame tests and reduced pkHRR and THR on all three substrates, though it unfortunately did not self-extinguish on any of the vertical flame samples [111]. Leistner, et al., followed with a similar tactic on PECO using chitosan and a polyphosphate as the base materials for a LbL FR coating, however melamine was introduced to form melamine polyphosphate during the coating process and found that with only 12 wt% addition to the fabric, the coated samples self-extinguished during vertical flame testing, seen in Figure 2.6, and reduced the pkHRR [112]. The success of this coating was attributed to the formation of melamine polyphosphate in the coating which is a known effective flame retardant.

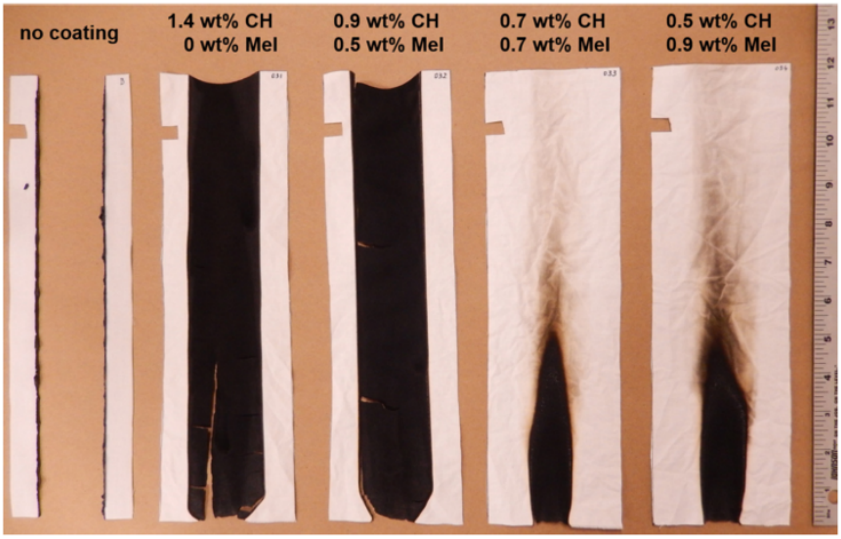

Figure 2.6: Fabric after vertical flame testing. Each coated sample had 12.5 ± 0.4 wt% deposited. Concentration of melamine in the cationic deposition solution is increasing from left to right. Concentration of PSP in the anionic solution was held constant at 2 wt%. Reproduced with permission from Reference [112]. Copyright 2015, Elsevier Ltd.

2.4.1.3 Coatings on Synthetic Fibers

Synthetic fibers, unlike cotton, melt when exposed to heat or flame since they are typically thermoplastics such as polyesters (PET) and polyamides (PAm). While fewer studies using LbL on synthetic fibers exist than on cotton and blends, some progress has been made towards understanding how to best apply LbL to PET or PAm 6,6 and achieve improvements in FR behavior. Carosio, et al., applied a coating based on oppositely charged silica particles on PET fabric and was able to eliminate melt-dripping and reduced the pkHRR by up to 20% [113]. It was observed that smaller silica particles resulted in a more uniform coating, however the coating became unstable at higher thicknesses, whereas the larger silica particles, with increased surface charge were more stable regarding flakiness of the coating. A

following study by the same group used zirconium phosphate (ZrP) paired with PDDA, POSS, or silica on PET fabric [34]. The PDDA/ZrP coatings increased the time to ignition by a significant 86%, while the POSS/ZrP coating had the greatest reduction in pkHRR of 26%. Apaydin, et al., took a different approach with PAm 6,6 and PET by using similar phosphorous and nitrogen based coatings as seen with many of the natural fiber LbL FR coatings [114]. PAH and PSP were used in a first study on PAm 6,6 and 40 BL reduced the pkHRR by 36%. It was suggested that the coating was able to alter the degradation pathway of the PAm 6,6. A follow up study focused on the addition of TiO2 into a PAH/PSP coating by forming QLs of PAH/PSP/PAH/TiO2 [115]. It was found that only minor improvements occurred on the PET fabric compared to the PAm 6,6 and that the TiO2 did not provide significant benefit over the PAH/PSP film alone. This study points out an important issue that is coatings need to be tailored for the specific substrate. Both PET and PAm 6,6 are thermoplastic fabrics, but their chemistries are different and the chemistry of the flame retardant as such might not perform equally. This is one of the major benefits of LbL in that the coating chemistry and functionality can easily be adapted to suit a specific material. Pan, et al., has produced the most significant improvements to date on PET fabrics with a 4QL, 4 wt% coating using inorganic nanoparticles (MMT and titanate nanotubes) with chitosan to reduce the pkHRR and THR by 48% and 36% respectively [71]. This study would suggest that the melting behavior and high heat release rates of at least PET fabrics might best be flame retarded by inorganic nanoparticles. It would be interesting to see if the results translate to other synthetic fabrics and how the coating stands to open flame testing.

2.4.2 Layer-by-Layer Flame Retardant Coatings on Foam

Open cell polyurethane (PU) foam is used extensively in furniture cushions, packaging, and in the transportation industry due to its high degree of flexibility and comfort. With that comes extreme flammability that can contribute to a large heat release and rapid fire spread mainly due to melt dripping during the burning process. Toxic smoke release also contributes to the danger of PU foam in a fire because the degradation creates toxic isocyanate and diol precursors which then can be inhaled during a fire, potentially causing suffocation. Due to its complex structural characteristics, applying a coating to prevent any or all of these hazards while maintaining the desirable characteristics that define its popularity can be difficult. The LbL technique by its very nature can overcome this problem, as coating thickness can be adjusted nanometers at a time while achieving a conformal coating and maintaining intrinsic substrate properties.

2.4.2.1 Polyurethane-Based Foams

Kim, et al., grew bilayers of PAA and PEI both suspending carbon nanofibers (CNF) on PU foam [116]. Four bilayers of this system lead to a 40% reduction of pkHRR and prevented the formation of a melt drip puddle during burning. This was a promising first step especially considering that only 4% loading of the CNF reduced the pkHRR the same amount as 20% loaded halogenated FR materials. Laufer, et al., published the first example of clay in LbL FR for PU foam by using CH and MMT to create a fully renewable coating which at 10 bilayers reduced the pkHRR by 52% and shielded the interior of the foam from degradation [117]. The protective char layer that is formed can be clearly seen in Figure 2.7 where the burned region and protected region after a bench-scale torch test are viewed under SEM to show how the insulating layer completely protected the underlying foam. The use of MMT

to protect PU foam was extended by Cain, et al., who eliminated melt dripping and reduced pKHRR by 55% with 4 TL of PSP, PAH and MMT [118]. The overall weight added to the foam was less than the CH/MMT system which suggests the polymer layers were more efficient at charring. Continuing the use of MMT, Li, et al., explored effects of solution concentration and showed that higher solution concentrations led to better flame retardant properties [67]. This study also tested the resiliency of the coating after compression. The flame retardant capability only slightly decreased after compression testing. To assess the viability of this technology on large scale applications, Kim, et al., showed that 2 BL of a MMT containing coating significanly reduced the pkHRR of a full scale chair while eliminating melt dripping and retaining the original chair shape after the test [119]. Li, et al., explored the effects of using DNA in an attempt to incorporate improved char formation between clay layers using sustainable materials [120]. Mixing DNA with CH and depositing with MMT resulted in the fastest growing film with the greatest incorporation of MMT. A 51% reduction in pkHRR was observed with a 10 BL coating. This study emphasized the importance of the content of clay in these systems. Unlike with cellulosic materials, it is difficult to interact with the degradation of PU foam directly, so it is clear that an effective strategy is to expedite the development of an exterior barrier to limit heat and mass transfer during burning.

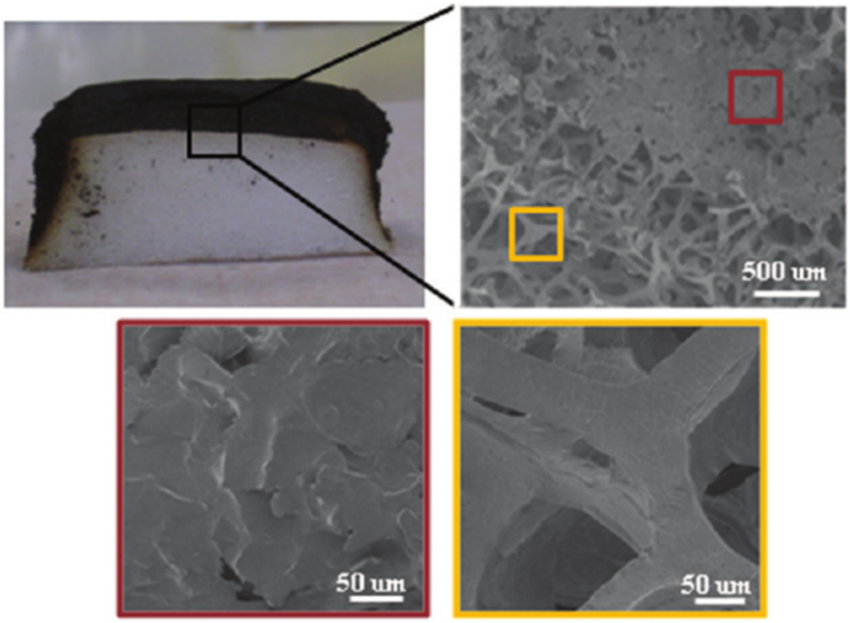

Figure 2.7: Digital and SEM images of cross sections of foam coated with 10 BL CH/MMT. The red box shows the thermal shield created by the coating and the yellow box shows undamaged foam. Reproduced with permission from Reference [117]. Copyright 2012, American Chemical Society.

Pan, et al., added carbon nanotubes (CNT) to CH and deposited with MMT and alginate (AL) in a TL system [121]. At 8 TL a 65% reduction in pkHRR was observed, and generation of detectable CO_2 and CO was greatly reduced. This system generated a percolated network of MMT/CNT with a total weight gain of only 4 wt% at 8 TL. In analysis of the pyrolysis products, it was determined that the initial stages of PU foam degradation during burning were unchanged. Instead, the MMT/CNT created a barrier that limited transfer of heat and mass and limited oxygen exposure to unburned fuel (i.e., PU foam).

Cain, et al., was able to reduce the processing steps down to 1 BL of PEI and VMT, which resulted in a reduction in pkHRR by 54% and smoke release by 31%

while eliminating melt dripping [122]. It was suggested that this remarkable increase in performance was due the order of magnitude larger aspect ratio exhibited by VMT over MMT which reduces gaps that allow heat and mass transfer. This is an important step in realizing the viability of LbL as a commercial strategy by greatly reducing the processing time. Patra, et al., built on this idea and developed an all nano-particle film consisting of one BL of boehmite (BMT) and VMT [123]. Melt dripping in coated samples was not observed and smoke release and pkHRR were reduced by a factor of 2. Because BMT is an alumina hydrate, it is able to undergo endothermic dehydration which acts as a heat sink, and the resulting Al_2O_3 acts as an insulating barrier. This effect was also observed when Yang, et al., assembled a variety of films containing layered double hydroxides (LDH) and/or MMT with PAA and PEI as polymeric binders [124]. It was shown that LDH containing films exhibited the largest reduction in pkHRR ($\sim$40%) whereas TL and QL films containing MMT had a smaller reduction in pkHRR ($\sim$30%). While both MMT and LDH develop an insulating layer, the LDH undergoes endothermic dehydration which acts to cool the material and slows degradation. Alumina in LbL flame retardants was further investigated by Haile, et al., by building bilayers of PEI and PAA stabilized alumina trihydrate (ATH) [125]. Just 6 BL led to a 64% reduction in pkHRR and self-extinguished under torch testing. Once again this performance is likely due to the cooling effect from the dehydration and the formation of an insulating ceramic layer.

Work has also been completed based on non-platelet nanoparticles on foam, most notably nanotube particles. Pan, et al., was able to greatly reduce total smoke release and pkHRR by constructing trilayers of CH/TNT/AL [12]. At 6 TL, 5.7% mass gain, the pkHRR was reduced by 70% and TSR was reduced by 41%. The coating is not interacting with the underlying foam as absorption peaks for the pyrolysis

products match that of the uncoated sample. It is likely that the TNT acts as a physical barrier limiting the interfaces for heat to transfer and for the pyrolysis products to escape, and it was suggested that the TNT may actually be adsorbing some of the pyrolysis organic products. Pan, et al., also coated PU foam using AL-stabilized GO and β-FeOOH nanorods (FNR) with PEI in a hybrid TL system [126]. There was a notable reduction in pkHRR at 5 TL, but a film grown without FNR exhibited similar pkHRR. The coating with FNR also reduced the amount of detectable organic volatiles. It is clear from these examples that nano-particles, specifically clay particles, alumina hydrates and nanotubes aid greatly in reducing the flammability of PU foam. Tubular nanoparticles have also shown promise towards developing smoke suppressant coatings.

While nanoparticle-based coatings are very effective on polyurethane, there are also studies focused on all polymer systems. In one such study Laufer, et al., used CH and poly(vinyl sulfonic acid sodium salt) (PVS) on PU foam to create a self-extinguishing effect at 10 BL [127]. It is was suggested, as depicted in Figure 2.8, that the PVS broke down during combustion into SO_2 and other non-flammable gasses, which diluted combustible volatiles in the flame, inhibiting further degradation and flame spread. Unlike composite foams with similar FR functionality, this coating completely prevented melting and also formed a char layer on the surface in conjunction with the reported gas phase dilution. This allowed the coating to self-extinguish while also preventing future ignitions. Carosio, et al., treated PU foam with up to 5 QL of CH/PAA/CH/PPA which exhibited self-extinguishing behavior and eliminated melt dripping [128]. This likely acted as an intumescent system with the PPA catalyzing char formation of CH. Using completely renewable polymers, Wang, et al., assembled 10 bilayers of CH/AL resulting in a 66% reduction in pkHRR [129]. Both deposition species are carbohydrates, so it is most likely that

an insulating char layer was formed during combustion resulting in the observed reduction of pkHRR. Carosio, et al., created an all polymer intumescent system utilizing CH and poly(allylamine diphosphonate) (PAHDP) [130]. Four BL reduced the pkHRR by 55% but the smoke release was significantly increased and the preservation of the foam was not especially effective as the sample was charred throughout. The same group was also able to rapidly deposit CH/PPA which at 2 BL produced a coating that reduced pkHRR by 33% and eliminated melt drip [131]. This was accomplished by putting the samples through rollers which left it exposed to the coating solution for less than 1 second. By reducing processing time this could help streamline the process for large scale applications. These examples are efficient at reducing the pkHRR, however little of the underlying substrate is preserved after burning which is a dominating and beneficial feature of nanoparticle-based coatings.

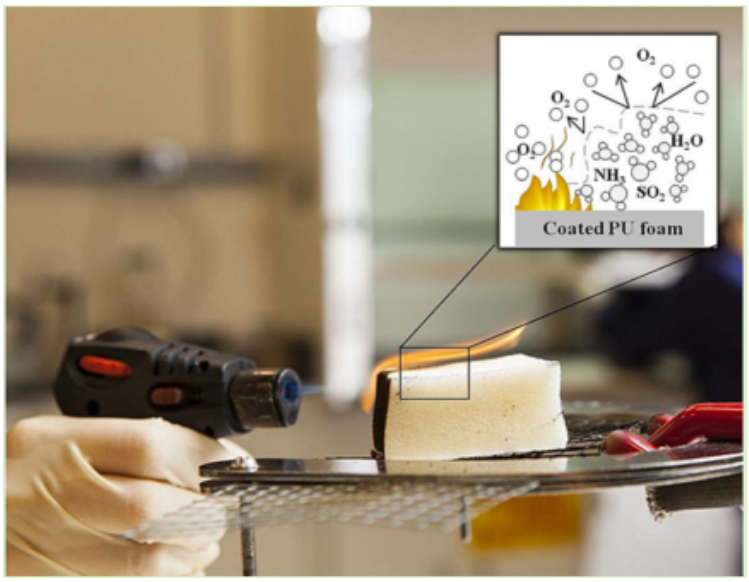

Figure 2.8: Abstract image showing proposed flame retardant mechanism of CH/PVS coating on polyurethane foam. Reproduced with permission from Reference [127]. Copyright 2013, American Chemical Society.

2.4.2.2 Other Foam Materials

Other foam materials have also benefited from LbL FR assemblies. PET foams are used in the food packing and the transportation industries. Carosio, et al., coated closed cell PET foam with a QL system consisting of either PDDA/PAA/PDDA/APP or PDDA/PAA/PDDA/DNA [132]. The coating with APP significantly outperformed the DNA coated samples due to increased phospohorus content and therefore incresed char formation facilitated by APP which eliminated melt drip and reduced the pkHRR by 25% compared to insignificant changes with the DNA assembled films. Melamine foam (MF) has also incurred research interest as a popular material for acoustic and thermal insulation in buildings. Melamine foam undergoes drastic shrinkage when exposed to the high temperatures of a fire. Yang, et al., used a simple intumescent system of CH/APP to reduce the flammability of MF and 2 BL yielding an 87% reduction in pkHRR, 77% reduction in THR, and reduced shrinkage during combustion [133]. Based on knowledge of phosphorus and melamine flame retardants, it is very likely that the coating has synergistic interactions with the melamine. The LOI was also increased from 34.5% to 47%. Polysiloxane foams (SiF) are highly porous and generally contain a large amount of flammable organic components which leads to a very flammable material that generates a large quantity of smoke during combustion. This has limited their potential commercial applications. Deng, et al., coated SiF with CH/MMT and CH/APP coatings in which CH/MMT proved to create a more effective barrier and smoke suppressant than CH/APP which follows the trends of previous examples [134]. Even at 21 BL there was only a modest reduction in pkHRR of $\sim$25%, but the TSR was decreased by 58%.

2.4.3 Layer-by-Layer Flame Retardant Coatings on Bulk Polymers and Other Substrates

2.4.3.1 Bulk Polymer Flame Retardant Layer-by-Layer

In 2011, around the same time studies started expanding to foam substrates, Laachachi, et al., grew LbL films on polylactide (PLA) sheets using what they considered to be a reinforced intumescent system containing an acid source, swelling agent, carbon source and an inorganic filler [35]. This coating utilized PAH and MMT as the primary layering materials and followed film growth with a soak in a PSP solution. The 60 BL coating, almost 20 μm in thickness, showed significant reductions in the flammability of the PLA substrate with and without the PSP addition. The PSP addition had the best results, increasing the time to ignition in cone calorimetry by a reported 123% and reducing the pkHRR by 37%, though these numbers were within error of the film without the PSP addition. This is significant when considering the bulk PLA is 2 mm in width and protected by a coating two orders of magnitude thinner, adding less than 2 wt% to the substrate. Apaydin, et al., published similar studies using PAH and MMT on bulk polyamide 6 [28]. It was observed that with 5 and 10 BL coatings, pkHRR increased, however with 20 BL there was a significant reduction in pkHRR of 62%. A follow-up study was completed to determine the flame retardant mechanism of this coating which is discussed in section 3.4.1 [13]. Building on the same concept as Laachachi and Apaydin, Guin, et al., developed chitosan and clay based coatings that prevented ignition of polystyrene (PS) films completely by incorporating amine salts to rapidly increase film growth while maintaining film structure [135]. Figure 2.9 shows that incorporating tris into the chitosan solution and pairing with VMT leads to a coating that prevented ignition of the PS when exposed to a butane torch in a flame-through test

that completely burns uncoated PS.

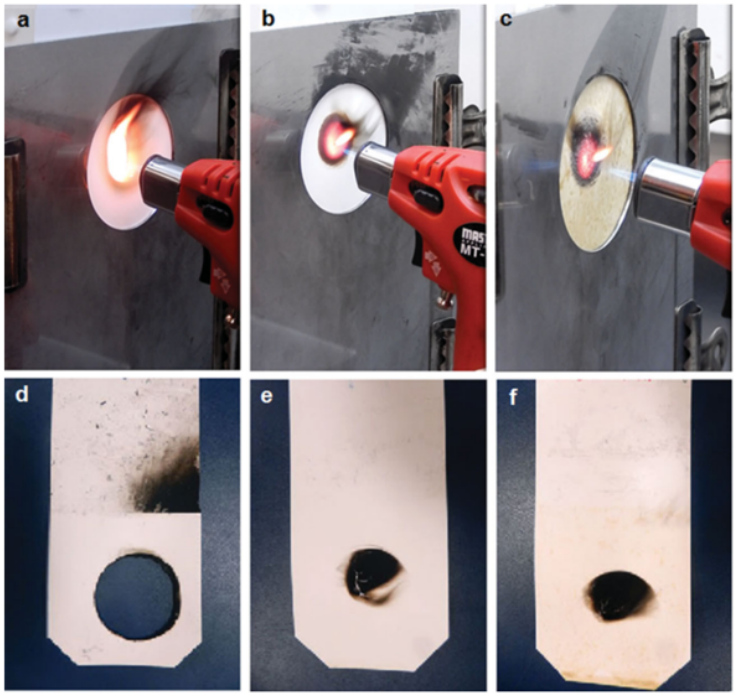

Figure 2.9: Pictures of flame-through torch tests 5 s after ignition of 3.2 mm thick PS plates: (a) control, (b) 8-BL CH+tris/MMT film added, or (c) 8-BL CH+tris/VMT film added. Pictures of the PS plates after 10 s flame-through torch test of the (d) control, (e) with a 3-BL CH+tris/MMT film added, or (f) with a 2-BL CH+tris/VMT film added. Reproduced with permission from Reference [135]. Copyright 2015, WILEY-VCH Verlag GmbH & Co. KGaA, Weinheim.

Other coatings on bulk polymer substrates include one by Alongi, et al., focused on polycarbonate (PC) and one by Farag, et al., focused on polyethylene (PE) and polystyrene [136, 137]. Alongi, et al., produced a coating on PC which contained UV-curable layers which were shown to improve thermal stability of the PC in air once cured [136]. The coating proved to be resistant to wash treatments in 50 °C water and also prevented melt dripping and suppressed smoke release during burning. Farag,

et al., used plasma treatment of substrates and plasma polymerization of PAH to promote adhesion to hydrophobic polymer substrates [137]. The coating of PAH and PSP reached approximately 1 m in thickness and was able to prevent melt dripping of the bulk substrate as well as increase the time to ignition which are both beneficial towards limiting/prolonging the flame spread to other objects in a fire scenario.

2.4.3.2 Other Layer-by-Layer Flame Retardant Studies

In the general sense, layer-by-layer is discussed as being applied to a surface, which is commonly assumed to be much larger than the materials being deposited. Several studies, however, have incorporated LbL to improve flame retardant properties of nanoparticles. In 2008, LbL was used by Lin, et al., to improve the thermal stability of lignocellulosic fibers from steam-exploded wood [138]. The coating of PDDA and MMT clay created significant char on the fibers acting as a barrier to prevent further decomposition of the fibers during any future thermal processing such as melt mixing in thermoplastic matrices. Wei, et al., took a similar approach to flame retarding sisal fibers, another cellulosic material, by depositing layers of CH/MMT [139]. This is the same coating seen previously on polyurethane foam and cotton fabric, though it appears in this case that while the FR properties as shown through TGA and MCC were improved, a clay-based coating on cellulose does not provide the same potential FR benefit as a phosphorus-based coating could, as evidenced by the success of phosphorus-based LbL textile coatings. Kklkaya, et al., functionalized wood fibers using LbL assembly for the purpose of creating flame retardant paper and focused on the inclusion of typical charring chemistries [140]. In this study, chitosan and poly(vinylphosphonic acid) were deposited directly onto the fibers which were then used to form paper sheets. The paper sheets were tested using HFT and cone calorimetry and were found to be self-extinguishing and had a 49% reduction in

pkHRR with 20BL of CH/PVPA. These studies show that there are multiple ways to flame retard cellulosic fibers, though as evidenced through these fiber based studies as well as through studies on cellulose-based textiles, char catalyzing coatings perform better as cellulose itself is a good carbon source for char formation.

One of the more unique LbL coatings for improved FR properties was developed by Jiang, et al., through the coating of mesoporous silica particles with Co-Al layered double hydroxides and nitrate [141]. The particles were coated with 10BL and then embedded into epoxy resin to determine the flame retardant potential of these spherical particles. Cone calorimetry of the filled epoxy resin yielded significant improvements in FR properties. The pkHRR was reduced by 39%, the THR was reduced by 36%, and the TSR was reduced by 24% all with only a 2 wt% loading of LbL coated particles. While it made sense for these particles to be used as fillers for bulk material, it would be interesting to apply this LbL coating directly to a substrate. The FR mechanism for these coated particles in epoxy was also investigated and will be discussed in section 3.4.1. Wang, et al., worked on a similar study using brucite as the base for LbL deposition of 3-aminopropyltriethoxysilane (APTES) and nickel alginate (NiA) [142]. Technically the particles with added materials formed a single quadlayer of brucite/APTES/NiA/APTES which was then incorporated into ethylene-vinyl acetate resin in order to improve the flame retardant properties. Both the THR and pkHRR were significantly reduced. This would also be an interesting material to incorporate into LbL coatings on other polymer substrates due to the unique mechanism of action, involving endothermic FR through release of water and other non-combustible gases and through the catalysis of char formation by the Ni.

2.4.4 Understanding and Scaling Layer-by-Layer Flame Retardants

2.4.4.1 Mechanistic Studies on Layer-by-Layer Flame Retardants

As seen in the previous sections, a wide variety of flame retardants have been developed using layer-by-layer assembly for range of polymeric materials. A vast majority of these studies are adapting previous flame retardant technologies into a multilayer coating format and following the assumption that the coatings would in theory perform under the same mechanisms. One of the simplest examples is the use of the word intumescent for nanocoatings containing similar chemistries to common intumescent systems, i.e. a carbon source, spumific, and acid donor. Little work has been done to truly determine the mechanism of flame retardancy of these nanometer scale thin films. In 2014, Apaydin, et al., performed a mechanistic study of the flame retardant performance of PAH/MMT bilayers on a polyamide substrate [13]. Cone calorimeter, pyrolysis-combustion flow calorimetry, analysis of the condensed phase, and analysis of the decomposition gases were all studied to get an understanding of how the coating was able to achieve the flame retardant improvements. Analysis during cone calorimeter suggested that the temperature of the sample gradually increased until the degradation of PAH occurred, which released different volatile products including ammonia, water, carbon monoxide and carbon dioxide which all slowed down the ignition of the sample. It was also suggested that a majority of the released products from the degradation of the PAH are retained in the condensed phase due to the intrinsic barrier properties of the coating. The polyamide 6 degrades after the PAH and contributes to the released products that are also trapped in the forming char causing it to swell at the surface of the substrate. Evidence of both degraded PAH and PA6 was found at the surface of the char layers. The conclusion was that the mode of action of the coating, as depicted in Figure 2.10, only occurs in

the condensed phase which was confirmed by pyrolysis-combustion flow calorimetry (PCFC) results.

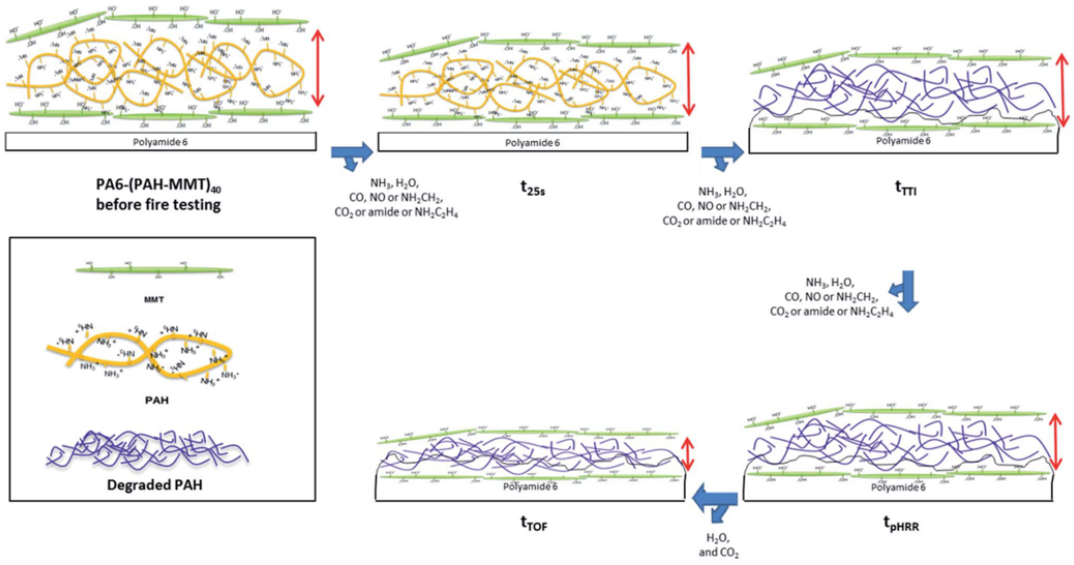

Figure 2.10: The mechanism of $(PAH\text{-}MMT)_n$ flame retardant coating shown various stages. Reproduced with permission from Reference [13]. Copyright 2014, The Royal Society of Chemistry.

Another mechanistic study was carried out on LbL coated silica particles that were dispersed in epoxy as flame retardant filler [141]. As previously described in section 3.3.2, only 2 wt% loading of these particles had significant impact on the flame retardancy of the epoxy composite. The flame retardant mechanism was studied through the analysis of thermal conductivity, char residue, and the degradation products of the epoxy and resulting composites. Thermal conductivity was reduced with the inclusion of the nanoparticles, suggesting that the low thermal conductivity and high surface area of the mesoporous silica particles limited heat and mass diffusion. The char residue of the nanocomposite was analyzed using Raman spectroscopy

and it was found that the nanoparticles catalyzed graphitized char during the epoxy combustion as opposed to the glassy carbon char seen in the neat epoxy residue. It was also noted that the nanocomposite formed a more continuous and cohesive char layer which combined with the improved thermal properties of the graphitized char, is beneficial for the inhibition of heat, mass, and oxygen exchange. Analysis of the pyrolysis products suggested that the silica can act as an efficient solid acid for the catalytic degradation of polymers leading to the formation of lower carbon number products, which were then readily dehydrogenated and catalyzed into char by the Co-Al LDH. Much like understanding the flame retardant mechanism is important for the development of future improved FR coatings, developing methods to scale up these coatings is important to realize the potential of these coatings to replace existing flame retardants in industry.

2.4.4.2 Scalability of Layer-by-Layer Flame Retardants

One of the largest pitfalls of layer-by-layer, especially in the technologies infancy, has been processing time. Deposition times of 20 min or more were used to deposit single layers in multilayer assemblies, which is not reasonable for any sort of commercialization of the technology. LbL has come a long way since then and now the more common deposition times are closer to 1 min or less. Other methods of deposition, straying from dip coating, have been studied, including spray coating which is an industrially viable technique. For flame retardants, the hurdle for rapid deposition falls on the wide variation in substrate morphologies. As mentioned, spray coating is a promising deposition method that is quick and reduces material use while also eliminating risk of solution contamination that could occur through repetitive dipping into solution baths. Alongi, et al., and Carosio, et al., started spray coating polyester and cotton fabrics respectively to speed up the deposition process and both

cases showed promising results, translating the coatings from dip process to a more efficient spray process [143, 144].

Chang, et al., and Mateos, et al., built roll-to-roll deposition systems similar to a padding system already used in the fabric industry in order to demonstrate the potential to streamline coating large quantities of fabric in a continuous line process that could easily adapt into current factory technologies [145, 146]. Figure 2.11 shows a photo of Mateos, et al., automated deposition system. Both cases showed reproducible results across the large coated samples. Chang and coworkers also introduced a new LbL recipe that achieved very significant reductions in flammability using PEI, clay, urea and diammonium phosphate [145]. Another downside to LbL that is also evident in these two scale-up studies, is the effect on fabric mechanical properties that are related to comfort of the material. It is rarely discussed, but many studies show evidence of bridging of the coatings between fabric fibers, and this bridging reduces fabric physical properties by increasing the overall stiffness. Guin, et al., devised a way to eliminate bridging of the fibers while maintaining the flame retardant properties of the coating using ultrasonication during the rinse steps of the coating process [36]. This allowed the loosely adhered polyelectrolytes to be removed more effectively during the rinse step, preventing the fibers to adhere to each other while the coating is being applied. Wash resistance after the coating is applied is another factor to consider when developing flame retardants for fabrics, since fabrics commonly undergo hundreds of wash cycles in their lifetime. The nature of water-based deposition focused on electrostatic interactions poses a problem when these coatings are exposed to heated water baths full of detergents that are specifically designed to remove non-covalently linked materials from the fabric surface. Carosio, et al., attempted to produce a LbL coating that was UV-curable in order to covalently bond the coating after deposition [147]. Washing did not completely remove the flame

retardant properties, however, the coating was resistance without curing was not reported so it is difficult to know how much the curing improved the wash-resistance of the coating. A similar study was completed on bulk polycarbonate by the same group which showed that PC melt dripped without curing the coating while the cured coatings of 5 QL prevented melt dripping before and after being washed [136]. Covalent-bonding is certainly a desirable method of permanently sealing the LbL coatings to the surface of whatever flammable surface is being protected, however this will need significant work moving forward.

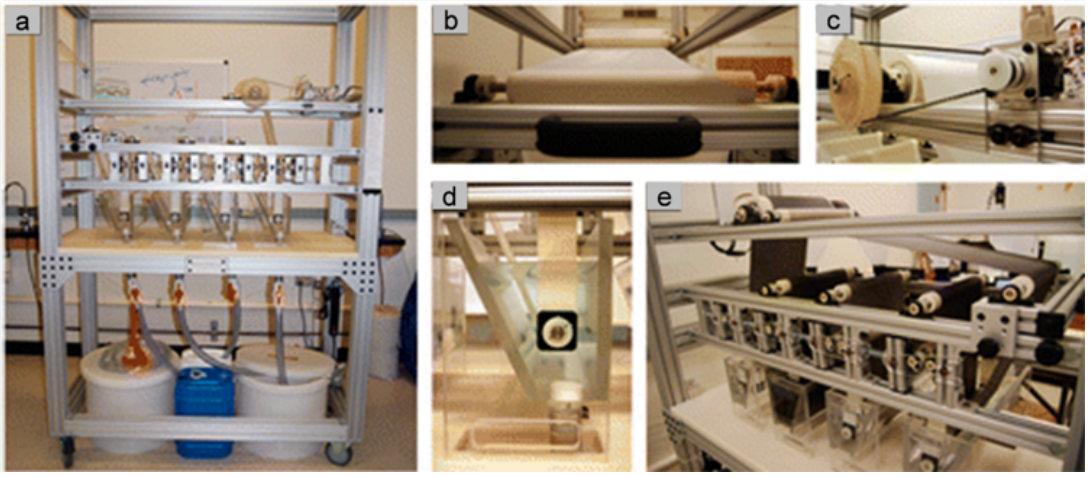

Figure 2.11: (a) Image of the pilot coater and pictures showing (b) the tensioner, (c) operating motor, (d) solution bath, and (e) a sample of fabric being coated. Reproduced with permission from Reference [146]. Copyright 2014, American Chemical Society.

Studies have been completed on fabric towards making LbL FR coatings a scalable technology, however not as much work has been published doing the same on foam. Two studies focused on creating single layer LbL coatings in order to reduce processing steps on polyurethane foam while still achieving significant reductions in

flammability of the foam [122, 123]. A more recent study has focused on the rapid deposition of layer-by-layer coatings using 0.5 second deposition steps [131]. Kim, et al., performed a study on foam that did not necessarily show any progress towards improving the LbL process for scale up on foam, but instead they showed that the LbL FR coating is visibly better on a large-scale furniture mockup flammability test, as seen in Figure 2.12 [119].

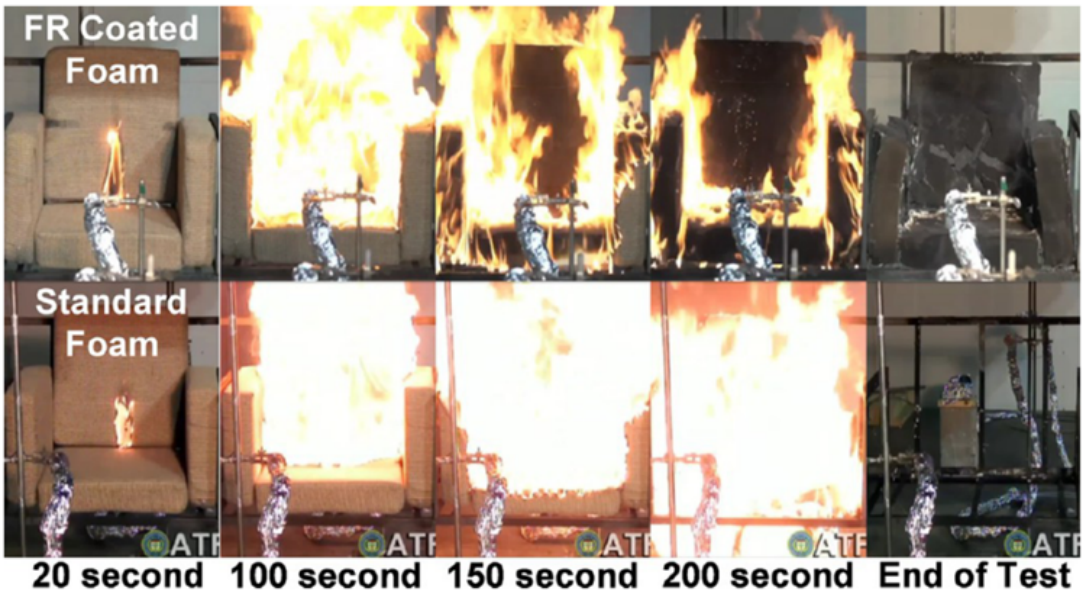

Figure 2.12: Images pulled from video records of a real scale fire test of an upholstered chair. Reproduced with permission from Reference [119]. Copyright 2014, American Chemical Society.

Layer-by-layer is a promising technology for imparting flame retardance to polymeric materials. A significant body of work has shown significant advances in flame retarding specific materials based on polymer type. After a decade of development, layer-by-layer FR is starting to reach the stages of study that are focused on making

this technology viable for commercial applications and hopefully the success of this technology will allow for more rigorous fire regulations to be installed to increase global fire safety.

2.4.5 Perspective and Conclusion

The increased usage of polymeric materials over the past century has made it difficult to maintain fire-safe environments. The increased regulation on flame retardants is also making it more difficult to flame retard materials using existing technologies. Layer-by-layer assembly is an up and coming technology platform being directed towards flame retarding materials due to its ease of use and tunable nature. Now safer flame retardant chemistries can easily be applied to a wide variety of materials as shown in this review, making this technology a significant step forward to producing safe flame retardants for polymeric materials. While it is possible that LbL FR technology is advanced enough to start being vetted for introduction as a marketable product, there are still some issues remaining that need to be ironed out before this technology widespread adoption in the market. One of the largest factors affecting cost and scalability is quantity of processing steps and time and fortunately these hurdles have been recognized by the community and are being addressed through various means. Some studies have taken LbL inspired coating chemistries and developed polyelectrolyte complexes that can deposit coatings in a single deposition step which may become a viable alternative coating technique for certain substrates [148, 149, 150]. Cost of materials is another issue since studies are all on laboratory scale, incorporating currently available cost effective materials has not been a focus and while a large percentage of studies have focused on environmentally safe and renewable materials, these materials are not necessarily ready to be produced cost effectively so this will take time. Coating durability will be anoter major issue to be

assessed moving forward because the coatings are being design for materials that will undergo significant wear-and-tear so the coatings must be able to last and remain effective.

The first LbL FR coating was created in 2006 and in the past decade, dozens more have been developed. Applicable substrates have expanded from textiles to foams, bulk polymers and even nanoparticles. The unique ability of LbL to deposit materials in layered fashion has allowed current flame retardant additive technologies to be adapted into nanoscale coatings that are prepositioned to directly interact with the polymer/flame interface. LbL also facilitates the incorporation of multiple FR mechanisms simultaneously which may allow for the discovery of new FR synergisms. It is very likely that the rapid expansion of studies and improved results on a multitude of substrates will result in commercial LbL flame retardants within the next decade.

3. INTUMESCING MULTILAYER THIN FILM DEPOSITED ON CLAY-BASED NANOBRICK WALL TO PRODUCE SELF-EXTINGUISHING FLAME RETARDANT POLYURETHANE*

3.1 Introduction

Polymer-clay multilayer nanocoatings have been developed for multiple purposes [151, 75, 152, 35, 70, 153, 154, 28, 155] and have demonstrated the ability to reduce the flammability of polyurethane foam [117, 118, 119, 67]. Layer-by-layer assembly is a facile processing technique used to create thin films through sequential deposition of materials with complimentary functional groups, which are most often ionic [10]. Ten bilayers (BL) of chitosan and clay was shown to add only 4 wt% to ester-based foam and reduce its heat release rate by 52% [117]. These nanobrick wall thin films provide protection through a condensed phase mechanism in which the clay forms a ceramic shell, breaking the pyrolysis cycle [156]. A trilayer (TL) film, deposited with montmorillonite clay, polyallylamine hydrochloride (PAH) and polysodium phosphate (PSP) showed improved results [118]. In this case, PAH and PSP acted as an intumescent mortar for the clay nanobricks. Intumescent systems are typically composed of four basic components: a carbon source, acid donor, blowing agent and a binder [157]. Several LbL-deposited intumescent recipes have been created for various substrates [119, 35, 11, 79, 80]. In most cases, the nanocoatings polymer backbones (and sometimes the substrate) are able to act as the carbon source and a phosphate-rich molecule acts as the acid donor. Blowing agents produce non-flammable gases when exposed to heat. Often, blowing agents are nitrogen-rich molecules, but it has also been suggested that substrates (e.g. polyurethane) and

*Reprinted with permission from Reference [1]. Copyright 2014, Springer Science+Business Media New York

carbon sources can act as blowing agents [158, 159, 160]. Layer-by-layer coatings by design do not require a separate binder. Even with the advances in LbL coatings on PUF, flashover is a persistent problem. Typically these nanocoatings prevent melt dripping of polyurethane, but the flame spreads over the surface of the foam, leaving only the interior unharmed [117, 118, 122].

In this section, a nanobrick wall is deposited to provide structural support and provide time for an intumescent coating (deposited on top as a second sequence of layers) to work more effectively. This unique stacked coating combines a highly ordered clay nanocoating that behaves as a thermal shield and an intumescing nanocoating to prevent flashover at the foams surface. The clay layers are composed of chitosan (CH) and vermiculite (VMT). Vermiculite is a high aspect ratio clay that provides good coverage of the PUF surface with relatively few layers [122]. The intumescing layers are composed of CH and ammonium polyphosphate (APP). In this case, CH acts as the carbon source and APP acts as the acid donor. Gases released from the polyurethane degradation and from the decomposition of chitosan in the LbL coating behave collectively as the blowing agent [158, 159, 160]. Now the benefits of two common flame retarding systems are better utilized by separating them on the nanoscale in a single coating. This concept offers an environmentally benign alternative to current flame retardant treatments that are undergoing heavy scrutiny by various agencies worldwide.

3.2 Experimental

3.2.1 Materials

Unless indicated, all materials were used as received. Natural vermiculite (VMT) (Microlite 963++, 7.5 wt% in water) clay dispersion was supplied by Specialty Vermiculite Corp. (Cambridge, MA). Chitosan (CH) (MW = 60,000 g/mol) was pur-

chased from G.T.C. Bio Corporation (Qingdao, China). Ammonium polyphosphate (APP) (Exolit AP 422, n > 1000) was supplied by Clariant Corp. (Charlotte, NC). Poly(acrylic acid) (PAA) solution (MW = 100,000 g/mol, 35 wt% in water), sodium hydroxide pellets (anhydrous) (reagent grade, 98%), nitric acid (red, fuming, HNO_3 > 90%), and hydrochloric acid (ACS reagent 37%) were purchased from Sigma-Aldrich (Milwaukee, WI). Polyether-based polyurethane foam (PUF) (foam type 1850, no additives), with a density of 28 kg/m^3 (1.75 lbs/ft^3), was purchased from Future Foam (High Point, NC).

3.2.2 Layer-by-Layer Deposition

All aqueous solutions were prepared with ∼18 MΩ deionized (DI) water. 1 wt% PAA solutions were prepared and altered to pH 2 using 2M HNO_3. The dissociated nitrates interact with the polar functionality and protonation of the polyurethane, producing a positive net charge on the surface of the PUF that leads to strong adhesion of anionic PAA. 1 wt% APP solutions (1 wt% APP, 11.1 wt% 1M NaOH, 11.1 wt% 1M HCl, and 76.8 wt% DI water) were prepared by first mixing APP in water until a homogenous suspension was obtained. NaOH was then added and the solution was mixed until completely dissolved (a noticeable increase in viscosity occurs). Finally, HCl was added to reduce viscosity. All components were added in the amounts mentioned relative to the final solution mass. This method was adapted from a previously established procedure [80]. Solutions of 0.1 wt% CH were prepared in pH 1.7 water (adjusted with 1M HCl). 1 wt% VMT suspensions were prepared in DI water. PAA, CH, and VMT mixtures were rolled for 24 hrs before use, while APP was used immediately upon preparation. CH and APP solutions were altered to pH 5 using 1M NaOH and VMT was used unaltered at pH 7.5. All foam samples were thoroughly rinsed in DI water, dried at 70°C, and stored in a dry

box prior to coating. LbL assemblies were fabricated on PUF in ambient conditions using the process depicted in Figure 3.1. After the rinsing steps, towel wringers were used to remove excess water before dipping in the next solution. Each deposition solution had a designated rinse bucket to avoid cross contamination and rinse water was replaced after every 10 bilayers. After depositing the desired number of layers, the foam was dried at 70°C for 3 hrs and then stored in a dry box prior to testing. Weights were taken 10 min after being removed from dry box, both before and after coating, to determine the weight percent of coating added to the foam.

3.2.3 Thermal Stability, Flammability and Combustion of Foam

A butane hand torch (TriggertorchTM MT-76K, Master Appliance Corp., Racine, WI) was used to apply a direct flame (approximately 1300°C) to foam samples to screen coating effectiveness. The foam was placed on top of a metal grating inside a fume hood, at a height of 25.4 cm, and exposed to the torch flame for 10 s. The flame was held perpendicular to the center of the foams side wall. Cone calorimetry was performed at the University of Dayton Research Institute (UDRI) using a FTT Dual Cone Calorimeter at one heat flux (35 kW/m^2) with an exhaust flow of 24 L/s. This testing followed the standardized cone calorimeter procedure (ASTM E1354-11). Samples were 10 x 10 x 2.5 cm and were wrapped in aluminum foil on one side as per the ASTM E1354 standard. Data collected carried an error of ±10% and was calculated using a specimen surface area of 100 cm^2. All samples were tested in triplicate.

3.2.4 Electron Microscopy

Surface images were acquired using a JEOL JSM-7500F field emission SEM. Each sample was first sputter coated with 4 nm of Pt/Pd to reduce charging in the beam. Cross-sectional images were obtained using an FEI Tecnai G2 F20 TEM, with a

ZrO_2/W Schottky field emitter gun, at 200kV acceleration voltage and a Gatan Tridiem GIF-CCD. Samples were prepared by embedding a small section of the PUF in Epofix (EMS, Hatfield, PA) resin overnight and cutting approximately 90 nm thick sections, using an Ultra 45° diamond knife (Diatome, Hatfield, PA), onto 300 mesh formvar and carbon coated copper Lacey grids.

3.3 Results and Discussion

Fire retarding behavior was evaluated as a function of CH/APP bilayers stacked on top of CH/VMT bilayers. The layer-by-layer assembly process is depicted schematically in Figure 3.1. The cartoon of the final stacked coating looks a lot like the real system shown in Figure 3.2. This TEM cross-sectional micrograph is from the thicker part of the 290-1005 nm range observed on the surface of foam coated with 4 BL CH/VMT and 20 BL CH/APP. The large variation in thickness was found though imaging many sample sets and is attributed to the dipping and squeezing deposition on foam. Some of the intumescent is likely transferred when two pore walls of the foam touch during squeezing.

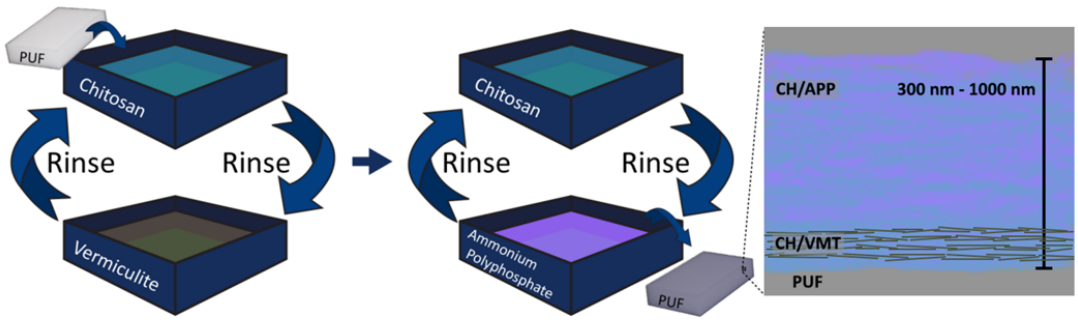

Figure 3.1: Schematic of layer-by-layer deposition steps, showing clay-based bilayers deposited, followed by intumescent layers. The cartoon at the right shows the final stacked coating on foam.

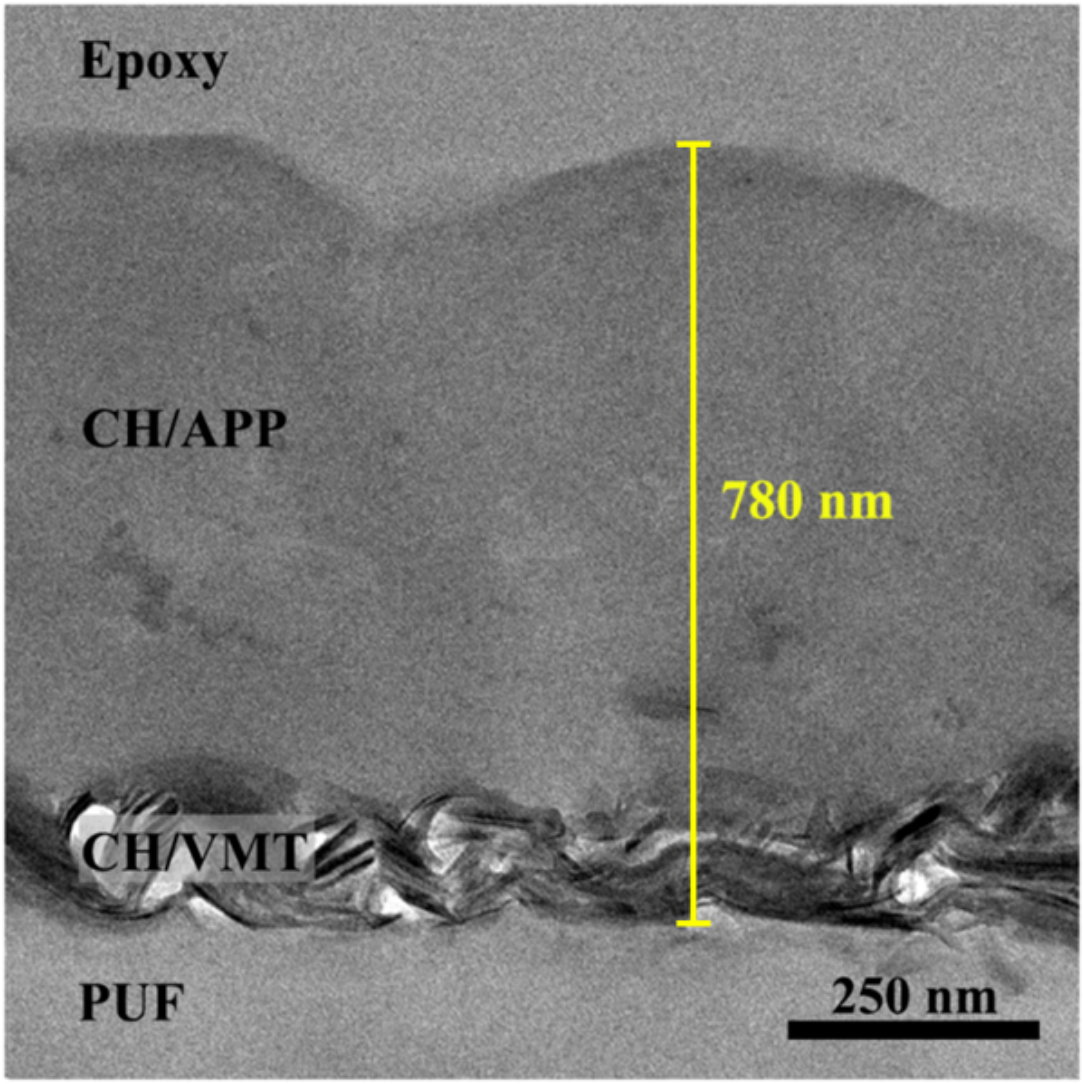

Figure 3.2: TEM micrograph showing a cross section of the 4 BL chitosan/clay and 20 BL chitosan/ammonium polyphosphate stacked coating. The yellow line highlights the thickness of the stack.

The flammability of coated and uncoated foam was initially evaluated using a butane torch, as shown in Figure 3.3. Burn time, remaining residue, shape retention, and microstructure of torched samples were measured. Uncoated foam exhibited typical polyurethane behavior by igniting upon exposure to the flame and then melting.

As the foam melted, drips of molten polymer formed a melt pool that ignited cotton beneath. This melt drip phenomenon is a major concern due to its propensity to spread fire to flooring, drapes and neighboring furniture.

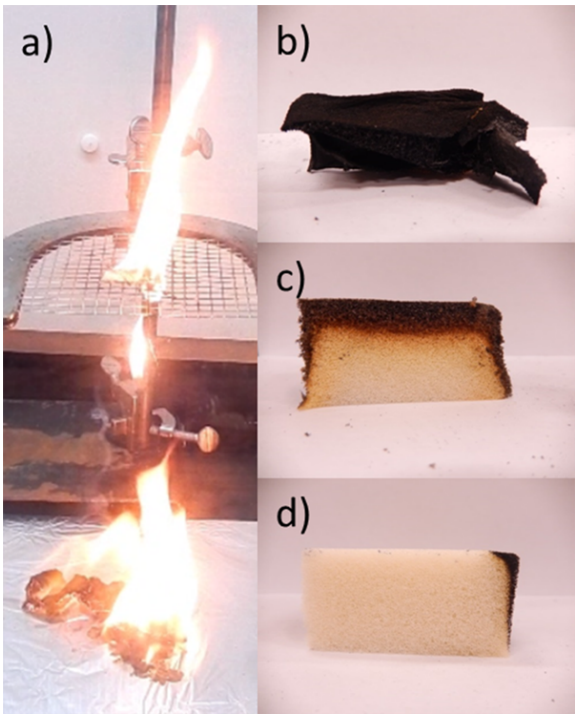

Figure 3.3: Digital images of uncoated and coated polyurethane foam after exposure to the flame from a butane torch. Uncoated polyurethane (a) is shown dripping molten polymer 26 s after torch exposure, igniting an underlying bed of cotton. Each coated sample is shown as a cross-section: (b) 20 BL CH/APP, (c) 4 BL CH/VMT, and (d) stacked coating. In each image, the right side of the foam was exposed to the butane torch for 10s.

Foam coated with only 20 BL CH/APP did not prevent the complete decomposition of the foam because the PUF began to collapse and degrade prior to activation of the intumescent charring. This coating did slow the burn and reduce melt dripping. It is very important for intumescing systems to activate before the substrate

degrades to allow the char layer to trap evolved gases and form a swollen thermal shield that separates the heat/flame from the fuel source. Figure 3.4(a) and (b) shows SEM images of intumescent coated foam after exposure to the torch. The coating is completely collapsed with no evidence of remaining polyurethane. The remaining char is riddled with holes that were formed by the early release of gasses that would have acted as the blowing agent if this intumescent system was able to activate before the degradation and volatilization of the foam substrate. This type of intumescent coating is able to effectively protect cotton, which has a much higher degradation temperature [36, 11].

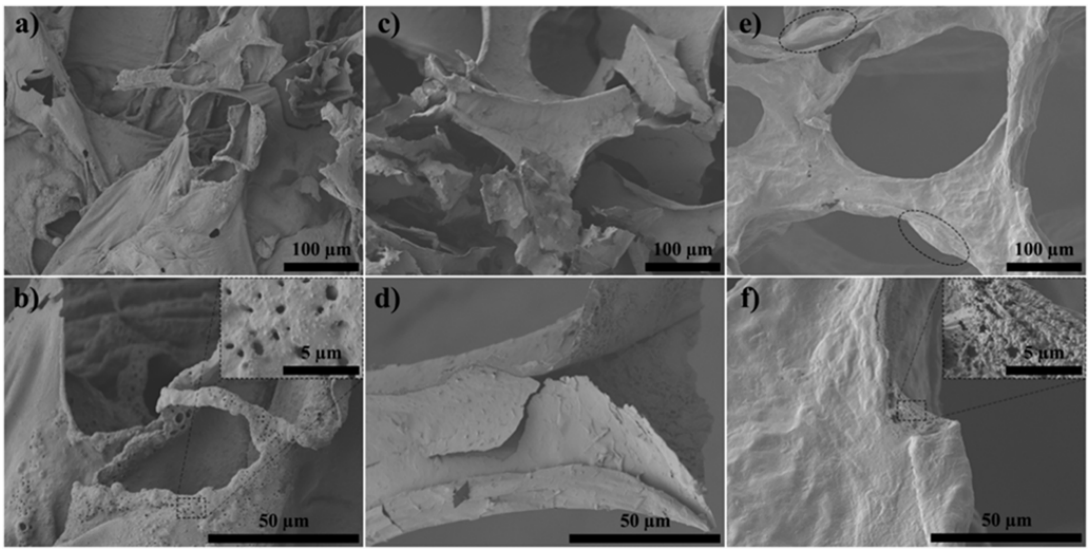

Figure 3.4: SEM micrographs of coated polyurethane foam after exposure to a butane torch flame for 10s. Each sample was taken from the region directly burned by the flame: (a-b) 20 BL CH/APP, (c-d) 4 BL CH/VMT, and (e-f) stacked coating.

When the foam is coated with four bilayers of chitosan and vermiculite, a variation of previously studied PUF flame retarding coatings [117, 118, 119, 67], an inorganic

thermal shield was formed upon exposure to the torch. This thin clay-based coating prevented complete decomposition of the foam, with samples retaining 60% of their weight. Figure 3.3(c) shows that the flame spread across the outer surface of the foam, but did not completely penetrate the interior. A gradient can be seen through the foam, transitioning from black char to a deep yellow color to white undamaged foam. The yellow color in the transition from charred to pristine foam is believed to be from both oxidative and thermal decomposition of the foam [161]. This is indicative of charred layers that form a thermal barrier that prevents the heat of the fire from reaching the interior of the foam. This coating shows significant improvement over uncoated PUF and that coated with the intumescing system, but the flashover still presents a hazard. SEM images of the remaining char for this coating (Figure 3.4(c) and (d)) show a well preserved coating that formed a shell of the original foam structure. This clay coating was thought to be able to provide enough protection to allow time for the intumescing coating to activate before the PUF degraded, thus preventing flashover and providing greater material retention.

Intumescing layers were stacked on top of the 4 BL CH/VMT to prevent the foam from collapsing before the intumescent could activate. Figure 3.3 shows that combining the two systems prevented flashover and reduced the overall flammability of the polyurethane. Increasing the amount of intumescing coating on top of the clay nanocoating resulted in an increased percentage of foam that remained unharmed by the torch. With 20 CH/APP bilayers, an average of 86 wt% foam residue remained (with a standard deviation of 8 wt%). This deviation is a result of some samples not igniting at all (97 wt% residue) and only charring where the flame touched the sample. In the worst case, the flame spread over the top surface and parts of the sides before extinguishing ($\sim$74 wt% residue). This flame-stopping ability is a result of the formation of an intumescent char layer that arrests further burning. A transition

can be seen from the charred foam to the undamaged foam in Figure 3.3(d), which provides visual evidence of a thermal gradient similar to that seen in the clay coating (Figure 3.3(c)), but on a smaller scale. Prior to further testing it was speculated that the minimal degradation below the thin char layer was due to the combination of the inorganic barrier and a successfully activated intumescent layer. Figure 3.4(e) and (f) shows microscopic images of the stacked coating from the charred region to show that the coating did exhibit swelling. It should be noted that this coating experienced slight shrinking in the char that causes the structure to appear dehydrated. The inset of Figure 3.3(f) shows a good example of the nanointumescent behavior. This location on the edge of the strut appears to have been cracked, allowing for the isocyanates and other foam volatiles to act as additional blowing agents that generated the nanoscale bubble formation. Bubbles were also seen in other regions, but the general structure showed smoother surfaces with a more large-scale swelling of the coating. Figure 3.5 shows an image taken deeper in the foam (at the transition from the charred to yellow region) show a better representation of the swelling prior to the total decomposition of the underlying polyurethane foam.

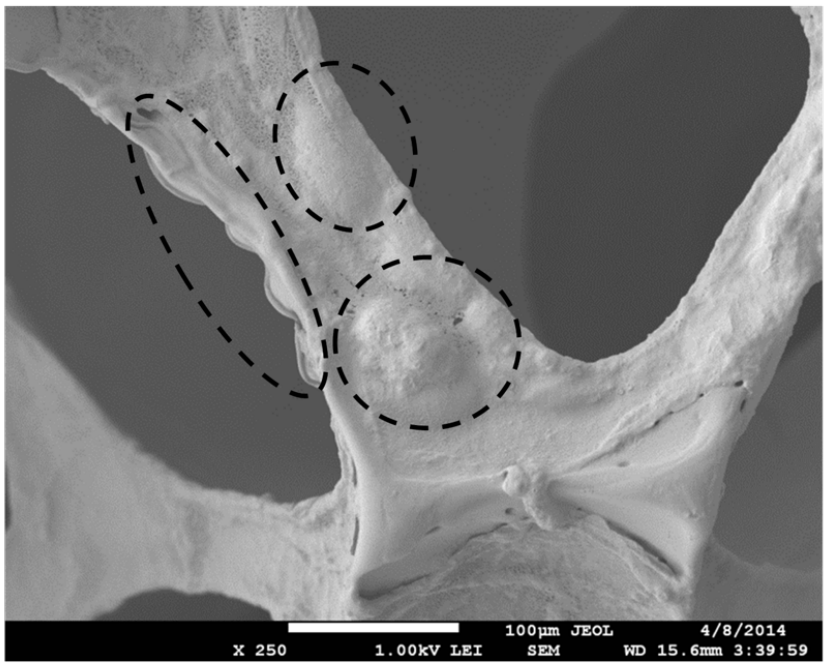

Figure 3.5: SEM micrograph of polyurethane foam coated with 20 BL CH/APP on 4 BL CH/VMT. The circles are highlighting the swollen coating after exposure to the heat from the torch in the region behind the char.

In addition to qualitative torch testing, cone calorimetry (ASTM E-1354-07) was performed on control and coated foam in an attempt to quantitatively assess the thermal barrier properties of this stacked thin film assembly [162, 163]. Foams coated with only 4 BL of CH/VMT, only 20 BL of CH/APP and a combination of 4 clay bilayers with 10, 15, and 20 BL of intumescent on top, were evaluated and compared to uncoated foam. The PUF was exposed to a constant heat flux, while heat release rate (a measure of a materials flammability) was measured [164]. Figure 3.6 shows the heat release rate as a function of time for the various coating combinations. Following ignition, heat quickly transferred through the uncoated foam, forming

a fully developed fire. The control foam collapsed into a pool of molten polymer as the polyurethane began to degrade. The smaller peak heat release (around 25 s) originated from the isocyanate/polyol decomposition and then the burning melt pool quickly generated a much larger peak heat release rate (HRR). This high peak HRR then rapidly declined as the material made the transition into combustible volatiles. Only a stain on the foil test pan remained after completion of the test.

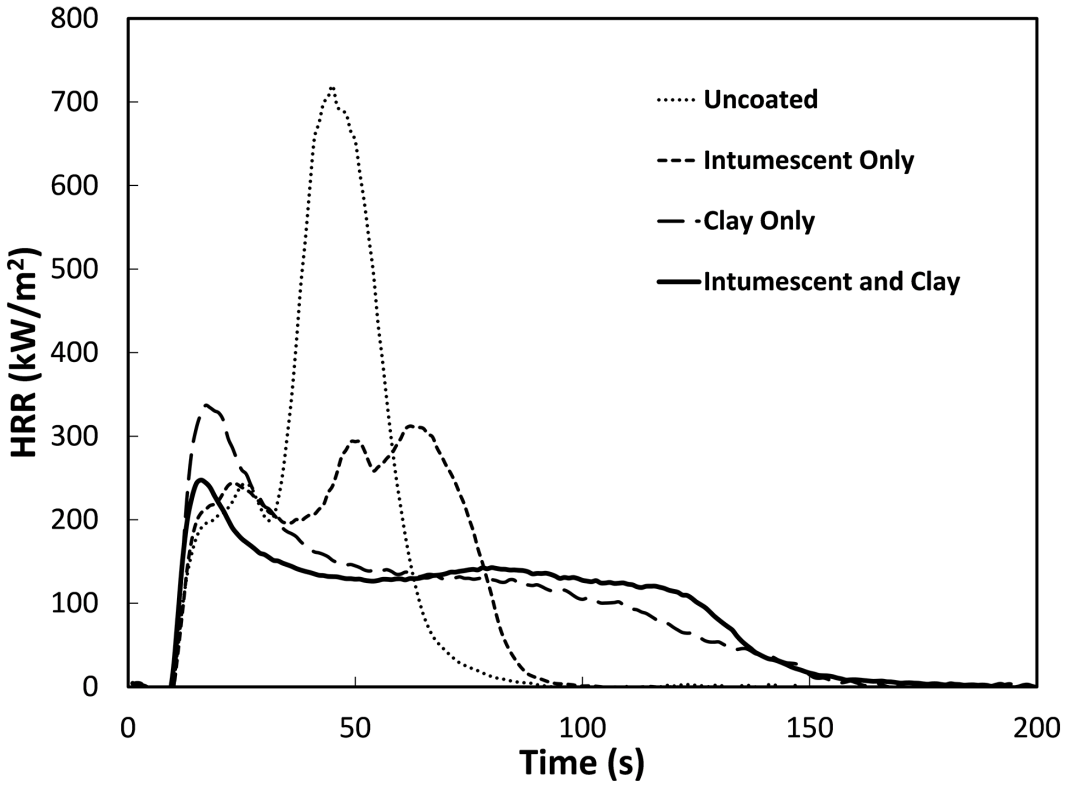

Figure 3.6: Heat release rate as a function of time for coated and uncoated foam.

Foam coated with only intumescent (20 BL CH/APP) exhibited a heat release rate trend similar to the uncoated foam. An initial peak in HRR, comparable to the uncoated sample, was followed by two considerably lower peaks. This reduced peak

HRR is likely due to the lack of liquefaction observed with the torch exposure. The coating formed a thin, crisp char that slowly shrunk as the sample burned, leaving only 34.5 wt% residue after it extinguished. This sample exhibited the greatest reduction in total heat release as well as the greatest total smoke release, shown in Table 3.1. It is possible that the increased smoke release is correlated to the lower total heat release stemming from incomplete degradation of the polymer components. This could be an effect of the polyurethane degrading within the confined char of the coating rather than in the burning liquid pool formed by the uncoated foam.

Table 3.1: Cone calorimeter results for polyurethane foam with and without nanocoatings.

	Coating wt% (%)	pkHRR (kW/m^2)	Avg HR (kW/m^2)	THR (MJ/m^2)	TSR (m^2/m^2)	MARHE (kW/m^2)
Uncoated	0	735	273	19.5	146	318
20 BL CH/APP	16.1	333	201	16.5	312	212
4 BL CH/VMT	3.1	337	132	18	63	188
Stacked Coating	19.9	250	126	17.4	206	139

Foam coated with only clay (4 BL CH/VMT) was the only system to show a reduction in smoke release, which is commonly observed with clay-based LbL coatings [117, 118]. Heat release rate was typical of previously studied coatings, showing rapid ignition and char formation, with little shrinkage. Clay-only coatings are also characterized by a quick rise to the peak heat release rate, which is slightly larger than the initial peak of the uncoated foam, followed by a steady decline until extinguished. This higher initial peak is believed due to chitosan between the clay in the coating, or

from the clay itself. Clay has been suggested to initially promote combustion through catalytic sites until the protective shell is formed [77]. This result also suggests the coating is activating before the PUF, which is ideal. Early activation minimizes the contribution of polyurethane to the fire by quickly forming the protective barrier, reducing the overall fire threat.

The stacked coating displayed a HRR trend with traits from both individual coatings (clay and intumescent). Samples coated with 10, 15 and 20 BL of chitosan and APP were tested, but due to the similarity of the results and small progressive trend showing improvement with higher intumescing bilayers, the combination containing 20 BL CH/APP (with 4 BL CH/VMT underneath) is the focus here. The peak HRR occurred quickly and the peak is narrow, similar to the clay-only coating, but the lower value is more similar to the initial peaks for the uncoated and intumescent-only samples. This was followed by a low plateau and what could be a second very broad peak just before the foam extinguished. It appears that the char formed after ignition is eventually burned through and the remaining protected polymer is consumed. The reduction in the peak HRR between the clay-only and stacked samples suggests that the clay layers are not impacted initially, or else there would have been a greater initial HRR peak. This further suggests that the lower peak heat release rate is related to the intumescing layers.

In summary, combining 4 BL of chitosan and clay with 20 BL of chitosan and ammonium polyphosphate resulted in a 66% reduction in peak HRR for polyurethane foam. This is one of the greatest peak reductions ever reported for an LbL coating on polyether-based PUF. While the 20 BL intumescent-only coating had the greatest reduction in total heat release, the stacked system still reduced the total heat released by nearly 11%. The maximum average rate of heat emission (MARHE) is reduced in all coated samples, with the greatest reduction observed in the combination coating

(56%). The MARHE is a useful parameter for ranking materials in terms of ability to support flame spread to other objects [165], meaning the clay-intumescent stack is the least likely to spread a fire to another object. This unique combination of two flame retardant mechanisms in a single nanocoating serves to render a commonly used material in home furnishings largely inflammable. This same type of coating could potentially be used for other commonly used materials that are prone to melt dripping in a fire (e.g., nylon and polyester fabrics).

3.4 Conclusion

Polyurethane decomposes into highly flammable melt-pools, when exposed to fire, and then releases toxic gases [161]. This melt pool formation can be completely avoided with a protective coating containing clay that provides a ceramic thermal shield [117, 118, 119, 67]. This study successfully showed that the combination of two multilayer recipes, stacked on top of one another, can provide a synergistic effect and greatly improve the flame retardant properties of PUF. With four clay layers and 20 intumescing bilayers, a peak heat release reduction of 66% was realized. This is among the greatest reductions reported for polyurethane foam. This stacked coating also showed a 56% reduction in the MARHE, suggesting the coated foam would be less than half as likely to spread a flame to a new source in a real fire scenario. This coating did produce more smoke, so it will be important to assess the toxicity and origin of this smoke relative to that of current flame retardants. This study highlights the power and versatility of layer-by-layer nanocoatings for flame retardant purposes. Stacking layers to combine mechanisms of action provides the opportunity to render nearly any substrate antiflammable. This is especially important for materials whose processing and mechanical behaviors are adversely influenced by adding flame retardant filler to the bulk.

4. CARBON NANOTUBE MULTILAYER NANOCOATINGS PREVENT FLAME SPREAD ON FLEXIBLE POLYURETHANE FOAM*

4.1 Introduction

In the case of flame retardant foam, layer-by-layer coatings prepared with layered silicate materials (i.e., clays) act as a thermal shield [1, 122]. These nanocoatings significantly reduce heat release rate and smoke release of polyurethane foam. More recently, assemblies have been prepared with multi-walled carbon nanotubes (MWNTs) and titanate nanotubes [12, 166]. All studies of LbL-coated foam report the elimination of melt dripping and reduction of heat release rate. Heat release rates measured via cone calorimetry are useful for determining the viability of coatings or fillers to reduce flammability [163]. Other testing methods, such as vertical and horizontal flame tests, focus on the ignitability of samples as well as the flame propagation rate and burn time. These are important metrics linked to real world fire scenarios. Most LbL flame retardant coatings for polyurethane are char forming and act in the condensed phase, so they generally extend burn time even as they reduce heat release. Few of these coatings have been able to withstand the rigorous open flame tests required for various applications (e.g., British Standard 5852 Crib 5 test in the UK).

This section describes a nanotube-based coating that exhibits vast improvement in cone calorimetry testing, but also dramatically reduces flame spread and burn time in open flame tests. Pyrene-modified branched polyethylenimine (PEI-Py), poly(acrylic acid) (PAA), and multi-wall carbon nanotubes (MWNT), shown in Figure 4.1, were used to create a flame suppressing nanocoating on polyurethane foam.

*Reprinted with permission from Reference [37]. Copyright 2015, WILEY-VCH Verlag GmbH & Co. KGaA, Weinheim.

These LbL coatings not only prevent melt dripping and maintain structural integrity of foam after exposure to a flame, they reduce heat release rate and total smoke release. One variation of the coating is able to self-extinguish during horizontal and vertical burn testing, which has never before been demonstrated with foam using LbL technology. This MWNT-based coating provides a viable alternative to brominated additives for open-celled foam.

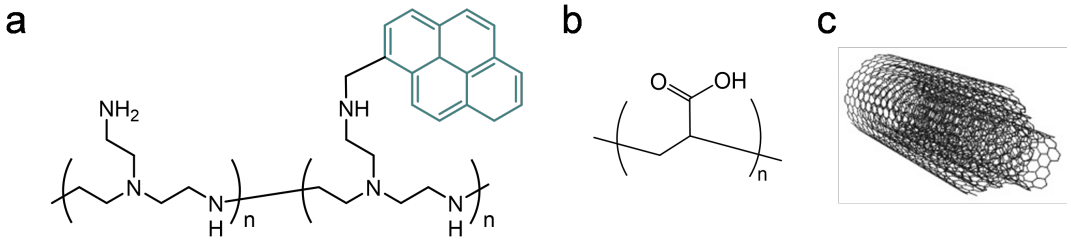

Figure 4.1: Chemical structures of (a) pyrene-modified branched polyethylenimine, (b) poly(acrylic acid) and (c) multi-wall carbon nanotube.

4.2 Experimental

4.2.1 Materials

Poly(acrylic acid) (PAA, M_W=100 kg/mol, 35 wt% in water) and branched polyethylenimine (PEI, M_W=25 kg/mol) were purchased from Sigma-Aldrich (Milwaukee, WI). Polyethylenimine with pyrene groups (PEI-Py) was synthesized via a reductive amination reaction [167]. Multi-walled carbon nanotubes (MWNT) were obtained from Bayer MaterialScience (12-15 nm outer and 4 nm inner wall diameter, 1+ μm length, C $\geq$ 95 wt%; Leverkusen, Germany). All aqueous solutions were prepared with 18.2 MΩ deionized water and rolled for 12 h. Solutions of 1.0 wt% PAA, which functioned as a surface treatment for polyurethane foam [127], were altered

to pH 2 with 2 M HNO_3 prior to deposition. MWNT (0.1 wt%) were dispersed in 0.1 wt% PAA solution (altered to pH 4 with 1 M NaOH) and 0.1 wt% PEI-Py solution (altered to pH 9 with 1 M NaOH), followed by tip sonication (Model VCX750; Sonics & Materials, Inc., Newtown, CT) at 50% amplitude for 1 h. Note: a 1200.5 g solution is composed of 3.43 g PAA solution, 1.2 g MWNT, and 1195.37 g deionized water. Solutions were used immediately after sonication.

4.2.2 Substrates

Silicon wafers (P-doped, single side polished (1 0 0), 500 nm thick) were purchased from University Wafer (South Boston, MA) and used to obtain thickness measurements with a profilometer. A quartz crystal microbalance (QCM), utilizing 5 MHz gold/titanium-electrode quartz crystals (Maxtek, Inc.; Cypress, CA), was used to obtain mass deposited per layer. Polyurethane foam (type 1850, 1.75 lbs/ft^3 density) was purchased from Future Foam (High Point, NC).

4.2.3 Layer-by-Layer Deposition

In preparation for deposition, silicon wafers and QCM crystals were exposed to oxygen plasma to ensure adequate negative surface charge. All two-dimensional substrates were coated using a homebuilt robotic coating system [168], where substrates were rinsed with deionized water and dried with filtered air following each dip into aqueous polyelectrolyte suspensions. Fabrication of the anti-flammable multilayer thin film on 3D substrates was applied by hand, where flexible polyurethane foam was fully compressed three times in each solution (ensuring uniform compression across the surface) and excess material was removed as foam was wrung out through towel wringers. All foam was submerged in a 1.0 wt% PAA solution for 30 sec in order to enhance the negative surface charge on the foam prior to the deposition of the nanocoatings. During this step, the carboxylic groups present on the polyanion

have the ability to hydrogen bond with the polyurethane surface. Treated substrates were then dipped into the PEI-Py and PAA-based solutions for 5 min each. All subsequent layers were deposited with 1 min dip times. Deposition solutions were changed every third bilayer in order to avoid depletion of the carbon nanotubes. Foam samples were placed in a 70 °C oven for 3 h immediately following deposition.

4.2.4 Thin Film Characterization

A P6 profilometer (KLA-Tencor; Milpitas, CA) was used to determine LbL film thickness. A Maxtek Research Quartz Crystal Microbalance (Cypress, CA) was used to obtain mass deposition of each individual layer on Au/Ti crystals. Coated polyurethane substrates were imaged using a field-emission scanning electron microscope (FESEM) (Model JSM-7500F, JEOL; Tokyo, Japan). Freeze fractured samples were placed on an aluminum stub and sputter coated with 4 nm of platinum/palladium alloy prior to imaging. Post-burn cone samples were not sputter coated when imaged using SEM.

4.2.5 Thermal Characterization

Thermal stability of control and coated polyurethane samples ($\sim$ 30 mg) and individual chemical components ($\sim$ 15 mg) were evaluated using a Q-50 thermogravimetric analyzer (TA Instruments; New Castle, DE) in an air atmosphere under a heating ramp rate of 10 °C/min, from room temperature up to 600 °C. Cone calorimetry was operated according to ASTM E-1354-12 at the University of Dayton Research Institute using a FTT Dual Cone Calorimeter (exhaust flow of 24 L/s). Samples (10 x 10 x 2.5 cm) were placed in an aluminum foil pan and exposed to a heat flux of 35 kW/m^2, with a data uncertainty of $\pm$10%. Horizontal flame testing was operated according to ASTM standard D 5132-04 in an HC-2 model horizontal flame cabinet (Govmark; Farmingdale, NY). Samples (10 x 32 x 1.3 cm) were

placed between U-shaped, non-corroding, metal frames and exposed to a 38 mm perpendicular flame for 15 sec to measure flame speed. Vertical flame testing was operated according to ASTM standard D6413-08 in a 701-S model vertical flame cabinet (Govmark; Farmingdale, NY). Samples (8.9 x 30.5 x 1.3 cm) were hung vertically in metal frames and exposed to a flame for 12 sec to measure vertical flame resistance. Samples were examined using a UV Black Ray B100 series light (365 nm) (UVP; Upland, CA) to analyze burn distance of the coated samples after horizontal and vertical burn testing.

4.3 Results and Discussion

4.3.1 Construction and Characterization of LbL Films

Layer-by-layer deposition of thin films prepared with polymer-stabilized nanoparticles is strongly influenced by pH and particle dispersion method. Previous studies have shown that polyethylenimine grows exponentially with poly(acrylic acid) under appropriate pH conditions. [169]. This occurs when the charge density of these weak polyelectrolytes is low, causing them to assume more coiled conformations. The exponential growth arises from polymer interdiffusion (at pH 10 for PEI and pH 4 for PAA). In this study, PEI was modified with pyrene, using a previously described method [167], in an effort to improve stability of the carbon nanotubes in the cationic solution as well as increase char formation. It was determined that the modified PEI-Py deposited thickest at pH 9 due to removal of some chargeable groups during the pyrene modification. Thicker growth reduces the number of layers required to achieve adequate film performance, thereby reducing processing time and complexity.

The method of nanoparticle dispersion/stabilization holds equal importance to deposition pH conditions. It was shown by Jan et al. that growth and resistance of

carbon black assemblies was altered by adjusting which solution was used to stabilize the carbon black for deposition [170]. A similar study using PEI-functionalized MWNT deposited discrete MWNT layers between PAA and PEI layers, forming a trilayer system [166]. This trilayer system did not provide optimal incorporation of MWNT into the system. In the present study, MWNT was successfully stabilized in both PEI-Py and PAA using tip sonication. The optimal flame retardant coating was determined using four recipes. Each recipe is denoted $[\text{PEI-Py/PAA}]_X$, where X denotes the number of bilayers deposited. Recipe A [PEI-Py+MWNT/PAA+MWNT] represents the maximum opportunity for MWNT incorporation. Recipe B [PEI-Py/PAA+MWNT] and Recipe C [PEI-Py+MWNT /PAA] only have nanotubes in one of the two deposition solutions, while Recipe D [PEI-Py/PAA] is the thin film control without any carbon nanotubes.

The open-celled polyurethane foam used to evaluate effectiveness of the MWNT-based coatings is a three-dimensional substrate that has high surface area and non-uniform curvature. In order to characterize thickness and mass deposition it was necessary to first apply these assemblies onto two-dimensional, flat substrates (silicon wafers and Ti-Au plated quartz crystals). Silicon wafers were used to measure thickness via profilometry, as shown in Figure 4.2(a). All of the recipes (A, B, C, and D) exhibited similar growth trends, with a slow initial growth for the first three bilayers that transitioned to a thicker linear growth regime after four bilayers. At 9 BL, thicknesses ranged between 480 and 620 nm, with greater thickness linked to an increased amount of MWNT in the film. Based on thickness, it appears that recipes A and B have the greatest inclusion of MWNT. Stabilizing MWNT in PEI-Py (Recipe C) generates only a minimal growth increase over the nanotube-free system (Recipe D). Based on mass deposition per layer, as determined by quartz crystal microbalance (Figure 4.2(b)), Recipe B was the most promising (i.e., deposited the

most mass). It has been shown for PEI/PAA assemblies that growth eventually becomes diffusion limited and mass deposited per layer reaches a steady-state maximum [171]. Recipe A takes the most layers to reach the diffusion-limited growth regime because MWNT limits diffusion between the two polymers. PAA seems to interact more strongly with MWNT than PEI-Py (i.e., PAA+MWNT layers contain more nanotubes), indicated by a sharp increase in mass per PAA layer when MWNT is included. In Recipe B, the PEI-Py is able to interdiffuse with the PAA+MWNT layers allowing for the quickest transition into the linear growth phase, where overall MWNT is maximized per bilayer.

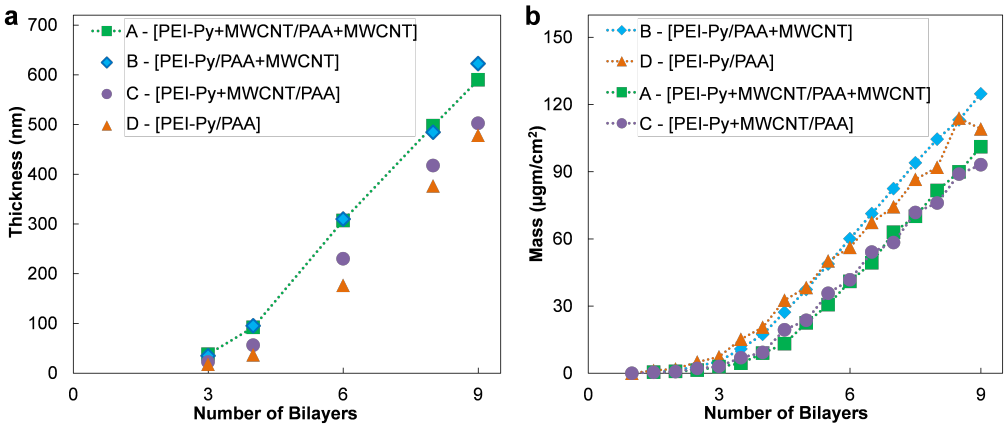

Figure 4.2: (a) Thickness and (b) mass deposition of LbL thin films as a function of the number of bilayers deposited.

Coupling the mass with the thickness reveals that Recipe B is the second densest of the films at 2.0 g/cm^3, only surpassed by the control film (Recipe D), which was much thinner (with a density of 2.28 g/cm^3). The nanotube-free control system has a higher density because of increased interactions between the polymer layers,

while higher density of the other films is likely due to a greater inclusion of MWNT in the film. As mentioned earlier, the properties of particle-containing thin films can be altered by the way in which the particles are introduced into the system, using cationic or anionic suspension in this case. Particle content in a given film is expected to alter the properties of that film. Greater multiwalled carbon nanotube concentration is expected to improve thermal stability and flame retardancy of the foam substrate.

4.3.2 Thermal Stability

Thermal stability of 6 BL coated and uncoated polyurethane foam was evaluated with thermogravimetric analysis. As shown in Figure 4.3, there was little difference in the initial degradation temperature of the polyurethane with or without coating. At 285 °C there is a deviation in the degradation pathway of the uncoated foam, as evidenced by a decreased rate of mass loss. Typical polyurethane degradation occurs in two or three steps [172, 173, 174, 175, 176]. The first step is the degradation of hard segments, forming isocyanates and alcohols, primary or secondary amines and olefins, and carbon dioxide. The second and third steps correspond to the thermal decomposition of soft polyol segments. It is likely that LbL coatings prevent formation of a melt pool during degradation, which creates the difference in mass loss observed in Figure 4.3. Despite exhibiting faster degradation initially, MWNT-containing LbL films maintain 10-15% higher weight retention during the soft segment degradation phase due to the MWNT stability up to approximately 475 °C. Using the [PEI-Py/PAA] data as a baseline at 475 °C suggests that Recipe A contains 44 wt% MWNT, Recipe B contains 38 wt% MWNT, and Recipe C contains 33 wt% MWNT. This assumes any mass remaining greater than the [PEI-Py/PAA] film is purely MWNT. Beyond 550 °C, all LbL coatings begin to degrade completely,

with Recipe B having the highest thermal stability in this region (up to 565 °C). The nanocoatings are slowing the mass loss rates as chars are set up, which may also be changing some of the decomposition chemistry of the polyurethane.

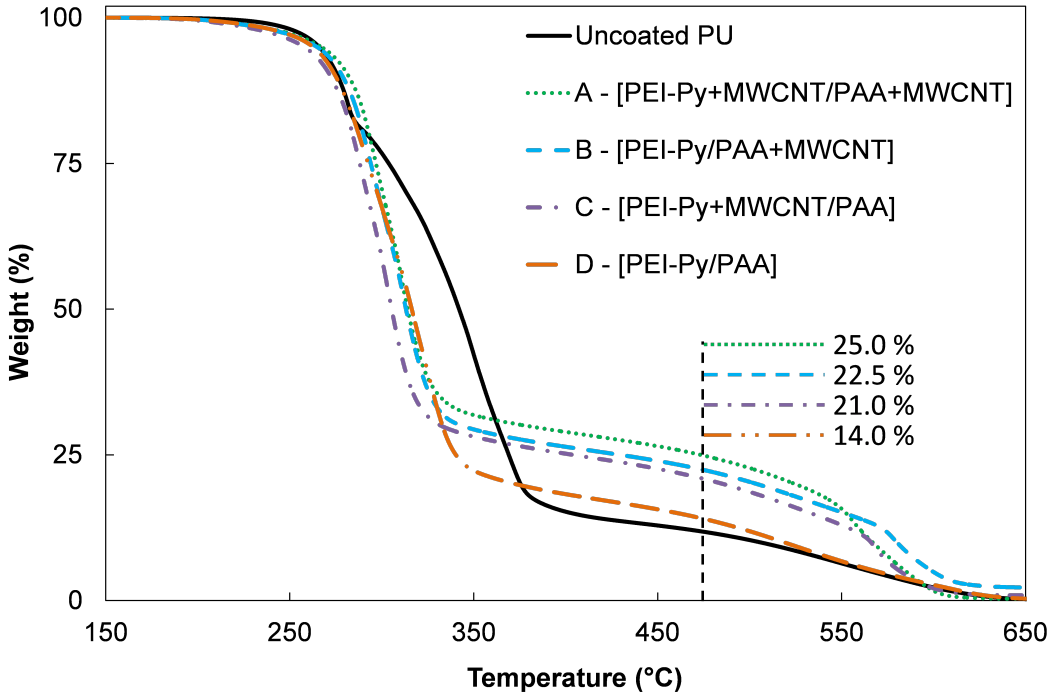

Figure 4.3: Mass loss as a function of temperature during heating of uncoated foam and foam coated with 6 BL of Recipes A-D. Weight remaining at 475 °C is marked because it is used to calculate weight loading of MWNT in the coatings.

4.3.3 Flame Retardant Behavior of LbL Films

Cone calorimetry was used to quantitatively assess fire performance by measuring time to ignition (TTI), peak heat release rate (pkHRR), total mass loss, total heat release (THR) and total smoke release (TSR) using oxygen consumption calorimetry [163]. Heat release is important in fire safety because it has been found to be the

most important predictor in fire loss events and determining if people have enough time to escape a burning room/compartment [164]. In this case, foam is exposed to a set heat flux, ranging from 10-100 kW/m^2, designed to resemble heat intensity experienced in a fire situation and the heat released is measured as a function of time. The filler-rich barrier, in this case carbon nanotubes, forms after the sample is exposed to a critical temperature and is able to delay mass loss corresponding to the lower heat release rate over a longer period of time. As mass loss is decreased, the amount of fuel consumed in the flame decreases and a lower HRR is achieved. The flammability properties of this barrier largely depend on the concentration and dispersion of nanofiller [177, 178]. Figure 4.4 shows the heat release curves tested at 35 kW/m^2 for uncoated polyurethane and for each of the four recipes used in this study, as well as post burn scanning electron microscope (SEM) images for Recipes B and D after exposure to cone testing. The SEM images reveal the ability of the MWNT-containing samples to retain the foam structure at the microscopic scale after exposure to fire. Uncoated polyurethane (and the samples coated without MWNT) show two evident peaks, with the first peak corresponding to the pyrolysis of diisocyanate compound and the second corresponding to the polyol pyrolysis [172, 179]. Recipe D only provided a small reduction in the pkHRR (∼16%), but as shown in Table 4.1, [PEI-Py/PAA]$_6$ increased HRR, THR, and TSR by 4%, 2.6%, and 24%, respectively (relative to uncoated polyurethane foam). When MWNT is added to the system, all three variations showed dramatic reduction of pkHRR (of at least 67%) and completely eliminated the second peak observed in both uncoated and polymer-only coated samples. Clearly the addition of MWNT and the char formation barrier formed is responsible for the reduction in flammability measured by the cone calorimeter.

The MWNT bring another advantage to improving the fire safety of the PU

foam by preventing the dripping/melt flow during burning. This is evident when looking at the char remaining after the test is complete. Uncoated PU melts within the aluminum pan and this melt pool undergoes rapid combustion, releasing a high amount of heat. Coated samples with MWNT have a low heat release rate and strong char formation that maintained the original structure, which suggests these nanocoatings prevent the melt dripping phenomenon. Lack of melt dripping is helpful when trying to prevent the spread of a flame and prevent radiant heat feedback from burning pool fires that is observed with polyurethane foam in real-world fires [180]. The MWNT-containing samples also exhibit a major improvement in total smoke release, reducing it as much as 80%. This is one of the highest reported smoke reduction values for LbL flame retardant films on polyurethane [12, 1, 123, 122]. Reducing smoke release can reduce the risk of injury in fire situations by allowing for better visibility to reach exits and also lowering irritant gases that can exacerbate the toxicity of other gases commonly released in fires such as carbon monoxide. Having the lowest weight addition of 18 wt% (similar to common flame retardant additives), further testing (flame spread, open flame testing) was focused on Recipe B [PEI-Py/PAA+MWNT] because weight added is an important metric (everything else being equal) when thinking about efficacy and minimizing processing steps.

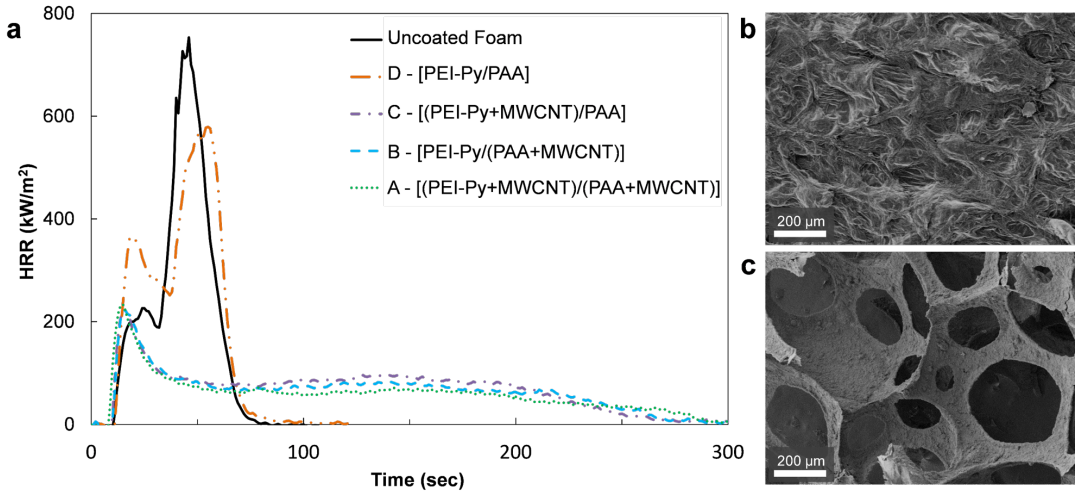

Figure 4.4: (a) Cone calorimeter heat release rate as a function of time (under 35 kW hr heat flux) for uncoated polyurethane foam and foam coated with 6 BL of Recipes A-D. The SEM images show samples coated with (b) recipe D and (c) Recipe B after exposure to cone testing.

Table 4.1: Weight addition, peak heat release rate, total heat release and total smoke release for 6 BL coated polyurethane foam.

Recipe	Wt Addition (%)	pkHRR (kW/m^2)	THR (MJ/m^2)	TSR (m^2/m^2)
Uncoated	—	727 ± 51	19.5 ± 0.6	147 ± 6
A	31.8 ± 0.5	238 ± 14	17.7 ± 1.4	30 ± 2
B	17.7 ± 0.3	235 ± 11	19.0 ± 1.2	33 ± 4
C	22.9 ± 0.1	232 ± 14	18.8 ± 0.8	35 ± 3
D	11.8 ± 0.2	610 ± 42	20.0 ± 0.4	183 ± 9

Horizontal flame testing (HFT) is used to monitor the ability of a flame to spread across samples. Uncoated polyurethane and 3 and 6 BL [PEI-Py/PAA+MWNT] samples were horizontal burn tested to measure flame speed and to determine the thin films ability to eliminate polyurethane melt dripping. The 355 mm test holder is divided into 3 sections (38 mm, 255 mm, and 64 mm), as shown in ASTM standard D5132-04. Burn rate is a measurement of the length the flame travels (in the 255 mm segment) divided by the time it took the flame to travel the measured distance. Since the flame did not reach the first scribed line in any of the 6 BL test runs, burn rate for all samples is redefined as the measurement of the distance the leading edge of the flame front propagates across the specimen, divided by the time the specimen remains burning after being in contact with the 15 sec flame.

HFT samples had coated weight gains 11 wt% and 24 wt% for 3 and 6 BL of Recipe B [PEI-Py/PAA+MWNT], respectively. Greater weight gain for 6 BL, compared to 18 wt% for cone calorimetry, is due to the change in sample dimensions that required a modest adjustment to the coating method. Still shots of uncoated polyurethane and 3 and 6 BL coated samples, at 34 sec after the flame was removed, are displayed in the top row of Figure 4.5. Cotton fabric was placed at the bottom of the burn chamber to magnify the visual effect of melt dripping (these samples are not included in calculations of average burn data to be sure the cotton did not adversely influence the results). The portion of the uncoated sample that comes in contact with the flame melts and drips, causing the cotton at the bottom of the test chamber to ignite. The flame propagates across the polyurethane for an average of 32 $\pm$ 24 sec (after the 15 second flame exposure) and an average distance of 83 $\pm$ 35 mm before it extinguishes. The average burn rate for all uncoated polyurethane samples is 181 55 mm/min. Both 3 and 6 BL [PEI-Py/PAA+MWNT] coated samples eliminate melt dripping. It takes the flame front an average of 310 $\pm$ 60 sec to propagate an

average of 275 ± 50 mm across 3 BL coated samples, while 6 BL coated samples only burn for an average of 45 ± 7 sec and produce an average char length of 30 ± 10 mm. The average burn rate for 3BL coated samples is 53 ± 3 mm/min, while it is 39 ± 8 mm/min for 6 BL coated samples, which is slightly more than four times slower than the uncoated sample. Although the flame remains on the nanocoated samples longer than the uncoated specimens, samples coated with 6 BL of [PEI-Py/PAA+MWNT] prevent melt dripping and completely diminish the ability of the flame to propagate.

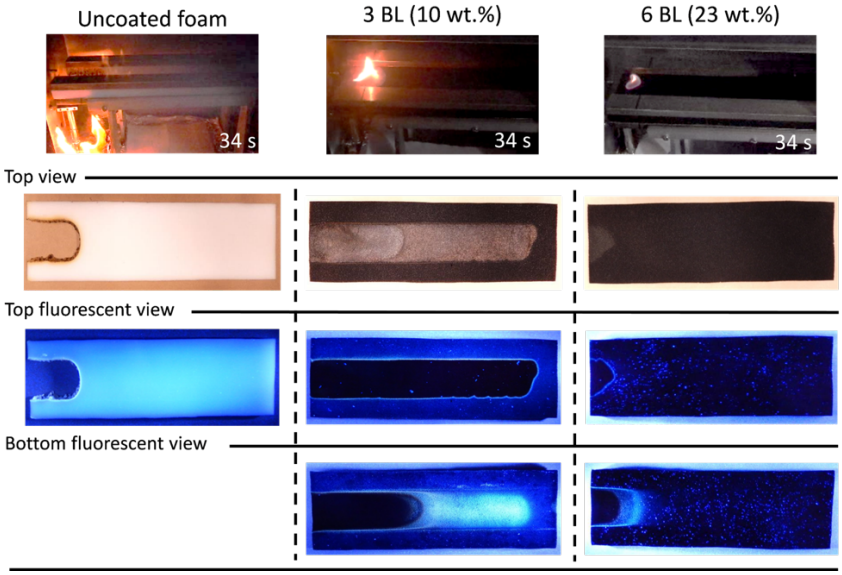

Figure 4.5: Horizontal flame test results showing uncoated foam in the left column, 3BL of Recipe B in the middle column and 6BL of Recipe B in the right column. Samples are imaged at 34 seconds into the burn test for the top row and post burn test below the top row. Fluorescent views highlight the char regions as solid black.

Figure 4.5 shows black light images of the samples after horizontal flame testing, which reveal the extent of burn damage. The coated samples have a gray/white discoloration under visible light, but appear black under UV light, allowing for more

accurate char length measurements. Fluorescent images of 3 BL coated samples reveal a significantly shorter char length for the bottom-view than the top-view, demonstrating that the bottom-side of the sample was exposed to a heat gradient as the flame traveled over the 1.3 cm thick foam and was extinguished. With 6 BL, there was no melt dripping and the flame did not propagate. The HFT displays the ability of a flame to spread across a surface when the ignition source is placed at one side of the sample and flame propagation is driven largely by thermal decomposition chemistry. The vertical burn test, similar to the HFT, shows the ability of a sample to withstand flame propagation when the ignition source is below the bulk of the sample, and also assesses flame spread due to thermal decomposition, but adds in the effects of bouyancy. In general, vertical flame spread is faster than that observed due to horizontal flame spread. By testing both vertical and horiztonal flame spread, which will be real-world geometries in fire events, a better understanding of the fire safety performance is obtained.

Uncoated polyurethane foam and foam coated with 3, 6 and 9 BL (12 wt%, 24 wt% and 44 wt% gain, respectively) of [PEI-Py/PAA+MWNT] (Recipe B) were prepared for vertical flame testing (VFT) to measure ignitability and flame spread. The burner was applied to the midpoint of the lowest portion of the hanging specimen at a 45 degree angle to avoid molten and flaming material from dripping into the burner. The flame was in contact with the sample for 12 sec. Afterflame time is reported as the average time the flame remained on the sample after the ignition source was removed. As expected, Figure 4.6 shows that within seconds of exposure to the flame from the burner, flames fully engulfed the entire 30.5 cm tall uncoated sample and molten, flaming drips fell to the bottom of the test chamber. Uncoated samples were consumed in an average of 61 $\pm$ 58 sec. Uncoated sample vertical burn behavior was erratic with the best performing sample extinguishing prior to removal

of the source flame and the worst burning completely over a period of 115 sec. Although the flame propagated the entire length of the 3 BL coated specimens, the coating completely prevented melt dripping. With 6 BL of [PEI-Py/PAA+MWNT], char length and flame time after removal of the ignition source decreased by an average of 27% and 69%, respectively. Samples coated with 9 BL self-extinguished when the ignition source was removed and had an average char length of 135.5 $\pm$ 3.7 mm. When viewed under the UV light, it can be seen that the true charred region is limited to the area exposed directly to the flame source. It is an impressive achievement to not only eliminate melt dripping of polyurethane foam, but to also completely prevent flame propagation in this vertical test orientation. Based on the results from cone calorimetry, HFT and VFT, it is clear that [PEI-Py/PAA+MWNT] is one of the most effective coatings ever reported for stopping fire on open-celled polyurethane foam.

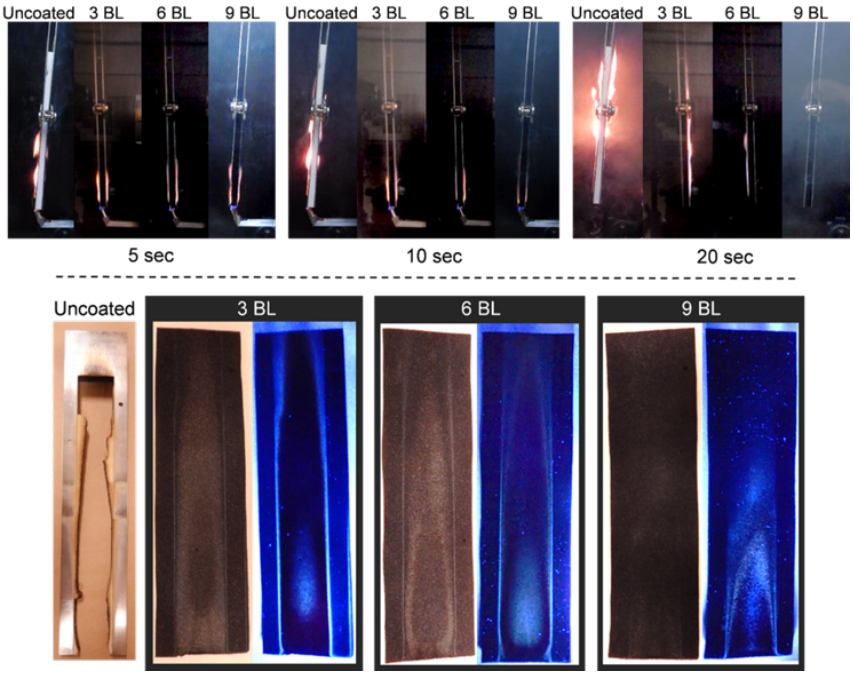

Figure 4.6: Top: vertical flame test results showing uncoated and 3, 6 and 9 BL coated samples at 5, 10, and 20 sec after ignition of the flame source. Bottom: images of charred regions after vertical flame test. In each case, the left image was produced using visible light, while the right image was produced using UV light for each sample.

4.4 Conclusion

This study demonstrates that a MWNT-based layer-by-layer assembly is capable of significantly reducing the flammability of polyurethane foam. TGA analysis revealed that the coatings contained up to 44 wt% MWNT. Cone calorimetry revealed that these coatings significantly reduced peak heat release rate, by at least 67%, and reduced total smoke release by up to 80%. It was found that only 6 BL of PEI-Py/PAA+MWNT could prevent horizontal flame spread and 9 BL was able to completely prevent vertical flame propagation. Melt dripping was eliminated with just 3 BL. The mechanism of flame retardancy, like that observed with poly-

mer nanocomposites and other LbL systems, is the formation of a robust char layer that slows mass loss and inhibits melt flow. This MWNT-based nanocoating allows the coated foam to retain its shape, burn with lower intensity, and have diminished flame spread. With relatively few layers, this coating exhibits the best flame retardant behavior reported in the open literature for open-celled polyurethane foam. Very few systems, even with very high weight addition (> 30wt%) can withstand a true vertical flame test.

5. CONE CALORIMETRY ASSESSMENT OF FABRIC AND FOAM ASSEMBLIES FOR IMPROVED TESTING METHODS

5.1 Introduction

Materials fire risk assessments typically focus on a single material's flammability due to the need for fundamental understanding of the fire physics and chemistry. This is particularly true for bench scale methods used to understand materials flammability behavior in an effort to develop new fire safety solutions. Many existing fire safety engineering test methods were designed and engineered to work with single materials or simple composites, not complex assemblies. Despite the common benchtop testing trend of focusing on one material, it is the full-scale fire behavior that drives codes and standards so there is a perceived disconnect between bench scale testing and full scale testing. When testing new pre-commercial material for fire safety, bench scale testing is conducted first to save on cost and material. Additionally, bench scale emissions are reduced (i.e., more environmentally friendly) relative to full scale fire tests. It is easy to understand why bench scale tests are preferred when considering cost and emission issues, but if the bench scale test does not correlate well to the full scale fire scenario the worth is questionable. Some bench scale tests do not always correctly mimic all of the full scale fire physics that will determine if a material is safe to use, but some existing bench scale tests are appropriate and, with simple modifications, can mimic full-scale fire behavior quite well. One such bench scale test is the cone calorimeter [181, 182], which works well for composites [183, 184, 54], wire and cable systems [185, 186], plastic electronic enclosures [187], and tests requiring heat release measurements [188]. While cone calorimetry is not a good fit for everything [163], it is a powerful tool for fully understanding material fire behavior

in well ventilated, forced combustion fire scenarios where time to escape (as dictated by heat release of the burning material) is important [164].

Despite the availability of this test method, there is little published data on interactions between foam and fabric interactions when tested via cone calorimetry, especially in the development of new fire safe solutions for furniture. This section explores how different foams (with and without flame retardant) behave in the cone calorimeter when covered with different types of fabric, having various flammability ratings. The objective of this work was to determine if the cone calorimeter can accurately screen performance in foam and fabric assemblies prior to full scale fire testing. In other words, can the cone calorimeter identify flammability parameters that may be able to predict pass/fail performance, especially in complex foam and fabric assemblies? Initial tests using standard materials serve as a set of controls, setting a baseline for comparison with a new flame retardant coating prepared from an aqueous polyelectrolyte complex (PEC). Testing these assemblies with PEC coated fabric will show if there are possible benefits of using PEC coatings for protecting fabric and foam assemblies.

5.2 Materials and Methods

5.2.1 Materials

All fabrics described in this study were purchased from Greenhouse Fabrics, Inc (High Point, NC). White BS5852 reference fabric is a 100% polyester standard reference fabric used in BS 5852 tests with a weight of 203 g/m^2 (6.0 oz/yd^2). 456-28 Bermuda fabric is also 100% polyester with a weight of 227 g/m^2 (6.7 oz/yd^2). A6041 Oak fabric is a 50:50 polyester and cotton blend with a weight of 214 g/m^2 (6.3 oz/yd^2). A7344 Icecaps fabric is 100% cotton (220 g/m^2 (6.5 oz/yd^2)). The foams (flame retardant and non-flame retardant (NFR)) were produced by Chem-

tura / Great Lakes Solutions and were polyether based polyurethane (∼1.5 lbs/ft^3, ∼4 scfm). The flame retardant polyurethane foam contained 19 parts per 100 of Chemtura Firemaster 600 (a proprietary phosphorus-bromine system) and 25 parts per 100 of melamine.

Branched polyethylenimine (M_W = 25,000 g/mol), sodium hexametaphosphate (also named poly(sodium phosphate)), citric acid monohydrate, and sodium chloride were purchased from Sigma-Aldrich (Milwaukee, WI). PEI is first dissolved into 18.2 MΩ deionized (DI) water followed by adding PSP to create a 5:10 wt% solution of PEI:PSP. A pH 2 buffering solution is prepared by adding 1.05 wt% citric acid monohydrate and 1.72 wt% NaCl (50 mM, ionic strength = 300 mmol).

5.2.2 Thin Film Deposition

The PEC solution was placed in a homebuilt trough provided by Chemtura which allowed for a 142 cm by 71 cm (56 in by 28 in) piece of fabric to be coated at one time while minimizing amount of solution needed. The fabric was pulled through the trough, containing 3300g of PEC solution, at a rate of approximately 0.3 cm/s (or 7 in/min). At a given moment, 9 cm (3.5 in) of fabric were submersed meaning each fiber of the cotton fabric was immersed in the PEC solution for approximately 30 seconds. This residence time was chosen based on previous work using this PEC coating method [150], however this cotton fabric is of a heavier weight than the referenced study and required two deposition cycles to obtain similar weight gain described previously. The full procedure consisted of immersion in the PEC solution, dry at 70°C for 25 min, a second immersion in the PEC solution, a second 25 min dry at 70°C, and an 8 min soak in the pH 2 buffering solution to lock the coating to the fabric by dropping the environment below the pH at which the complex is water soluble. This allowed the fabric to be squeezed and rinsed in DI water to

remove excess buffering solution. This was followed by a final wringing of the fabric to remove excess DI water and then the sample was dried at 70°C.

5.2.3 Flame Retardant Tests

The fabrics were tested on both flame retardant and non-flame retardant PU foam in cone calorimeter. Fabrics were cut into four pieces approximately 31.8 cm by 14 cm (12.5 in by 5.5 in). Foams were cut into 10 cm by 10 cm by 2.54 cm (4 in by 4 in by 1 in) samples. The fabric pieces were then wrapped around the PU foam and sewn together using Kevlar thread and a 7.6 cm (3 in) needle as per ASTM E1474. Pictures of the prepared samples are shown in Figure 5.1.

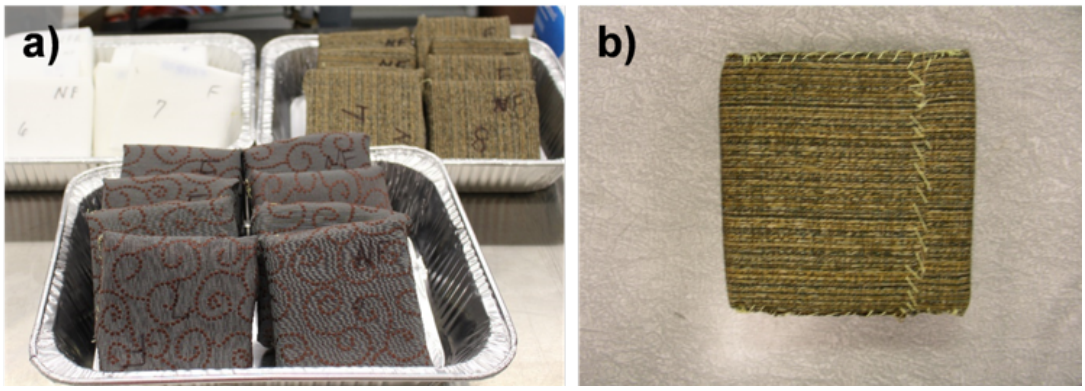

Figure 5.1: Pictures of fabric sewn onto foam pieces to be measured in cone calorimetry.

Cone Calorimeter experiments were conducted on a FTT Dual Cone Calorimeter at two heat fluxes (25 kW/m^2 and 35 kW/m^2) with an exhaust flow of 24 L/s using the standardized cone calorimeter procedure (ASTM E1354-12). Samples were wrapped in aluminum foil on one side as per the ASTM E1354 standard. Data collected from all samples is believed to have an error of ± 10% and was calculated

using a specimen surface area of 100 cm^2. All samples were tested at least in triplicate as per the ASTM E1354 standard. A fourth sample was tested when three samples had scattered results. A heat flux of 25 kW/m^2 was used for the reference, Bermuda, and Oak fabric samples. A heat flux of 35 kW/m^2 was used on coated and uncoated Icecaps cotton fabric samples.

In addition to cone calorimetry, a secondary test was performed to assess the flame retardant behavior of the coated cotton on PU foam. This test was designed as a qualitative testing method for this study. A butane hand torch (TriggertorchTM MT-76 K, Master Appliance Corps., Racine, WI) was used to apply a direct flame (approximately 1300°C) to the fabric and foam assemblies. The torch was set such that the inner blue flame length was 2.5 cm (1 in) and outer transparent blue flame was approximately 5 cm (2 in) total length. The samples were prepared by wrapping two 5 cm by 5 cm by 2.5 cm (2 in by 2 in by 1 in) foam pieces joined in an L-shape using a steel paperclip with coated or uncoated cotton fabric sewn onto the front face of the foam. The torch was applied to the creased region of the L-shape mini-couch in a manner that the inner blue flame was within 2 cm from being in contact with the cotton fabric. The uncoated sample was exposed to the torch for only 10 seconds for safety reasons, while the coated fabric was exposed for 100 seconds to demonstrate robustness of the coating.

5.3 Results and Discussion

The first three sets of samples were tested to measure the effects of combining foam and fabric in the cone calorimeter and were tested with a 25 kW/m^2 heat flux. Multiple fabric types were used to determine if different fabric compositions would or would not affect the heat release. Foam composition (with and without flame retardant) was also considered in testing. These series of tests will serve as a

baseline for future studies going deeper into understanding why testing fabric and foam together in cone calorimetry is beneficial.

5.3.1 Reference Polyester Fabric

The BS5852 white reference fabric was tested on both neat and flame retarded PU foam. Immediately upon exposure to the cone heater, the sample began to smoke and the surface fabric began to curl and deform quickly, followed by igniting and splitting open. The underlying foam began to collapse and liquefy, eventually leading to the fabric and foam assembly shrinking down into a burning mass that slowly burned to completion. The aluminum foil sample pan deformed during burning such that the cone heater shutters could not be closed at the end of the test. Figure 5.2(a) shows heat release rate average curves for the NFR and FR sample sets with the white reference fabric. When analyzing the heat release rate curves (prior to averaging the curves), there was some scatter noted due to the irregular deformation and fire behavior of the fabric at ignition. The data showed an average reduction in peak heat release rate (pkHRR) of 23% between the NFR and FR foam samples. FR foam showed better reproducibility, though tests with other fabrics showed better reproducibility with both foams. In both cases, the final chars, seen in Figure 5.2(b,c), appeared very similar because in each case, the foam melted, collapsed, and left very little char residue.

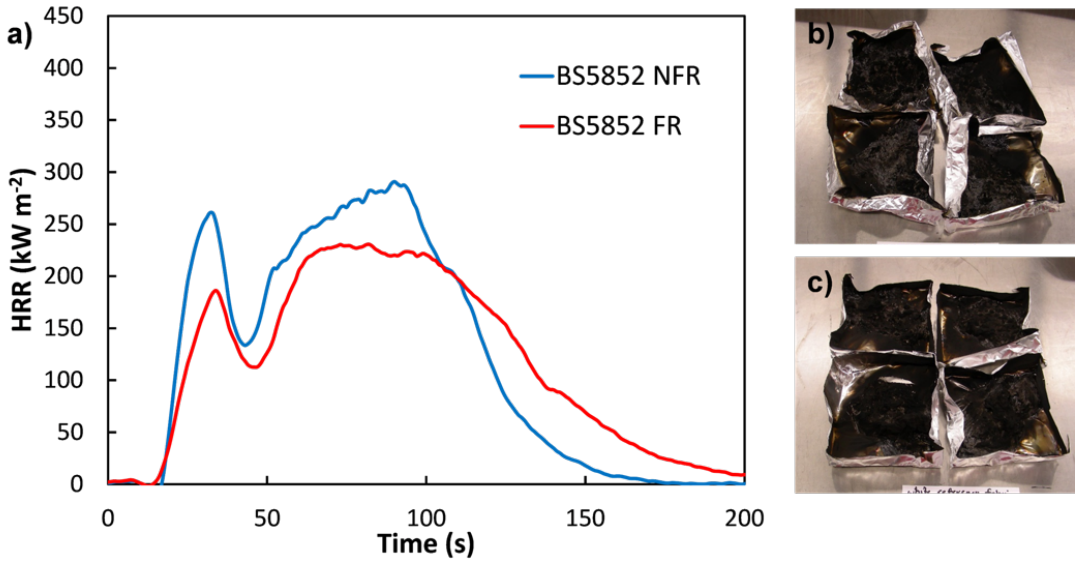

Figure 5.2: (a) HRR curves averaged for samples made with white reference BS5852 fabric with non-flame retarded foam and flame retarded foam. (b) Image of four NFR foam with reference fabric sample pans after cone testing. (c) Image of four FR foam with reference fabric sample pans after cone testing.

5.3.2 Commercial Polyester Fabric

The 456-28 Bermuda fabric behaved similarly to the white reference fabric as the samples began to smoke instantly upon exposure to the heater, quickly split open and pulled away from the foam. The splitting was so rapid that pieces of the fabric broke away from the sample and fell out of the cone calorimeter sample holder area while still burning. It is likely that there is higher than expected error in the mass loss data for samples with this fabric. The foam collapsed and fully liquefied. Unlike other samples in this study, the aluminum foil did not deform at this point and the shutters could be closed at the end of the test. The averaged HRR curves in Figure 5.3(a) show that the first peak is nearly gone for the FR foam containing sample. The data shows an average reduction in pkHRR of 15.9% and there was some scattered

data between samples for both FR and NFR foams. The burned samples appeared to contain significantly more black char evenly distributed in the sample pan, as seen in Figure 5.3(b,c).

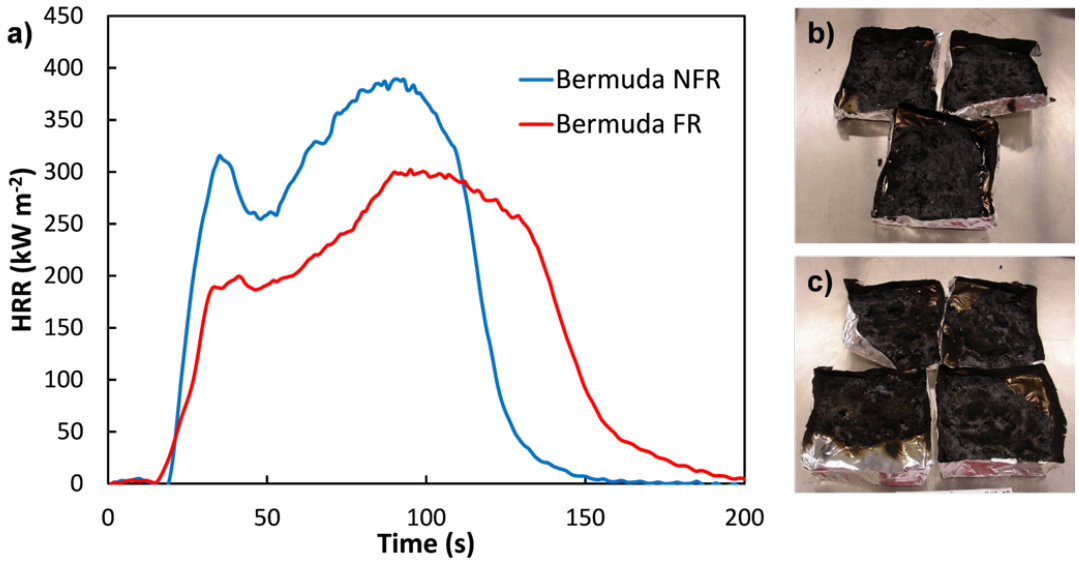

Figure 5.3: (a) HRR curves averaged for samples made with 456-28 Bermuda fabric with non-flame retarded foam and flame retarded foam. (b) Image of three NFR foam with Bermuda fabric sample pans after cone testing. (c) Image of four FR foam with Bermuda fabric sample pans after cone testing.

5.3.3 Polyester-Cotton Blend Fabric

The A6041 Oak fabric performed slightly different initially as the fabric did not curl or deform initially. It did not curl back until after ignition when it finally split open. Otherwise, the fire behavior was similar as the foam fully liquefied and the samples collapsed. The aluminum foil deformed at the end of the test similar to the BS5852 reference fabric, preventing the shutters from closing. The data shows an average reduction in pkHRR of 10.8%, showing less difference between NFR and FR

foams than the BS5852 reference and Bermuda fabrics. The HRR curves in Figure 5.4(a) differ from previous samples as well in that the FR foam containing sample shows a decline in HRR at a similar time and rate as the NFR foam containing sample. The Oak fabric samples had more reproducible results between measurements as well. Figure 5.4(b,c) shows the final chars had a mixture of white and black char and some of the fabric weave was still noticeable. This is likely due to the addition of cotton in the fabric makeup of these samples as cotton is more prone to rapid char formation than polyester.

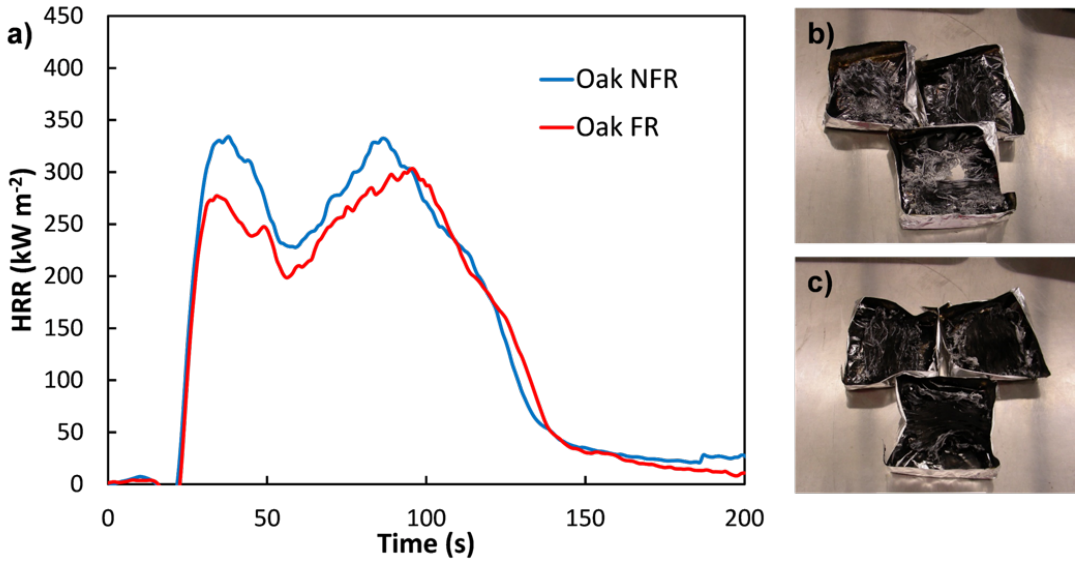

Figure 5.4: (a) HRR curves averaged for samples made with A6041 Oak fabric with non-flame retarded foam and flame retarded foam. (b) Image of three NFR foam with Oak fabric sample pans after cone testing. (c) Image of three FR foam with Oak fabric sample pans after cone testing.

5.3.4 Comparison of Polyester and Polyester-Cotton Fabrics

Table 5.1 shows a summary of results for each sample from which some general trends are observed. The foam type has the largest effect on flammability amongst the samples. This is expected since the foam is the majority of the flammable mass in each sample. FR foam samples have lower total heat release (THR) and pkHRR values compared to NFR samples for the same fabric type. FR foam also tends to generate higher levels of total smoke release (TSR) than NFR foam, though fabric type appears to significantly affect smoke output. Again, this result is expected since the FR foam contains a vapor phase flame retardant system (phosphorus-bromine) which inhibits combustion therefore resulting in higher levels of smoke release. The pure polyester fabric samples produced more smoke as well compared to the cotton containing samples. The overall lowest flammability combination seems to be the BS5852 reference fabric with the FR foam. The cotton/polyester blend (A6041 Oak) fabric performed better than the 100% polyester (456-28 Bermuda) fabric likely because 50% of the flammable polyester is replaced with less flammable and lower heat release cotton fiber. The Bermuda fabric, while 100% polyester just like the reference fabric, likely had worse flammability because it is thicker and has more flammable mass present.

Table 5.1: The average 25 kW/m^2 heat release data for assemblies of BS5852, Bermuda, and Oak fabrics with NFR and FR foam.

Fabric Sample	Foam	T_{ig} (s)	pkHRR (kW/m^2)	Avg HRR (kW/m^2)	Mass Lost (%)	THR (MJ/m^2)	TSR (m^2/m^2)
BS5852	NFR	13	327	170	87.7	24.1	704
BS5852	FR	11	251	138	84.7	23.5	794
Bermuda	NFR	12	396	253	92.3	31.0	573
Bermuda	FR	13	333	219	82.6	30.7	816
Oak	NFR	15	343	226	91.1	28.0	329
Oak	FR	17	306	210	87.8	26.1	541

All of the samples exhibited a two peak behavior. Each sample had very similar behavior with the outer fabric layer igniting first, followed by bursting open or melting back which led into the secondary heat release peaks as the foam fully liquefied and burned. Therefore, some of the HRR curves may be due to physical effects of flammability. It is interesting and notable to observe how the fabric fails at this heat flux when exposed to a radiant heat source (as opposed to a spot ignition source). This two peak behavior is also notably different than what is seen with typical polyurethane foams tested in cone calorimeter without surface fabrics present [172]. The normal two peak HRR curve for polyurethane due to the two step thermal decomposition behavior of the foam appears to be altered by the presence of fabric. Each fabric appears to have a slightly different effect on the two peaks (most notably the first peak). The peaks appear to be further separated from each other and more or less prominent in some cases and the fabric composition has a definite effect on the intensities of both the first and second HRR peaks.

5.3.5 Cotton Fabric

A7344 Icecaps (100% cotton) fabric was also tested using this fabric and foam combination method. In this portion of the study however, a coating was also applied to the fabric to demonstrate a potential flame retarding mechanism for upholstered foam applications. In these tests, the heat flux deviated from previous tests. A higher heat flux of 35 kW/m^2 was used (compared to 25 kW/m^2). When testing at the lower heat flux in previous samples, ignition behavior was consistent, but there were some erratic results post ignition. Sometimes higher heat fluxes will address the issue of consistency, especially for flame retardant materials which is relevant for the flame retardant polyelectrolyte coating applied to the cotton fabric. For this reason, only general comparisons will be made between these samples and previous samples. The focus of this portion is on the introduction of the PEC nanocoating and its effectiveness as a flame retardant for the fabric and foam assemblies.

Table 5.2 shows a summary of the Icecaps samples results with and without the polyelectrolyte complex coating on both NFR and FR foam tested at 35 kW/m^2. The results show minor differences between the NFR and FR foams when tested with the A7344 Icecaps fabric without the nanocoating. When the nanocoating is applied, the results change dramatically. The coating added 21.8 $\pm$ 0.4 wt% to the Icecaps cotton and leads to a significant decrease in heat release and overall flammability regardless of whether NFR or FR foam was used. This is evidence that the coated fabric does have a flame retardant effect, including some delays in time to ignition. The PEC coated fabric improves almost every measured property in the cone calorimeter with the exception of possibly total smoke release. The improvement in properties is significant and noteworthy. A more complete description of testing behavior and results are described for each sample set below.

Table 5.2: The average 35 kW/m^2 heat release data for assemblies of coated and uncoated Icecaps cotton with NFR and FR foam.

Fabric Sample	Foam	T_{ig} (s)	pkHRR (kW/m^2)	Avg HRR (kW/m^2)	Mass Lost (%)	THR (MJ/m^2)	TSR (m^2/m^2)
Uncoated	NFR	9	374	198	94.8	28.9	191
Uncoated	FR	7	403	195	90.2	27.2	295
Coated	NFR	11	299	159	76.7	20.8	195
Coated	FR	11	319	140	76.7	20.7	301

5.3.5.1 Uncoated Cotton

The NFR and FR foam and uncoated cotton fabric samples behaved similarly in that they began smoking immediately upon exposure to the cone heater, igniting shortly afterward. The surface blackened and the foam collapsed inside the fabric during burning. Some glowing (smolder) was noted towards the end of the test as the fabric began to curl and deform (FR foam samples had less deformation at the end). Unlike previous tests with the polyester containing fabrics, the cotton fabric did not split open and instead remained intact and carbonized during testing. Heat release rate curves shown in Figure 5.5(a) showed the classic two peak behavior of PU foam and very little difference between the NFR and FR foam containing samples. The pkHRR actually show an increase of 7.8% on average from NFR to FR foam, though the averaged HRR curves show little difference if any in pkHRR due to some scatter in time to pkHRR of the FR samples. The final chars of the NFR samples seen in Figure 5.5(b) show the remaining curled up carbonized fabric which could be opened up and, while mostly hollow, did retain some small pieces of char/foam

residue. The final chars of the FR samples (Figure 5.5(c)) had carbonized fabric that remained pliable (can move and bend without breaking), though it was torn easily. Again, small pieces of foam residue were found within the fabric shells at the end of the test. Both NFR and FR sets with Icecaps fabric are significant improvements over the previously tested fabrics as there is more tangible char remaining even at a higher heat flux due to the char forming nature of the cotton, further signifying that fabric composition plays an important role in overall flammability.

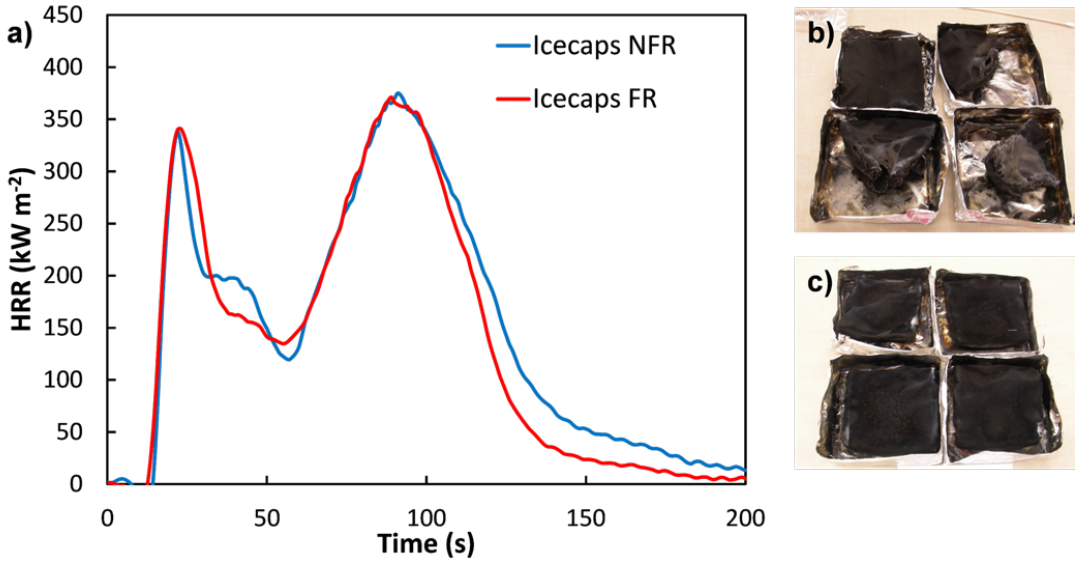

Figure 5.5: (a) HRR curves averaged for samples made with A7344 Icecaps fabric with non-flame retarded foam and flame retarded foam. (b) Image of four NFR foam with Icecaps fabric sample pans after cone testing. (c) Image of four FR foam with Icecaps fabric sample pans after cone testing.

5.3.5.2 Coated Cotton

Fire behavior for the NFR foam and coated cotton fabric was similar to the uncoated samples with a deviation in the initial heat release rate growth. The initial

heat release growth rate was slower and there were small white (relative to the black surface) flames on the surface of the sample, likely resulting from addition of phosphorus to the surface of the sample in the form of sodium hexametaphosphate within the polyelectrolyte complex coating. Figure 5.6(a) shows the averaged heat release rate curves. The slower initial HRR growth is noted by the lowered intensity of the first peak and addition of a more noticeable secondary peak of 150 kW/m^2 around 40-45 seconds. This secondary peak is somewhat evident in the uncoated samples, but is mostly overshadowed by the first peak. These samples are also very reproducible. The final char of the coated fabric on NFR foam (Figure 5.6(b)) maintained the shape of the original assembly and the outer fabric was stiff. The charred outer fabric contained a hollow inner core with some foam residue and fragments.

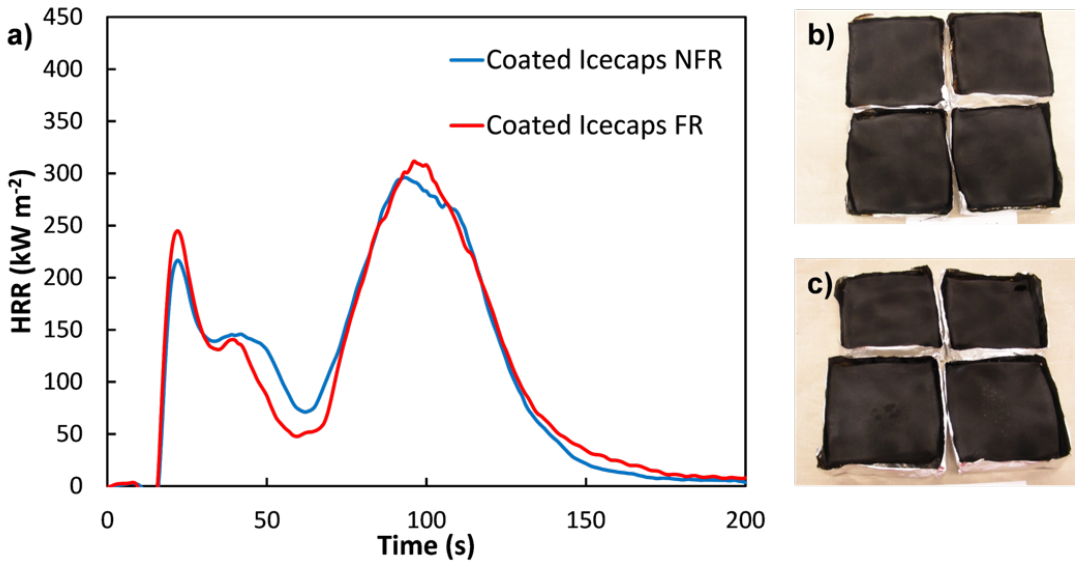

Figure 5.6: (a) HRR curves averaged for samples made with A7344 Icecaps fabric coated with PEC with non-flame retarded foam and flame retarded foam. (b) Image of four NFR foam with coated Icecaps fabric sample pans after cone testing. (c) Image of four FR foam with coated Icecaps fabric sample pans after cone testing.

The coated cotton fabric with FR foam showed different behavior, though still significant improvement over the uncoated counterpart. Unlike in the NFR foam samples, the FR foam samples with coated fabric had erratic self-extinguishing events in a couple of the samples around 50 seconds into the test, requiring the spark to be reinserted. This re-ignition behavior caused much more irregular HRR curves, but this is not to be mistaken for poor results. This behavior actually suggests a more robust flame retardant performance for this combination of fabric and foam, even though it appears that the pkHRR increased by an average of 6.7% from the coated fabric on NFR foam samples. The final chars (Figure 5.6(c)) were very similar to NFR foam in that the outer fabric retained the shape and contained small pieces of foam residue and char inside.

5.3.5.3 Butane Torch Test

A separate qualitative test was performed on these cotton based fabric and foam assemblies in order to further exemplify how robust this PEC coating is in regards to flame retarding the fabric and foam assembly. For this test, a slightly different set-up was used for the assembly as seen in Figure 5.7 in order to create a corner region for the flame to be applied. The torchs inner blue flame was brought within 1" of the sample surface and held in place for 100 seconds. This could not be done for the sample without a coating as the flame from the sample became too large and it was not safe to hold the torch in place. For this reason, only 10 second exposure was used for uncoated fabric. Figure 5.7(a-d) shows the uncoated sample as it slowly burned over a total of 200 seconds leaving char residue under a small piece of charred cotton fabric that remained intact. Within the short 10 second exposure, the torch burned a hole through the fabric and the foam, quickly igniting and propagating a flame on both. The coated sample is shown in Figure 5.7(e-i). Even after 100 seconds,

the fabric was not penetrated by the torch. The flame on the surface of the sample immediately extinguished with no propagation once the torch was removed (Figure 5.7(g)). There was a charred area around the location where the flame contacted the surface of the assembly, and the outer areas of the fabric remained undamaged as there was no flame spread during the torch exposure. The charred region cracked upon handling of the sample and closer inspection underneath this region showed that the foam receded from the fabric during the test (Figure 5.7(i)). The fabric allowed the foam to safely melt away from the heat without igniting or propagating a flame.

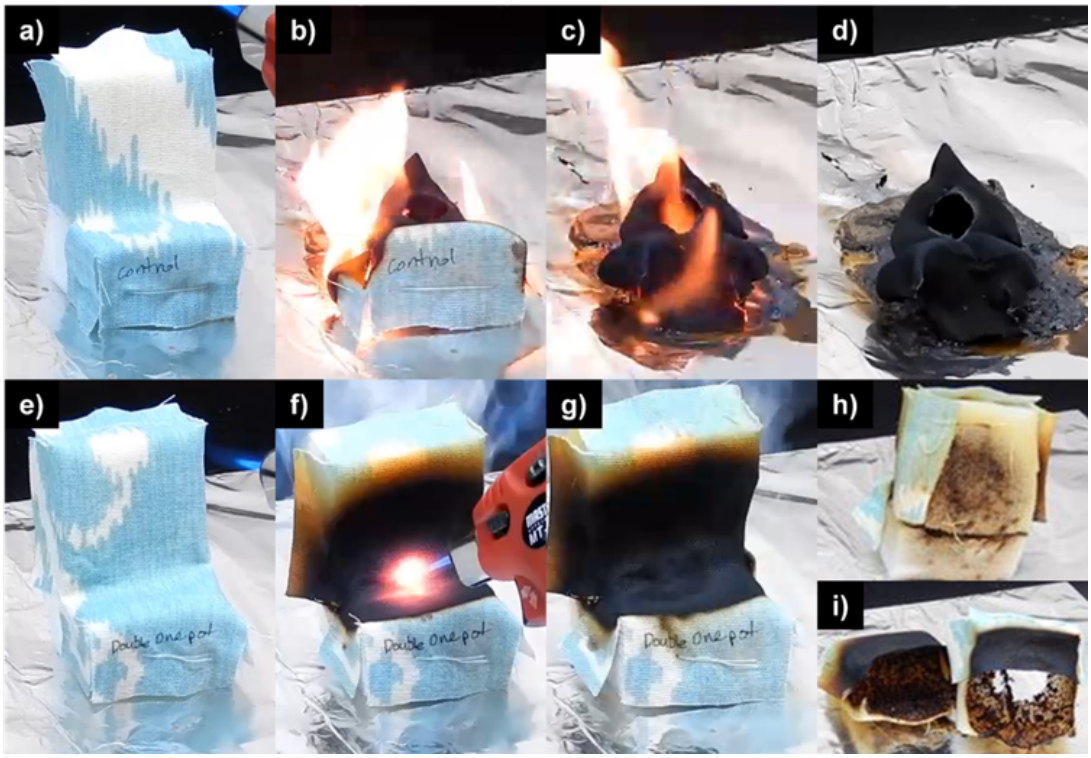

Figure 5.7: Pictures of uncoated Icecaps cotton on NFR foam (a) before the 10 second butane torch exposure, (b) 50 seconds after exposure, (c) 100 seconds after exposure, and (d) the final extinguished sample. Pictures of coated Icecaps cotton on NFR foam are shown (e) before the 100 second butane torch exposure, (f) 50 seconds of exposure, (g) immediately after removal of torch at 100 seconds of exposure, (h) back of sample showing foam structure intact, and (i) inside the burned sample showing where the foam melted away from the heat during torch exposure.

5.4 Conclusion

It is evident from the results in this paper that fabric and foam do interact with one another during fire events and therefore it makes sense to study foam and fabric combinations when developing new flame retardant materials. Cone calorimetry results showed that fabric composition had notable effects on heat release and heat release rate growth. The fabric composition effects also behaved differently when

switching from NFR foam to FR foam samples. Polyester materials tested in this paper have higher heat release and form very little char when compared to cotton fibers which form char and have lower heat release. This was seen when comparing the 50/50 cotton/polyester blend fabric (A6041 Oak) with the 100% polyester fabric (456-28 Bermuda) as the cotton containing sample contributed less to the additional heat release when compared to the 100% polyester. The BS5852 reference fabric contributed the least to heat release, though this is likely due to the fabric being thinner and therefore added little additional fuel to the overall system. It is concluded for these reasons that fabric type and composition do affect heat release in the test despite the majority of the fuel present being polyurethane.

Along with the ability to differentiate between fabrics, the cone calorimeter data showed differences between flame retarded and non-flame retarded foam. However, the sample set in this report is small and other fabric and foam combinations with varying standalone results in other tests are recommended for future testing to determine what measurements in cone calorimeter can provide quantitative differentiation between samples as opposed to qualitative differentiation as described by this report. This report and the inlying results show that in order to properly understand upholstered furniture flammability at the bench scale, fabric and foam combinations should be considered in flame retardant material design and discovery work.

This is further exemplified through the results of the polyelectrolyte complex FR coating on cotton. This coating on cotton was able to significantly reduce the heat release rate of the system even at a higher heat flux and showed some self-extinguishing behavior. The PEC coatings provide robust flame retardant protection regardless of the underlying foam being flame retarded or not. The qualitative torch test shows protection of the fabric and foam combination from direct butane torch exposure through extinguishing the flame and preventing cracking of the fabric as

well as ignition of the foam. This is evidence that flame retardant nanocoatings could create thin barrier fabrics and this could be a potential method moving forward for flame retarding upholstered furniture.

6. CONCLUSIONS AND FUTURE WORK

6.1 Reductions to Polyurethane Foam Flammability

This dissertation has shown several improvements made to layer-by-layer flame retardant coatings for polyurethane foam. These improvements are significant additions to LbL FR literature as they show that not only can these coatings reduce the flammability of PU, but also have the potential to prevent flame spread completely when exposed to an open flame source. Barrier fabric development is another simple avenue of creating effective flame retardants for polyurethane. These advancements in flame retarding foam are significant and can be expanded upon. At this age of the technology, future works should also begin focusing on efficiency in order to bridge the gap from academia into scalable products. An overview of the findings and future work suggestions are provided here.

6.1.1 Stack LbL Assembly

It was shown in Section 3 that bilayers of CH/APP had minimal effect on the flammability of polyurethane foam until it was combined with a few layers of CH/VMT at which point the foam resisted flame spread [1]. The initial thermal stability of the CH/VMT layers provide a support structure for the CH/APP layers to form an expanded char layer. By combining 4 BL of CH/VMT and 20 BL of CH/APP, the fire from the butane torch test was unable to spread once the flame source was removed. This stacked LbL concept can be applied to other systems to benefit from two different mechanisms and achieve greater flame retardant properties.

6.1.2 Multiwalled Carbon Nanotube Multilayers

Section 4 showed the ability of carbon nanotubes interlaced in a LbL thin film composed of PEI-Py and PAA to flame retard polyurethane foam [37]. This bilayer system had several beneficial reductions to the PU flammability. Cone calorimetry showed both pkHRR and TSR were significantly reduced and open flame tests showed that the foam could withstand ignition in both vertical and horizontal orientations.

6.1.3 Cone Calorimetry Study and Barrier Fabric Development

The results of Section 5 support the idea that testing of individual materials that will later become part of a larger product for flammability may not be the most effective way of screening and developing flame retardants. Specifically for the case of upholstered foam furnishings, combinations of various fabrics with both FR and non-FR polyurethane foam resulted in different trends. Using cone calorimetry to test various combinations, possibly in conjunction with other testing methods, could lead to more efficient development of application specific flame retardants. To provide an example, it was shown that a simple polyelectrolyte coating on cotton fabric was able to significantly flame retard the fabric and foam combination.

6.2 Future Research Direction

6.2.1 Halloysite Nanotubes for Improved Flame Retardant Coatings

The results of Section 4 show that nanotubes can be a useful particle shape for imparting flame retardant properties on polyurethane foam. Carbon nanotubes, however, are still relatively expensive and are not necessarily environmentally friendly. In attempt to provide an environmentally benign alternative, halloysite nanotubes will be studied to determine if the clay-based nanotube structure provides similar benefits to the carbon nanotubes with regards to peak heat release rate and total

smoke release reduction. Initial experiments resulted in promising results as shown in Figure 6.1. Halloysite nanoparticles could provide an environmentally benign option for flame retarding polyurethane foam.

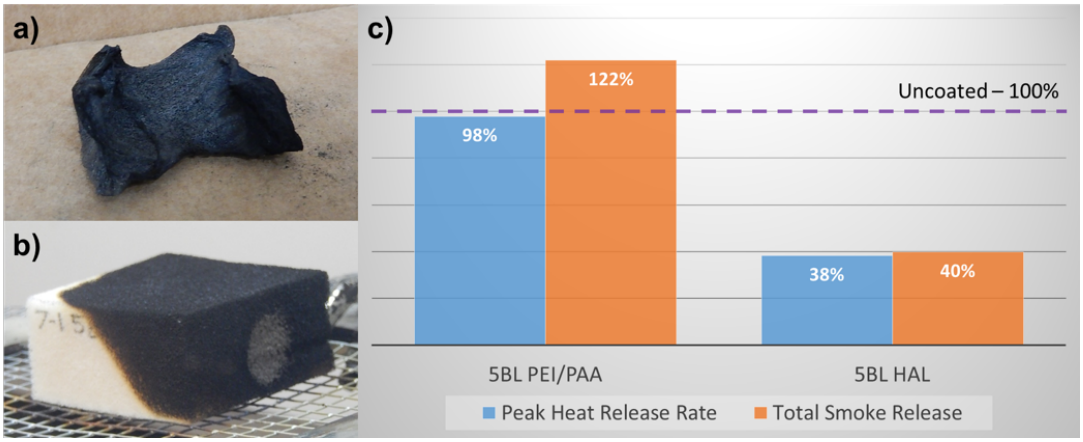

Figure 6.1: Images of (a) 5BL PEI/PAA and (b) 5BL PEI+HAL/PAA+HAL after exposure to a butane torch test. (c) Cone calorimetry results for peak heat release rate and total smoke release for 5BL coatings compared to uncoated polyurethane.

6.2.2 Boron Nitride Flame Retardant Study

Sections 3 and 4 as well as several other studies reviewed in Section 2 have shown the potential benefits of using thermally stable nanoparticles. Boron nitride nanosheets (BNNS) are thermally conductive and stable nanoparticles that have yet to be studied in LbL FR coatings. The mass increase from oxidation at high temperatures gives BNNS a unique benefit not observed for many other nanoparticles used to date. These would be an interesting nanoparticle to be studied for flame retardant properties as well as a general protective oxidation barrier due to the sheet-structure. This could possibly reduce aging of the coated substrate. Figure 6.2(a) shows initial torch test results of polyurethane coated with a BNNS-based

recipe. This coating could also serve as a good gas barrier, with a high growth rate, highlighted in Figure 6.2(b), and inclusion of impermeable sheets to a system already known for good gas barrier [169].

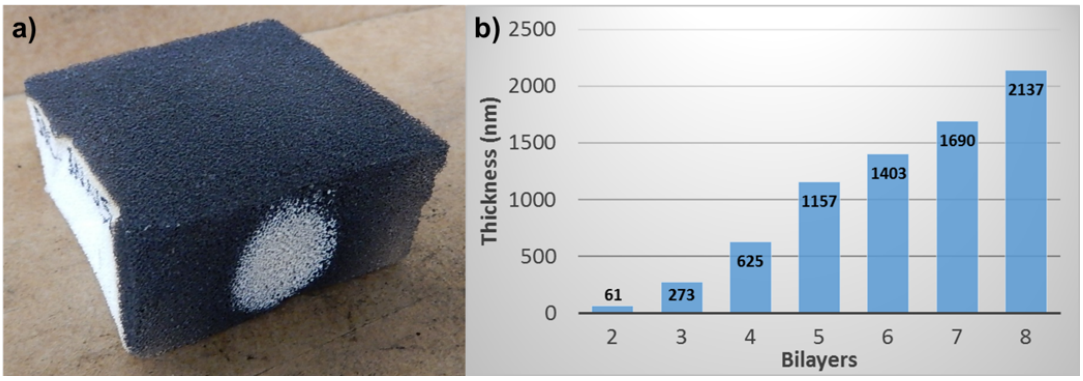

Figure 6.2: Image of polyurethane coated with a BNNS containing LbL coating after exposure to a butane torch test.

6.2.3 Spray Coating Flame Retardant Coatings on Polyurethane Foam

The use of LbL to deposit flame retardant nanocoatings on polymeric surfaces is still a rapidly growing field as outlined in Section 2. With the current research base, it is now questionable how transferable this technology will be to industrial scale. There are many processing steps to LbL and despite the significant reductions in flammability, scalability needs to be addressed. Studies have begun showing possible methods to scale, showing promising adaptations into current fabric assembly lines, however foam and other complex three dimensional substrates still require improvements. Spray coating is a successful platform for depositing LbL though it has limited ability to penetrate a porous foam to deposit a uniform coatings. However, the many coatings on foam show that the bulk of the material is protected from any

degradation. A study focused on penetration depth of spray coating polyurethane foam might reveal that an outer layer is all that is necessary to impart the same flammability reductions as dip coating. Initial results outlined in Figure 6.3 are very promising showing that the coating can self-extinguish in both torch and HFT tests as well as maintain flame retardant properties after conditioning.

-insert figure-

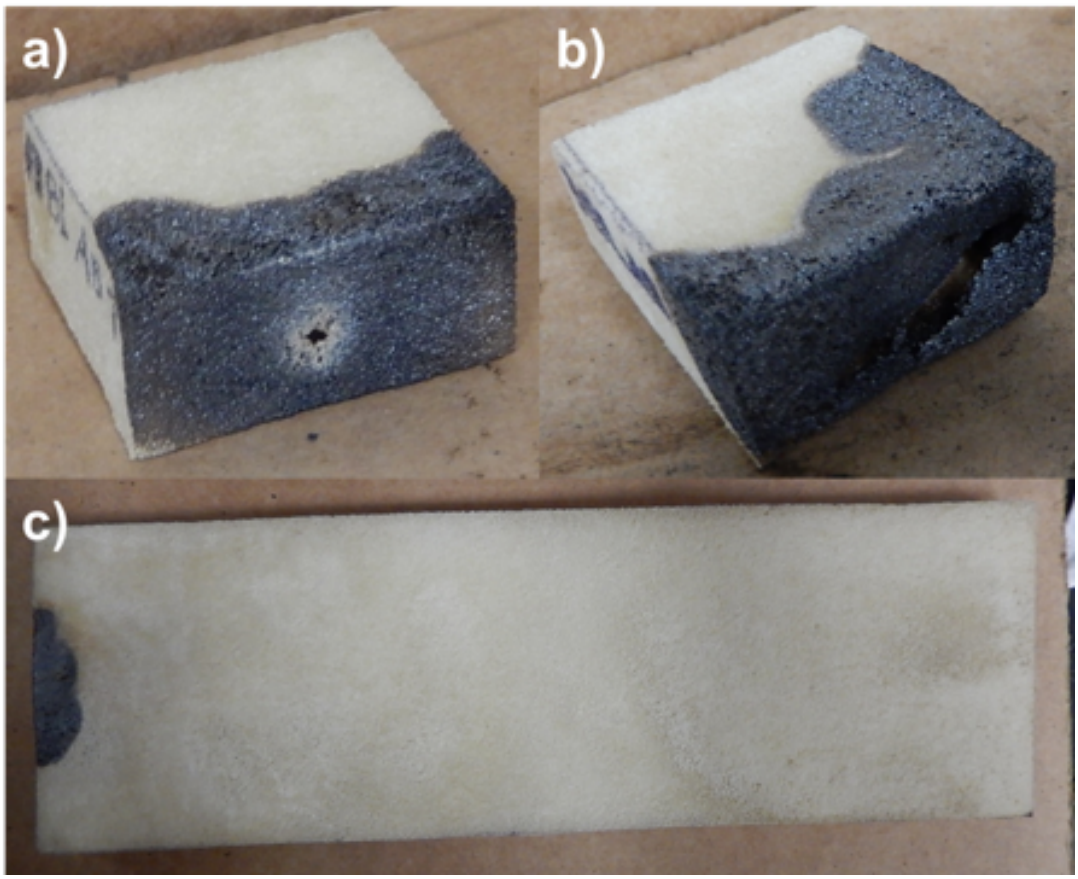

Figure 6.3: Images of polyurethane foam spray coated with 3BL of CH/VMT (a) before and (b) after compression conditioning and exposure to the butane torch test. (c) An image of 3BL CH/VMT spray coated and tested via a horizontal flame test.

REFERENCES

[1] K. M. Holder, M. E. Huff, M. N. Cosio, and J. C. Grunlan. Intumescing multilayer thin film deposited on clay-based nanobrick wall to produce self-extinguishing flame retardant polyurethane. *Journal of Materials Science*, 50(6):2451–2458, 2015.

[2] M. Ahrens. Home structure fires, 2015. http://www.nfpa.org/.

[3] A. Gharehbagh and Z. Ahmadi. *Polyurethane flexible foam fire behavior*. In-Tech, 2012. http://dx.doi.org/10.5772/47965.

[4] T. R. Hull and B. K. Kandola. *Fire retardancy of polymers: new strategies and mechanisms*. Royal Society of Chemistry: Cambridge, UK, 2009.

[5] W. E. Wilson, J. T. O'Donovan, and R. M. Fristrom. Flame inhibition by halogen compounds. *International Symposium on Combustion*, 12(1):929–942, 1969.

[6] F. Laoutid, L. Bonnaud, M. Alexandre, J. M. Lopez-Cuesta, and P. Dubois. New prospects in flame retardant polymer materials: from fundamentals to nanocomposites. *Materials Science and Engineering: R*, 63(3):100–125, 2009.

[7] H. R. Buser. Polybrominated dibenzofurans and dibenzo-p-dioxins: thermal reaction products of polybrominated diphenyl ether flame retardants. *Environmental Science and Technology*, 20(4):404–408, 1986.

[8] F. Rahman, K. H. Langford, M. D. Scrimshaw, and J. N. Lester. Polybrominated diphenyl ether (pbde) flame retardants. *Science of the Total Environment*, 275(1):1–17, 2001.

[9] P. O. Darnerud. Toxic effects of brominated flame retardants in man and in wildlife. *Environmental International*, 29(6):841–853, 2003.

[10] G. Decher. *Layer-by-Layer Assembly (Putting Molecules to Work)*, pages 1–21. Wiley Online Library: Weinheim, Germany, 2012.

[11] Y. C. Li, S. Mannen, A. B. Morgan, S. C. Chang, Y. H. Yang, B. Condon, and J. C. Grunlan. Intumescent all-polymer multilayer nanocoating capable of extinguishing flame on fabric. *Advanced Materials*, 23(34):3926–3931, 2011.

[12] H. F. Pan, W. Wang, Y. Pan, L. Song, Y. Hu, and K. M. Liew. Formation of layer-by-layer assembled titanate nanotubes filled coating on flexible polyurethane foam with improved flame retardant and smoke suppression properties. *ACS Applied Materials & Interfaces*, 7(1):101–111, 2015.

[13] K. Apaydin, A. Laachachi, T. Fouquet, M. Jimenez, S. Bourbigot, and D. Ruch. Mechanistic investigation of a flame retardant coating made by layer-by-layer assembly. *RSC Advances*, 4(82):43326–43334, 2014.

[14] F. Fang, X. Zhang, Y. D. Meng, X. Ding, C. Bao, S. Y. Li, H. Zhang, and X. Y. Tian. Boron-containing intumescent multilayer nanocoating for extinguishing flame on cotton fabric. *Cellulose*, 23(3):2161–2172, 2016.

[15] M. A. Priolo, K. M. Holder, T. Guin, and J. C. Grunlan. Recent advances in gas barrier thin films via layer-by-layer assembly of polymers and platelets. *Macromolecular Rapid Communications*, 36(10):866–879, 2015.

[16] K. M. Holder, B. R. Spears, M. E. Huff, M. A. Priolo, E. Harth, and J. C. Grunlan. Stretchable gas barrier achieved with partially hydrogen-bonded multilayer nanocoating. *Macromolecular Rapid Communications*, 35(10):960–964, 2014.

[17] L. Zhai, F. C. Cebeci, R. E. Cohen, and M. F. Rubner. Stable superhydrophobic coatings from polyelectrolyte multilayers. *Nano Letters*, 4(7):1349–1353, 2004.

[18] L. Zhang and J. Sun. Layer-by-layer codeposition of polyelectrolyte complexes and free polyelectrolytes for the fabrication of polymeric coatings. *Macromolecules*, 43(5):2413–2420, 2010.

[19] J. A. Lichter and M. F. Rubner. Polyelectrolyte multilayers with intrinsic antimicrobial functionality: the importance of mobile polycations. *Langmuir*, 25(13):7686–7694, 2009.

[20] J. A. Lichter, K. J. Van Vliet, and M. F. Rubner. Design of antibacterial surfaces and interfaces: polyelectrolyte multilayers as a multifunctional platform. *Macromolecules*, 42(22):8573–8586, 2009.

[21] B. S. Shim, J. Zhu, E. Jan, K. Critchley, and N. A. Kotov. Transparent conductors from layer-by-layer assembled swnt films: importance of mechanical properties and a new figure of merit. *ACS Nano*, 4(7):3725–3734, 2010.

[22] C. Huang, N. Grobert, A. Watt, C. Johnston, A. Crossley, N. P. Young, and P. S. Grant. Layer-by-layer spray deposition and unzipping of single-wall carbon nanotube-based thin film electrodes for electrochemical capacitors. *Carbon*, 61:525–536, 2013.

[23] E. Kharlampieva, V. Kozlovskaya, and S. A. Sukhishvili. Layer-by-layer hydrogen-bonded polymer films: From fundamentals to applications. *Advanced Materials*, 21(30):3053–3065, 2009.

[24] P. Kekicheff, G. F. Schneider, and G. Decher. Size-controlled polyelectrolyte complexes: Direct measurement of the balance of forces involved in

the triggered collapse of layer-by-layer assembled nanocapsules. *Langmuir*, 29(34):10713–10726, 2013.

[25] T. Boudou, T. Crouzier, C. Nicolas, K. Ren, and C. Picart. Polyelectrolyte multilayer nanofilms used as thin materials for cell mechano-sensitivity studies. *Macromolecular Bioscience*, 11(1):77–89, 2011.

[26] S. S. Shiratori and M. F. Rubner. ph-dependent thickness behavior of sequentially adsorbed layers of weak polyelectrolytes. *Macromolecules*, 33(11):4213–4219, 2000.

[27] L. Chang, X. X. Kong, F. Wang, L. Y. Wang, and J. C. Shen. Layer-by-layer assembly of poly (n-acryloyl-n '-propylpiperazine) and poly (acrylic acid): Effect of ph and temperature. *Thin Solid Films*, 516(8):2125–2129, 2008.

[28] K. Apaydin, A. Laachachi, V. Ball, M. Jimenez, S. Bourbigot, V. Toniazzo, and D. Ruch. Polyallylamine-montmorillonite as super flame retardant coating assemblies by layer-by layer deposition on polyamide. *Polymer Degradation and Stability*, 98(2):627–634, 2013.

[29] T. Guin, M. Krecker, D. A. Hagen, and J. C. Grunlan. Thick growing multi layer nanobrick wall thin films: Super gas barrier with very few layers. *Langmuir*, 30(24):7057–7060, 2014.

[30] R. A. McAloney, M. Sinyor, V. Dudnik, and M. C. Goh. Atomic force microscopy studies of salt effects on polyelectrolyte multilayer film morphology. *Langmuir*, 17(21):6655–6663, 2001.

[31] H. L. Tan, M. J. McMurdo, G. Q. Pan, and P. G. Van Patten. Temperature dependence of polyelectrolyte multilayer assembly. *Langmuir*, 19(22):9311–9314, 2003.

[32] S. T. Dubas, P. Kumlangdudsana, and P. Potiyaraj. Layer-by-layer deposition of antimicrobial silver nanoparticles on textile fibers. *Colloids and Surfaces A: Physicochemical and Engineering Aspects*, 289(1):105–109, 2006.

[33] Y. C. Li, J. Schulz, and J. C. Grunlan. Polyelectrolyte/nanosilicate thin-film assemblies: Influence of ph on growth, mechanical behavior, and flammability. *ACS Applied Materials & Interfaces*, 1(10):2338–2347, 2009.

[34] F. Carosio, J. Alongi, and G. Malucelli. alpha-zirconium phosphate-based nanoarchitectures on polyester fabrics through layer-by-layer assembly. *Journal of Materials Chemistry*, 21(28):10370–10376, 2011.

[35] A. Laachachi, V. Ball, K. Apaydin, V. Toniazzo, and D. Ruch. Diffusion of polyphosphates into (poly(allylamine)-montmorillonite) multilayer films: Flame retardant-intumescent films with improved oxygen barrier. *Langmuir*, 27(22):13879–13887, 2011.

[36] T. Guin, M. Krecker, A. Milhorn, and J. C. Grunlan. Maintaining hand and improving fire resistance of cotton fabric through ultrasonication rinsing of multilayer nanocoating. *Cellulose*, 21(4):3023–3030, 2014.

[37] K. M. Holder, A. A. Cain, M. G. Plummer, B. E. Stevens, P. K. Odenborg, A. B. Morgan, and J. C. Grunlan. Carbon nanotube multilayer nanocoatings prevent flame spread on flexible polyurethane foam. *Macromolecular Materials and Engineering*, 301(6):665–673, 2016.

[38] Y. Lvov, R. Price, B. Gaber, and I. Ichinose. Thin film nanofabrication via layer-by-layer adsorption of tubule halloysite, spherical silica, proteins and polycations. *Colloids and Surfaces A: Physicochemical and Engineering Aspects*, 198:375–382, 2002.

[39] A. Hao, I. Wong, H. Wu, B. Lisco, B. Ong, A. Sallean, S. Butler, M. Londa, and J. H. Koo. Mechanical, thermal, and flame-retardant performance of polyamide 11–halloysite nanotube nanocomposites. *Journal of Materials Science*, 50(1):157–167, 2015.

[40] L. Li, Z. Wu, S. Jiang, S. Zhang, S. Lu, W. Chen, B. Sun, and M. Zhu. Effect of halloysite nanotubes on thermal and flame retardant properties of polyamide 6/melamine cyanurate composites. *Polymer Composites*, 36(5):892–896, 2015.

[41] Y. Lvov, W. Wang, L. Zhang, and R. Fakhrullin. Halloysite clay nanotubes for loading and sustained release of functional compounds. *Advanced Materials*, 28(6):1227–1250, 2016.

[42] G. Camino, L. Costa, and M. Dicortemiglia. Overview of fire retardant mechanisms. *Polymer Degradation and Stability*, 33(2):131–154, 1991.

[43] J. H. Troitzsch. Fires, statistics, ignition sources, and passive fire protection measures. *Journal of Fire Sciences*, 34(3):171–198, 2016.

[44] P. Georlette, J. Simons, and L. Costa. *Halogen-containing fire-retardant compounds*. Marcel Dekker: New York, 2000.

[45] P. Georlette. *Applications of halogen flame retardants*. Woodhead Publishing: Cambridge, UK, 2001.

[46] J. Murphy. Flame retardants: trends and new developments. *Plastics, Additives and Compounding*, 3(4):16–20, 2001.

[47] A. Litzenburger. Criteria for, and examples of optimal choice of flame retardants. *Polymers & Polymer Composites*, 8(8):581–592, 2000.

[48] J. Green. Mechanisms for flame retardancy and smoke suppression - a review. *Journal of Fire Sciences*, 14(6):426–442, 1996.

[49] S. Levchik and C. A. Wilkie. *Char formation*, pages 171–215. Marcel Dekker: New York, 2000.

[50] E. M. Pearce, S. W. Shalaby, and R. H. Barker. *Retardation of combustion of polyamides*, pages 239–290. Springer: New York, 1975.

[51] A. B. Morgan and C. A. Wilkie. *Flame retardant polymer nanocomposites*. John Wiley & Sons: New Jersey, 2007.

[52] R. M. Aseeva and G. Zaikov. *Combustion of polymer materials*. Hanser: Munich, Germany, 1986.

[53] M. Lewin and E. Weil. *Mechanisms and modes of action in flame retardancy of polymers*, pages 31–68. Woodhead Publishing Limited: Cambridge, UK, 2001.

[54] B. K. Kandola and R. Toqueer-Ul-Haq. The effect of fibre content on the thermal and fire performance of polypropylene-glass composites. *Fire and Materials*, 36(8):603–613, 2012.

[55] E. D. Weil. *Synergists, adjuvants and antagonists in flame-retardant systems*, pages 115–145. Marcel Dekker: New York, 2000.

[56] S. Bourbigot, M. Le Bras, S. Duquesne, and M. Rochery. Recent advances for intumescent polymers. *Macromolecular Materials and Engineering*, 289(6):499–511, 2004.

[57] P. R. Hornsby and R. N. Rothon. *Fire retardancy of polymers: new applications of mineral fillers*. Royal Society of Chemistry: Cambridge, UK, 2005.

[58] B. Bann and S. A. Miller. Melamine and derivatives of melamine. *Chemical Reviews*, 58(1):131–172, 1958.

[59] G. F. Levchik, S. V. Levchik, A. F. Selevich, and A. I. Lesnikovich. The influence of ammonium pentaborate on combustion and thermal decomposition of polyamide 6. *Vestsi AN Belarusi*, (3):34–38, 1995.

[60] Y. Yang, X. Shi, and R. Zhao. Flame retardancy behavior of zinc borate. *Journal of Fire Sciences*, 17(5):355–361, 1999.

[61] R. K. Iler. Multilayers of colloidal particles. *Journal of Colloid and Interface Science*, 21(6):569, 1966.

[62] P. T. Hammond. Form and function in multilayer assembly: New applications at the nanoscale. *Advanced Materials*, 16(15):1271–1293, 2004.

[63] J. J. Richardson, M. Bjornmalm, and F. Caruso. Technology-driven layer-by-layer assembly of nanofilms. *Science*, 348(6233):1–11, 2015.

[64] F. X. Xiao, M. Pagliaro, Y. J. Xu, and B. Liu. Layer-by-layer assembly of versatile nanoarchitectures with diverse dimensionality: a new perspective for rational construction of multilayer assemblies. *Chemical Society Reviews*, 45(11):3088–3121, 2016.

[65] E. Kharlampieva and S. A. Sukhishvili. Hydrogen-bonded layer-by-layer polymer films. *Polymer Reviews*, 46(4):377–395, 2006.

[66] J. Alongi, F. Carosio, and G. Malucelli. Layer by layer complex architectures based on ammonium polyphosphate, chitosan and silica on polyester-cotton blends: flammability and combustion behaviour. *Cellulose*, 19(3):1041–1050, 2012.

[67] Y. C. Li, Y. S. Kim, J. Shields, and R. Davis. Controlling polyurethane foam flammability and mechanical behaviour by tailoring the composition of clay-

based multilayer nanocoatings. *Journal of Materials Chemistry A*, 1(41):12987–12997, 2013.

[68] D. A. Hagen, C. Box, S. Greenlee, F. Xiang, O. Regev, and J. C. Grunlan. High gas barrier imparted by similarly charged multilayers in nanobrick wall thin films. *RSC Advances*, 4(35):18354–18359, 2014.

[69] M. A. Priolo, D. Gamboa, K. M. Holder, and J. C. Grunlan. Super gas barrier of transparent polymer-clay multi layer ultrathin films. *Nano Letters*, 10(12):4970–4974, 2010.

[70] A. Zhuk, R. Mirza, and S. Sukhishvili. Multiresponsive clay-containing layer-by-layer films. *ACS Nano*, 5(11):8790–8799, 2011.

[71] Y. Pan, W. Wang, H. Pan, J. Zhan, and Y. Hu. Fabrication of montmorillonite and titanate nanotube based coatings via layer-by-layer self-assembly method to enhance the thermal stability, flame retardancy and ultraviolet protection of polyethylene terephthalate (pet) fabric. *RSC Advances*, 6(59):53625–53634, 2016.

[72] J. Bravo, L. Zhai, Z. Z. Wu, R. E. Cohen, and M. F. Rubner. Transparent superhydrophobic films based on silica nanoparticles. *Langmuir*, 23(13):7293–7298, 2007.

[73] Y. Zhao, Y. W. Tang, X. G. Wang, and T. Lin. Superhydrophobic cotton fabric fabricated by electrostatic assembly of silica nanoparticles and its remarkable buoyancy. *Applied Surface Science*, 256(22):6736–6742, 2010.

[74] T. J. Dawidczyk, M. D. Walton, W. S. Jang, and J. C. Grunlan. Layer-by-layer assembly of uv-resistant poly(3,4-ethylenedioxythiophene) thin films. *Langmuir*, 24(15):8314–8318, 2008.

[75] P. Podsiadlo, Z. Q. Liu, D. Paterson, P. B. Messersmith, and N. A. Kotov. Fusion of seashell nacre and marine bioadhesive analogs: High-strength nanocomposite by layer-by-layer assembly of clay and l-3,4-dihydroxyphenylaianine polymer. *Advanced Materials*, 19(7):949–955, 2007.

[76] Y. Kim, T. I. Ryu, K. H. Ok, M. G. Kwak, S. Park, N. G. Park, C. J. Han, B. S. Kim, M. J. Ko, H. J. Son, and J. W. Kim. Inverted layer-by-layer fabrication of an ultraflexible and transparent ag nanowire/conductive polymer composite electrode for use in high-performance organic solar cells. *Advanced Functional Materials*, 25(29):4580–4589, 2015.

[77] M. Zanetti, T. Kashiwagi, L. Falqui, and G. Camino. Cone calorimeter combustion and gasification studies of polymer layered silicate nanocomposites. *Chemistry of Materials*, 14(2):881–887, 2002.

[78] K. Srikulkit, C. Iamsamai, and S. T. Dubas. Development of flame retardant polyphosphoric acid coating based on the polyelectrolyte multilayers technique. *Journal of Metals, Materials and Minerals*, 16(2):41–45, 2006.

[79] G. Laufer, C. Kirkland, A. B. Morgan, and J. C. Grunlan. Intumescent multilayer nanocoating, made with renewable polyelectrolytes, for flame-retardant cotton. *Biomacromolecules*, 13(9):2843–2848, 2012.

[80] T. Zhang, H. Q. Yan, L. L. Wang, and Z. P. Fang. Controlled formation of self-extinguishing intumescent coating on ramie fabric via layer-by-layer assembly. *Industrial & Engineering Chemistry Research*, 52(18):6138–6146, 2013.

[81] F. Carosio, A. Di Blasio, J. Alongi, and G. Malucelli. Green dna-based flame retardant coatings assembled through layer by layer. *Polymer*, 54(19):5148–5153, 2013.

[82] H. F. Pan, L. Song, L. Y. Ma, Y. Pan, K. M. Liew, and Y. Hu. Layer-by-layer assembled thin films based on fully biobased polysaccharides: chitosan and phosphorylated cellulose for flame-retardant cotton fabric. *Cellulose*, 21(4):2995–3006, 2014.

[83] C. Negrell-Guirao, F. Carosio, B. Boutevin, H. Cottet, and C. Loubat. Phosphonated oligoallylamine: Synthesis, characterization in water, and development of layer by layer assembly. *Journal of Polymer Science Part B-Polymer Physics*, 51(16):1244–1251, 2013.

[84] F. Carosio, C. Negrell-Guirao, A. Di Blasio, J. Alongi, G. David, and G. Camino. Tunable thermal and flame response of phosphonated oligoallylamines layer by layer assemblies on cotton. *Carbohydrate Polymers*, 115:752–759, 2015.

[85] H. F. Pan, W. Wang, Y. Pan, L. Song, Y. Hu, and K. M. Liew. Formation of self-extinguishing flame retardant biobased coating on cotton fabrics via layer-by-layer assembly of chitin derivatives. *Carbohydrate Polymers*, 115:516–524, 2015.

[86] F. Fang, D. Z. Xiao, X. Zhang, Y. D. Meng, C. Cheng, C. Bao, X. Ding, H. Cao, and X. Y. Tian. Construction of intumescent flame retardant and antimicrobial coating on cotton fabric via layer-by-layer assembly technology. *Surface & Coatings Technology*, 276:726–734, 2015.

[87] X. Wang, M. Q. Romero, X. Q. Zhang, R. Wang, and D. Y. Wang. Intumescent multilayer hybrid coating for flame retardant cotton fabrics based on layer-by-layer assembly and sol-gel process. *RSC Advances*, 5(14):10647–10655, 2015.

[88] S. S. Chen, X. Li, Y. Li, and J. Q. Sun. Intumescent flame-retardant and self-healing superhydrophobic coatings on cotton fabric. *ACS Nano*, 9(4):4070–

4076, 2015.

[89] F. Carosio, G. Fontaine, J. Alongi, and S. Bourbigot. Starch-based layer by layer assembly: Efficient and sustainable approach to cotton fire protection. *ACS Applied Materials & Interfaces*, 7(22):12158–12167, 2015.

[90] H. F. Pan, L. Song, Y. Hu, and K. M. Liew. An eco-friendly way to improve flame retardancy of cotton fabrics: Layer-by-layer assembly of semi-biobased substance. *Energy Procedia*, 75:174–179, 2015.

[91] S. M. Mostashari and F. Fayyaz. Tg of a cotton fabric impregnated by sodium borate decahydrate ($na_2b_4o_7{\cdot}10h_2o$) as a flame-retardant. *Journal of Thermal Analysis and Calorimetry*, 93(3):933–936, 2008.

[92] M. Dogan, A. Yilmaz, and E. Bayramli. Synergistic effect of boron containing substances on flame retardancy and thermal stability of intumescent polypropylene composites. *Polymer Degradation and Stability*, 95(12):2584–2588, 2010.

[93] M. Dogan and E. Bayramli. Synergistic effect of boron containing substances on flame retardancy and thermal stability of clay containing intumescent polypropylene nanoclay composites. *Polymers for Advanced Technologies*, 22(12):1628–1632, 2011.

[94] M. Dogan and E. Bayramli. The flame retardant effect of aluminum phosphinate in combination with zinc borate, borophosphate, and nanoclay in polyamide-6. *Fire and Materials*, 38(1):92–99, 2014.

[95] Y. C. Li, J. Schulz, S. Mannen, C. Delhom, B. Condon, S. Chang, M. Zammarano, and J. C. Grunlan. Flame retardant behavior of polyelectrolyte-clay thin film assemblies on cotton fabric. *ACS Nano*, 4(6):3325–3337, 2010.

[96] Y. C. Li, S. Mannen, J. Schulz, and J. C. Grunlan. Growth and fire protection behavior of poss-based multilayer thin films. *Journal of Materials Chemistry*, 21(9):3060–3069, 2011.

[97] G. Laufer, F. Carosio, R. Martinez, G. Camino, and J. C. Grunlan. Growth and fire resistance of colloidal silica-polyelectrolyte thin film assemblies. *Journal of Colloid and Interface Science*, 356(1):69–77, 2011.

[98] S. S. Ugur, M. Sariisik, and A. H. Aktas. Nano-al2o3 multilayer film deposition on cotton fabrics by layer-by-layer deposition method. *Materials Research Bulletin*, 46(8):1202–1206, 2011.

[99] G. B. Huang, H. D. Liang, X. Wang, and J. R. Gao. Poly(acrylic acid)/clay thin films assembled by layer-by-layer deposition for improving the flame retardancy properties of cotton. *Industrial & Engineering Chemistry Research*, 51(38):12299–12309, 2012.

[100] G. B. Huang, J. G. Yang, J. R. Gao, and X. Wang. Thin films of intumescent flame retardant-polyacrylamide and exfoliated graphene oxide fabricated via layer-by-layer assembly for improving flame retardant properties of cotton fabric. *Industrial & Engineering Chemistry Research*, 51(38):12355–12366, 2012.

[101] D. S. Cheng, X. Y. Liu, J. H. Wu, and W. D. Yu. Self-assembled multilayer of silver nanoparticles on cotton fabric and its flame-retardant property. *Industria Textila*, 63(3):115–120, 2012.

[102] L. L. Wang, T. Zhang, H. Q. Yan, M. Peng, and Z. P. Fang. Modification of ramie fabric with a metal-ion-doped flame-retardant coating. *Journal of Applied Polymer Science*, 129(5):2986–2997, 2013.

[103] M. Lewin and M. Endo. Catalysis of intumescent flame retardancy of polypropylene by metallic compounds. *Polymers for Advanced Technologies*, 14(1):3–11, 2003.

[104] P. J. Davies, A. R. Horrocks, and A. Alderson. The sensitisation of thermal decomposition of ammonium polyphosphate by selected metal ions and their potential for improved cotton fabric flame retardancy. *Polymer Degradation and Stability*, 88(1):114–122, 2005.

[105] Y. L. Lam, C. W. Kan, and C. W. M. Yuen. Flame-retardant finishing in cotton fabrics using zinc oxide co-catalyst. *Journal of Applied Polymer Science*, 121(1):612–621, 2011.

[106] T. Zhang, H. Q. Yan, M. Peng, L. L. Wang, H. L. Ding, and Z. P. Fang. Construction of flame retardant nanocoating on ramie fabric via layer-by-layer assembly of carbon nanotube and ammonium polyphosphate. *Nanoscale*, 5(7):3013–3021, 2013.

[107] H. F. Pan, W. Wang, Y. Pan, W. R. Zeng, J. Zhan, L. Song, Y. Hu, and K. M. Liew. Construction of layer-by-layer assembled chitosan/titanate nanotubes based nanocoating on cotton fabrics: flame retardant performance and combustion behavior. *Cellulose*, 22(1):911–923, 2015.

[108] X. X. Chen, F. Fang, X. Zhang, X. Ding, Y. Y. Wang, L. Chen, and X. Y. Tian. Flame-retardant, electrically conductive and antimicrobial multifunctional coating on cotton fabric via layer-by-layer assembly technique. *RSC Advances*, 6(33):27669–27676, 2016.

[109] F. Carosio, J. Alongi, and G. Malucelli. Layer by layer ammonium polyphosphate-based coatings for flame retardancy of polyester-cotton blends. *Carbohydrate Polymers*, 88(4):1460–1469, 2012.

[110] J. Alongi, F. Carosio, and G. Malucelli. Influence of ammonium polyphosphate-/poly(acrylic acid)-based layer by layer architectures on the char formation in cotton, polyester and their blends. *Polymer Degradation and Stability*, 97(9):1644–1653, 2012.

[111] F. Carosio, J. Alongi, and G. Malucelli. Flammability and combustion properties of ammonium polyphosphate-/poly(acrylic acid)- based layer by layer architectures deposited on cotton, polyester and their blends. *Polymer Degradation and Stability*, 98(9):1626–1637, 2013.

[112] M. Leistner, A. A. Abu-Odeh, S. C. Rohmer, and J. C. Grunlan. Water-based chitosan/melamine polyphosphate multilayer nanocoating that extinguishes fire on polyester-cotton fabric. *Carbohydrate Polymers*, 130:227–232, 2015.

[113] F. Carosio, G. Laufer, J. Alongi, G. Camino, and J. C. Grunlan. Layer-by-layer assembly of silica-based flame retardant thin film on pet fabric. *Polymer Degradation and Stability*, 96(5):745–750, 2011.

[114] K. Apaydin, A. Laachachi, V. Ball, M. Jimenez, S. Bourbigot, V. Toniazzo, and D. Ruch. Intumescent coating of (polyallylamine-polyphosphates) deposited on polyamide fabrics via layer-by-layer technique. *Polymer Degradation and Stability*, 106:158–164, 2014.

[115] K. Apaydin, A. Laachachi, V. Ball, M. Jimenezd, S. Bourbigot, and D. Ruch. Layer-by-layer deposition of a tio2-filled intumescent coating and its effect on the flame retardancy of polyamide and polyester fabrics. *Colloids and Surfaces A-Physicochemical and Engineering Aspects*, 469:1–10, 2015.

[116] Y. S. Kim, R. Davis, A. A. Cain, and J. C. Grunlan. Development of layer-by-layer assembled carbon nanofiber-filled coatings to reduce polyurethane foam

flammability. *Polymer*, 52(13):2847–2855, 2011.

[117] G. Laufer, C. Kirkland, A. A. Cain, and J. C. Grunlan. Clay-chitosan nanobrick walls: Completely renewable gas barrier and flame-retardant nanocoatings. *ACS Applied Materials & Interfaces*, 4(3):1643–1649, 2012.

[118] A. A. Cain, C. R. Nolen, Y. C. Li, R. Davis, and J. C. Grunlan. Phosphorous-filled nanobrick wall multilayer thin film eliminates polyurethane melt dripping and reduces heat release associated with fire. *Polymer Degradation and Stability*, 98(12):2645–2652, 2013.

[119] Y. S. Kim, Y. C. Li, W. M. Pitts, M. Werrel, and R. D. Davis. Rapid growing clay coatings to reduce the fire threat of furniture. *ACS Applied Materials & Interfaces*, 6(3):2146–2152, 2014.

[120] Y. Li, Y. Yang, Y. S. Kim, J. R. Shields, and R. D. Davis. Dna-based nanocomposite bio-coatings for fire retarding polyurethane foam. *Green Materials*, 2(3):144–152, 2014.

[121] H. F. Pan, Y. Pan, W. Wang, L. Song, Y. Hu, and K. M. Liew. Synergistic effect of layer-by-layer assembled thin films based on clay and carbon nanotubes to reduce the flammability of flexible polyurethane foam. *Industrial & Engineering Chemistry Research*, 53(37):14315–14321, 2014.

[122] A. A. Cain, M. G. Plummer, S. E. Murray, L. Bolling, O. Regev, and J. C. Grunlan. Iron-containing, high aspect ratio clay as nanoarmor that imparts substantial thermal/flame protection to polyurethane with a single electrostatically-deposited bilayer. *Journal of Materials Chemistry A*, 2(41):17609–17617, 2014.

[123] D. Patra, P. Vangal, A. A. Cain, C. Cho, O. Regev, and J. C. Grunlan. Inorganic nanoparticle thin film that suppresses flammability of polyurethane with only a single electrostatically-assembled bilayer. *ACS Applied Materials & Interfaces*, 6(19):16903–16908, 2014.

[124] Y. H. Yang, Y. C. Li, J. Shields, and R. D. Davis. Layer double hydroxide and sodium montmorillonite multilayer coatings for the flammability reduction of flexible polyurethane foams. *Journal of Applied Polymer Science*, 132(14):1–8, 2015.

[125] M. Haile, S. Fomete, I. D. Lopez, and J. C. Grunlan. Aluminum hydroxide multilayer assembly capable of extinguishing flame on polyurethane foam. *Journal of Materials Science*, 51(1):375–381, 2016.

[126] H. F. Pan, Y. S. Lu, L. Song, X. T. Zhang, and Y. Hu. Construction of layer-by-layer coating based on graphene oxide/$\beta - feooh$ nanorods and its synergistic effect on improving flame retardancy of flexible polyurethane foam. *Composites Science and Technology*, 129:116–122, 2016.

[127] G. Laufer, C. Kirkland, A. B. Morgan, and J. C. Grunlan. Exceptionally flame retardant sulfur-based multilayer nanocoating for polyurethane prepared from aqueous polyelectrolyte solutions. *ACS Macro Letters*, 2(5):361–365, 2013.

[128] F. Carosio, A. Di Blasio, F. Cuttica, J. Alongi, and G. Malucelli. Self-assembled hybrid nanoarchitectures deposited on poly(urethane) foams capable of chemically adapting to extreme heat. *RSC Advances*, 4(32):16674–16680, 2014.

[129] X. Wang, Y. T. Pan, J. T. Wan, and D. Y. Wang. An eco-friendly way to fire retardant flexible polyurethane foam: layer-by-layer assembly of fully bio-based substances. *RSC Advances*, 4(86):46164–46169, 2014.

[130] F. Carosio, C. Negrell-Guirao, J. Alongi, G. David, and G. Camino. All-polymer layer by layer coating as efficient solution to polyurethane foam flame retardancy. *European Polymer Journal*, 70:94–103, 2015.

[131] F. Carosio and J. Alongi. Ultra-fast layer-by-layer approach for depositing flame retardant coatings on flexible pu foams within seconds. *ACS Applied Materials & Interfaces*, 8(10):6315–6319, 2016.

[132] F. Carosio, F. Cuttica, A. Di Blasio, J. Alongi, and G. Malucelli. Layer by layer assembly of flame retardant thin films on closed cell pet foams: Efficiency of ammonium polyphosphate versus dna. *Polymer Degradation and Stability*, 113:189–196, 2015.

[133] J. C. Yang, Z. J. Cao, Y. Z. Wang, and D. A. Schiraldi. Ammonium polyphosphate-based nanocoating for melamine foam towards high flame retardancy and anti-shrinkage in fire. *Polymer*, 66:86–93, 2015.

[134] S. Deng, W. Liao, J. Yang, Z. Cao, and Y. Wang. Flame-retardant and smoke-suppressed silicone foams with chitosan-based nanocoatings. *Industrial & Engineering Chemistry Research*, 55(27):7239–7248, 2016.

[135] T. Guin, M. Krecker, A. Milhorn, D. A. Hagen, B. Stevens, and J. C. Grunlan. Exceptional flame resistance and gas barrier with thick multilayer nanobrick wall thin films. *Advanced Materials Interfaces*, 2(11):1–7, 2015.

[136] J. Alongi, A. Di Blasio, F. Carosio, and G. Malucelli. Uv-cured hybrid organic-inorganic layer by layer assemblies: Effect on the flame retardancy of polycarbonate films. *Polymer Degradation and Stability*, 107:74–81, 2014.

[137] Z. R. Farag, J. F. Friedrich, S. Kruger, G. Hidde, and M. E. Moustapha. Adhesion promotion of thick polyphosphate-poly(allylamine) films onto polyolefin

substrates by plasma polymers. *Journal of Adhesion Science and Technology*, 30(3):231–246, 2016.

[138] Z. Y. Lin, S. Renneckar, and D. P. Hindman. Nanocomposite-based lignocellulosic fibers 1. thermal stability of modified fibers with clay-polyelectrolyte multilayers. *Cellulose*, 15(2):333–346, 2008.

[139] C. Wei, S. H. Zeng, Y. Y. Tan, W. Wang, J. Lv, and H. X. Liu. Impact of layer-by-layer self-assembly clay-based nanocoating on flame retardant properties of sisal fiber cellulose microcrystals. *Advances in Materials Science and Engineering*, 2015:1–7, 2015.

[140] O. Koklukaya, F. Carosio, J. C. Grunlan, and L. Wagberg. Flame-retardant paper from wood fibers functionalized via layer-by-layer assembly. *ACS Applied Materials & Interfaces*, 7(42):23750–23759, 2015.

[141] S. D. Jiang, Z. M. Bai, G. Tang, L. Song, A. A. Stec, T. R. Hull, Y. Hu, and W. Z. Hu. Synthesis of mesoporous silica@co-al layered double hydroxide spheres: Layer-by-layer method and their effects on the flame retardancy of epoxy resins. *ACS Applied Materials & Interfaces*, 6(16):14076–14086, 2014.

[142] Y. L. Wang, X. M. Yang, H. Peng, F. Wang, X. Liu, Y. G. Yang, and J. W. Hao. Layer-by-layer assembly of multifunctional flame retardant based on brucite, 3-aminopropyltriethoxysilane, and alginate and its applications in ethylene-vinyl acetate resin. *ACS Applied Materials & Interfaces*, 8(15):9925–9935, 2016.

[143] J. Alongi, F. Carosio, A. Frache, and G. Malucelli. Layer by layer coatings assembled through dipping, vertical or horizontal spray for cotton flame retardancy. *Carbohydrate Polymers*, 92(1):114–119, 2013.

[144] F. Carosio, A. Di Blasio, F. Cuttica, J. Alongi, A. Frache, and G. Malucelli. Flame retardancy of polyester fabrics treated by spray-assisted layer-by-layer silica architectures. *Industrial & Engineering Chemistry Research*, 52(28):9544–9550, 2013.

[145] S. C. Chang, R. P. Slopek, B. Condon, and J. C. Grunlan. Surface coating for flame-retardant behavior of cotton fabric using a continuous layer-by-layer process. *Industrial & Engineering Chemistry Research*, 53(10):3805–3812, 2014.

[146] A. J. Mateos, A. A. Cain, and J. C. Grunlan. Large-scale continuous immersion system for layer-by-layer deposition of flame retardant and conductive nanocoatings on fabric. *Industrial & Engineering Chemistry Research*, 53(15):6409–6416, 2014.

[147] F. Carosio and J. Alongi. Few durable layers suppress cotton combustion due to the joint combination of layer by layer assembly and uv-curing. *RSC Advances*, 5(87):71482–71490, 2015.

[148] M. Leistner, M. Haile, S. Rohmer, A. Abu-Odeh, and J. C. Grunlan. Water-soluble polyelectrolyte complex nanocoating for flame retardant nylon-cotton fabric. *Polymer Degradation and Stability*, 122:1–7, 2015.

[149] A. A. Cain, S. Murray, K. M. Holder, C. R. Nolen, and J. C. Grunlan. Intumescent nanocoating extinguishes flame on fabric using aqueous polyelectrolyte complex deposited in single step. *Macromolecular Materials and Engineering*, 299(10):1180–1187, 2014.

[150] M. Haile, C. Fincher, S. Fomete, and J. C. Grunlan. Water-soluble polyelectrolyte complexes that extinguish fire on cotton fabric when deposited as ph-cured nanocoating. *Polymer Degradation and Stability*, 114:60–64, 2015.

[151] Y. Lvov, K. Ariga, I. Ichinose, and T. Kunitake. Molecular film assembly via layer-by-layer adsorption of oppositely charged macromolecules (linear polymer, protein and clay) and concanavalin a and glycogen. *Thin Solid Films*, 284:797–801, 1996.

[152] S. Srivastava and N. A. Kotov. Composite layer-by-layer (lbl) assembly with inorganic nanoparticles and nanowires. *Accounts of Chemical Research*, 41(12):1831–1841, 2008.

[153] K. M. Holder, M. A. Priolo, K. E. Secrist, S. M. Greenlee, A. J. Nolte, and J. C. Grunlan. Humidity-responsive gas barrier of hydrogen-bonded polymer–clay multilayer thin films. *The Journal of Physical Chemistry C*, 116(37):19851–19856, 2012.

[154] M. A. Priolo, K. M. Holder, S. M. Greenlee, and J. C. Grunlan. Transparency, gas barrier, and moisture resistance of large-aspect-ratio vermiculite nanobrick wall thin films. *ACS Applied Materials & Interfaces*, 4(10):5529–5533, 2012.

[155] P. Tzeng, C. R. Maupin, and J. C. Grunlan. Influence of polymer interdiffusion and clay concentration on gas barrier of polyelectrolyte/clay nanobrick wall quadlayer assemblies. *Journal of Membrane Science*, 452:46–53, 2014.

[156] M. Bartholmai and B. Schartel. Layered silicate polymer nanocomposites: new approach or illusion for fire retardancy? investigations of the potentials and the tasks using a model system. *Polymers for Advanced Technologies*, 15(7):355–364, 2004.

[157] A. B. Morgan and J. W. Gilman. An overview of flame retardancy of polymeric materials: application, technology, and future directions. *Fire and Materials*, 37(4):259–279, 2013.

[158] G. Montaudo, E. Scamporrino, C. Puglisi, and D. Vitalini. Intumescent flame retardant for polymers. iii. the polypropylene–ammonium polyphosphate–polyurethane system. *Journal of Applied Polymer Science*, 30(4):1449–1460, 1985.

[159] G. Camino, L. Costa, and G. Martinasso. Intumescent fire-retardant systems. *Polymer Degradation and Stability*, 23(4):359–376, 1989.

[160] M. Ravey and E. M. Pearce. Flexible polyurethane foam. i. thermal decomposition of a polyether-based, water-blown commercial type of flexible polyurethane foam. *Journal of Applied Polymer Science*, 63(1):47–74, 1997.

[161] S. V. Levchik and E. D. Weil. Thermal decomposition, combustion and fire-retardancy of polyurethanesa review of the recent literature. *Polymer International*, 53(11):1585–1610, 2004.

[162] V. Babrauskas. Development of the cone calorimetera bench-scale heat release rate apparatus based on oxygen consumption. *Fire and Materials*, 8(2):81–95, 1984.

[163] B. Schartel and T. R. Hull. Development of fire-retarded materials - interpretation of cone calorimeter data. *Fire and Materials*, 31(5):327–354, 2007.

[164] V. Babrauskas and R. D. Peacock. Heat release rate: the single most important variable in fire hazard. *Fire Safety Journal*, 18(3):255–272, 1992.

[165] A. B. Morgan and W. Liu. Flammability of thermoplastic carbon nanofiber nanocomposites. *Fire and Materials*, 35(1):43–60, 2011.

[166] Y. S. Kim and R. Davis. Multi-walled carbon nanotube layer-by-layer coatings with a trilayer structure to reduce foam flammability. *Thin Solid Films*, 550:184–189, 2014.

[167] B. E. Stevens, P. K. Odenborg, M. A. Priolo, and J. C. Grunlan. Hydrophobically modified polyelectrolyte for improved oxygen barrier in nanobrick wall multilayer thin films. *Journal of Polymer Science Part B: Polymer Physics*, 52(17):1153–1156, 2014.

[168] D. Gamboa, M. A. Priolo, A. Ham, and J. C. Grunlan. Note: Influence of rinsing and drying routines on growth of multilayer thin films using automated deposition system. *Review of Scientific Instruments*, 81(3):036103, 2010.

[169] Y. Yang, M. Haile, Y. T. Park, F. A. Malek, and J. C. Grunlan. Super gas barrier of all-polymer multilayer thin films. *Macromolecules*, 44(6):1450–1459, 2011.

[170] C. J. Jan, M. D. Walton, E. P. McConnell, W. Jang, Y. S. Kim, and J. C. Grunlan. Carbon black thin films with tunable resistance and optical transparency. *Carbon*, 44(10):1974–1981, 2006.

[171] D. A. Hagen, B. Foster, B. Stevens, and J. C. Grunlan. Shift-time polyelectrolyte multilayer assembly: fast film growth and high gas barrier with fewer layers by adjusting deposition time. *ACS Macro Letters*, 3(7):663–666, 2014.

[172] R. H. Krämer, M. Zammarano, G. T. Linteris, U. W. Gedde, and J. W. Gilman. Heat release and structural collapse of flexible polyurethane foam. *Polymer Degradation and Stability*, 95(6):1115–1122, 2010.

[173] N. Grassie and G. Mendoza. Thermal degradation of polyether-urethanes: 5. polyether-urethanes prepared from methylene bis (4-phenylisocyanate) and high molecular weight poly (ethylene glycols) and the effect of ammonium polyphosphate. *Polymer Degradation and Stability*, 11(4):359–379, 1985.

[174] H. K. Lee and S. W. Ko. Structure and thermal properties of polyether polyurethaneurea elastomers. *Journal of Applied Polymer Science*, 50(7):1269–1280, 1993.

[175] Z. S. Petrović, Z. Zavargo, J. H. Flyn, and W. J. Macknight. Thermal degradation of segmented polyurethanes. *Journal of Applied Polymer Science*, 51(6):1087–1095, 1994.

[176] L. Lage and Y. Kawano. Thermal degradation of biomedical polyurethanesa kinetic study using high-resolution thermogravimetry. *Journal of Applied Polymer Science*, 79(5):910–919, 2001.

[177] T. Kashiwagi, F. Du, K. I. Winey, K. M. Groth, J. R. Shields, S. P. Bellayer, H. Kim, and J. F. Douglas. Flammability properties of polymer nanocomposites with single-walled carbon nanotubes: effects of nanotube dispersion and concentration. *Polymer*, 46(2):471–481, 2005.

[178] B. H. Cipiriano, T. Kashiwagi, S. R. Raghavan, Y. Yang, E. A. Grulke, K. Yamamoto, J. R. Shields, and J. F. Douglas. Effects of aspect ratio of mwnt on the flammability properties of polymer nanocomposites. *Polymer*, 48(20):6086–6096, 2007.

[179] J. Lefebvre, B. Bastin, M. Le Bras, S. Duquesne, C. Ritter, R. Paleja, and F. Poutch. Flame spread of flexible polyurethane foam: comprehensive study. *Polymer Testing*, 23(3):281–290, 2004.

[180] W. M. Pitts. Role of two stage pyrolysis in fire growth on flexible polyurethane foam slabs. *Fire and Materials*, 38(3):323–338, 2014.

[181] *ASTM E1354-15: Standard heat method for heat and visible smoke release rates for materials and products using an oxygen consumption calorime-*

ter. ASTM International: Pennsylvania. 2015. http://www.astm.org/cgi-bin/resolver.cgi?E1354-15.

[182] *ISO 5660-1: Reaction-to-fire tests - heat release, smoke production and mass loss rate - part 1: heat release (cone calorimeter method)*. International Organization for Standardization: Geneva, Switzerland. 2015. http://www.iso.org/.

[183] A. B. Morgan, N. A. Gagliardi, W. A. Price, and M. L. Galaska. Cone calorimeter testing of s2 glass reinforced polymer composites. *Fire and Materials*, 33(7):323–344, 2009.

[184] P. Patel, T. R. Hull, R. E. Lyon, S. I. Stoliarov, R. N. Walters, S. Crowley, and N. Safronava. Investigation of the thermal decomposition and flammability of peek and its carbon and glass-fibre composites. *Polymer Degradation and Stability*, 96(1):12–22, 2011.

[185] H. Breulet and T. Steenhuizen. Fire testing of cables: comparison of sbi with fipec/europacable tests. *Polymer Degradation and Stability*, 88(1):150–158, 2005.

[186] *ASTM D6113-11: Standard test method for using a cone calorimeter to determine fire-test response characteristics of insulating materials contained in electrical or optical fiber cables*. ASTM International: Pennsylvania. 2011. http://www.astm.org/cgi-bin/resolver.cgi?D6113-11.

[187] A. B. Morgan and M. Bundy. Cone calorimeter analysis of ul-94 v-rated plastics. *Fire and Materials*, 31(4):257–283, 2007.

[188] M. M. Hirschler. Flame retardants and heat release: review of data on individual polymers. *Fire and Materials*, 39(3):232–258, 2015.

[189] T. W. Kelley, P. F. Baude, C. Gerlach, D. E. Ender, D. Muyres, M. A. Haase, D. E. Vogel, and S. D. Theiss. Recent progress in organic electronics: Materials, devices, and processes. *Chemistry of Materials*, 16(23):4413–4422, 2004.

[190] J. Rhim, H. Park, and C. Ha. Bio-nanocomposites for food packaging applications. *Progress in Polymer Science*, 38(10):1629–1652, 2013.

[191] D. Brosteaux, F. Axisa, M. Gonzalez, and J. Vanfleteren. Design and fabrication of elastic interconnections for stretchable electronic circuits. *IEEE Electron Device Letters*, 28(7):552–554, 2007.

[192] D. A. Kunz, J. Schmid, P. Feicht, J. Erath, A. Fery, and J. Breu. Clay-based nanocomposite coating for flexible optoelectronics applying commercial polymers. *ACS Nano*, 7(5):4275–4280, 2013.

[193] M. S. White, M. Kaltenbrunner, E. D. Głowacki, K. Gutnichenko, G. Kettlgruber, I. Graz, S. Aazou, C. Ulbricht, D. A. Egbe, and M. C. Miron. Ultrathin, highly flexible and stretchable pleds. *Nature Photonics*, 7(10):811–816, 2013.

[194] J. Lange and Y. Wyser. Recent innovations in barrier technologies for plastic packaginga review. *Packaging Technology and Science*, 16(4):149–158, 2003.

[195] H. Chatham. Oxygen diffusion barrier properties of transparent oxide coatings on polymeric substrates. *Surface and Coatings Technology*, 78(1):1–9, 1996.

[196] P. Bertrand, A. Jonas, A. Laschewsky, and R. Legras. Ultrathin polymer coatings by complexation of polyelectrolytes at interfaces: suitable materials, structure and properties. *Macromolecular Rapid Communications*, 21(7):319–348, 2000.

[197] K. Ariga, Y. Yamauchi, G. Rydzek, Q. Ji, Y. Yonamine, K. Wu, and J. P. Hill. Layer-by-layer nanoarchitectonics: invention, innovation, and evolution.

Chemistry Letters, 43(1):36–68, 2014.

[198] M. A. Priolo, K. M. Holder, S. M. Greenlee, B. E. Stevens, and J. C. Grunlan. Precisely tuning the clay spacing in nanobrick wall gas barrier thin films. *Chemistry of Materials*, 25(9):1649–1655, 2013.

[199] D. Kim, P. Tzeng, K. J. Barnett, Y. Yang, B. A. Wilhite, and J. C. Grunlan. Highly size-selective ionically crosslinked multilayer polymer films for light gas separation. *Advanced Materials*, 26(5):746–751, 2014.

[200] P. Su, H. Hsu, and C. Liu. Layer-by-layer anchoring of copolymer of methyl methacrylate and [3-(methacrylamino) propyl] trimethyl ammonium chloride to gold surface on flexible substrate for sensing humidity. *Sensors and Actuators B: Chemical*, 178:289–295, 2013.

[201] J. Luo, Y. Chen, Q. Ma, R. Liu, and X. Liu. Layer-by-layer self-assembled hybrid multilayer films based on poly (sodium 4-styrenesulfonate) stabilized graphene with polyaniline and their electrochemical sensing properties. *RSC Advances*, 3(39):17866–17873, 2013.

[202] J. L. Lutkenhaus, K. D. Hrabak, K. McEnnis, and P. T. Hammond. Elastomeric flexible free-standing hydrogen-bonded nanoscale assemblies. *Journal of the American Chemical Society*, 127(49):17228–17234, 2005.

[203] S. Ishihara, N. Iyi, Y. Tsujimoto, S. Tominaka, Y. Matsushita, V. Krishnan, M. Akada, J. Labuta, K. Deguchi, and S. Ohki. Hydrogen-bond-driven homogeneous intercalationfor rapid, reversible, and ultra-precise actuation of layered clay nanosheets. *Chemical Communications*, 49(35):3631–3633, 2013.

[204] B. R. Spears, J. Waksal, C. McQuade, L. Lanier, and E. Harth. Controlled branching of polyglycidol and formation of protein–glycidol bioconju-

gates via a graft-from approach with peg-like arms. *Chemical Communications*, 49(24):2394–2396, 2013.

[205] N. J. Geddes, E. M. Paschinger, D. N. Furlong, F. Caruso, C. L. Hoffmann, and J. F. Rabolt. Surface chemical activation of quartz crystal microbalance gold electrodesanalysis by frequency changes, contact angle measurements and grazing angle ftir. *Thin Solid Films*, 260(2):192–199, 1995.

[206] D. K. Owens. The mechanism of corona and ultraviolet light-induced self-adhesion of poly (ethylene terephthalate) film. *Journal of Applied Polymer Science*, 19(12):3315–3326, 1975.

[207] W. Jang and J. C. Grunlan. Robotic dipping system for layer-by-layer assembly of multifunctional thin films. *Review of Scientific Instruments*, 76(10):103904, 2005.

[208] H. Lee, R. Mensire, R. E. Cohen, and M. F. Rubner. Strategies for hydrogen bonding based layer-by-layer assembly of poly (vinyl alcohol) with weak polyacids. *Macromolecules*, 45(1):347–355, 2012.

[209] G. Choudalakis and A. Gotsis. Permeability of polymer/clay nanocomposites: a review. *European Polymer Journal*, 45(4):967–984, 2009.

[210] R. Wilson, T. Plivelic, A. S. Aprem, C. Ranganathaiagh, S. A. Kumar, and S. Thomas. Preparation and characterization of eva/clay nanocomposites with improved barrier performance. *Journal of Applied Polymer Science*, 123(6):3806–3818, 2012.

[211] A. Walther, I. Bjurhager, J. Malho, J. Pere, J. Ruokolainen, L. A. Berglund, and O. Ikkala. Large-area, lightweight and thick biomimetic composites with

superior material properties via fast, economic, and green pathways. *Nano Letters*, 10(8):2742–2748, 2010.

[212] M. A. Priolo, D. Gamboa, and J. C. Grunlan. Transparent clay- polymer nano brick wall assemblies with tailorable oxygen barrier. *ACS Applied Materials & Interfaces*, 2(1):312–320, 2010.

[213] M. A. Priolo, K. M. Holder, D. Gamboa, and J. C. Grunlan. Influence of clay concentration on the gas barrier of clay–polymer nanobrick wall thin film assemblies. *Langmuir*, 27(19):12106–12114, 2011.

[214] E. L. Cussler, S. E. Hughes, W. J. Ward, and R. Aris. Barrier membranes. *Journal of Membrane Science*, 38(2):161–174, 1988.

[215] R. Liu, D. Schiraldi, A. Hiltner, and E. Baer. Oxygen-barrier properties of cold-drawn polyesters. *Journal of Polymer Science Part B: Polymer Physics*, 40(9):862–877, 2002.

APPENDIX A

STRETCHABLE GAS BARRIER ACHIEVED WITH PARTIALLY HYDROGEN-BONDED MULTILAYER NANOCOATING*

A.1 Introduction

Numerous electronics, food packaging, and pressurized systems require gas barrier layers [189, 190]. In many cases, this barrier needs to be flexible, resistant to humidity and stretchable [191, 192, 193]. Commonly used gas barrier layers include polymer films, ceramic thin films and metalization [194]. The drawback of inorganic barriers, such as metal-oxide coatings, is that they are neither flexible nor stretchable, have inherent pinholes and crack upon flexing, which diminishes their ability to block oxygen [195]. Flexible and transparent thin films have been produced, with gas barrier exceeding those of metal and metal oxides, using layer-by-layer (LbL) deposition of polymers and clay [69]. These thin films provide many of the desired properties for the applications mentioned above and could possibly displace current inorganic barriers, but they lack true stretchability. Some applications require the ability to stretch 10% or more without damage [193]. Pressurized elastomer systems, such as sports balls and tires, would benefit from a flexible and stretchable thin film barrier. These applications could be improved with a nanocoating that could provide a sturdy, flexible, and stretchable barrier that would reduce weight and/or material cost.

Layer-by-layer assembly is a facile process for depositing multifunctional thin films that has become increasingly popular since the 1990s [196, 10]. This pro-

*Reprinted with permission from Reference [16]. Copyright 2014, WILEY-VCH Verlag GmbH & Co. KGaA, Weinheim.

cess has been used to impart various properties[197] including gas barrier/separation [69, 198, 199], flame retardant [79, 117], antimicrobial [19], and sensing [200, 201]. The best gas barrier films make use of polyelectrolytes and nanoplatelets (e.g., clay) to form a tortuous path for gas molecules, forcing them to traverse long distances perpendicular to the direction of diffusion [69, 198]. This significantly reduces the total number of permeating molecules passing through the film in a given time. Many of these super oxygen barrier nanobrick wall films are created using electrostatic interactions that are akin to crosslinks, making them relatively glassy. Upon straining, the electrostatic bonds between the polymer and clay are strong enough to cause cracking within the film. Hydrogen-bonded assemblies have been shown to exhibit elastomeric behavior [202], which could allow the polymer to bond-slip along the basal plane of the clay during stretching [203]. The presence of some hydrogen-bonded layers could reduce the strain on the electrostatic layers, resulting in less movement of the platelets, reduced (or eliminated) film damage, and retained barrier. In the present study, the addition of a hydrogen-bonding layer to an otherwise electrostatically grown film resulted in a four times improvement over the barrier of neat PET and this barrier was maintained after undergoing a 10% strain. The electrostatically-bonded film lost 4350% of its barrier after stretching, whereas the hydrogen-bonded film lost only 17%.

A.2 Experimental

A.2.1 Materials

Cationic branched polyethylenimine (PEI) (M_W ~25,000 g/mol) was purchased from Sigma-Aldrich (Milwaukee, WI) and used as received. Polyglycidol (PGD) was synthesized according to a previously described method [204]. Natural sodium montmorillonite (MMT) clay was purchased from Southern Clay Products, Inc. (Gonzales,

TX) and used as received. Poly(ethylene terephthalate) (PET) film with a thickness of 179 μm was used as the substrate for oxygen transmission rate (OTR) testing and scanning electron microscopy. Single-side-polished, 500-μm-thick silicon wafers were purchased from University Wafer (South Boston, MA) and used for film growth measurements via ellipsometry.

A.2.2 Film Preparation

Solutions were prepared with deionized water and rolled for 24 hours to ensure homogeneity. Polyethylenimine and polyglycidol solutions were prepared at 0.1 wt% and montmorillonite solutions were prepared at 1 wt%. The pH of each solution was altered to the corresponding pH 3, 4, 5, or 10 using 1.0 M HCl. Silicon wafers were treated with piranha solution for 30 minutes prior to rinsing with water, acetone, and water again, and finally dried with filtered air before deposition [205]. Caution! Piranha solution reacts violently with organic materials and should be handled with extreme care. PET films were rinsed with water, methanol, and water again, dried with filtered air, and corona treated to create a negative surface charge prior to deposition [206]. Each appropriately treated substrate was then dipped into the PEI solution for 5 minutes, rinsed with deionized water, and dried with filtered air. The same procedure was followed with MMT. This initial bilayer served as an adhesive primer, as PGD does not electrostatically bond and therefore poorly adheres to the substrate. After this initial bilayer, a trilayer was formed by alternating dips of PGD, PEI, and MMT. Figure A.1 shows a schematic representation of the deposition process along with polymer and clay structures. All layers were deposited with one minute dip times until the desired number of trilayers (TLs) were deposited. For the electrostatically-bonded control film, the initial PEI/MMT primer was followed by repeated PEI/MMT depositions at 1 min until the desired number of bilayers (BLs)

were deposited. The TL films were grown at pH 3, 4, and 5 and in each case all solutions were adjusted to the same pH. The BL films were all grown with PEI at pH 10 and MMT at its unaltered pH of 9.8. All films were prepared using home-built robotic dipping systems similar to one previously described [207].

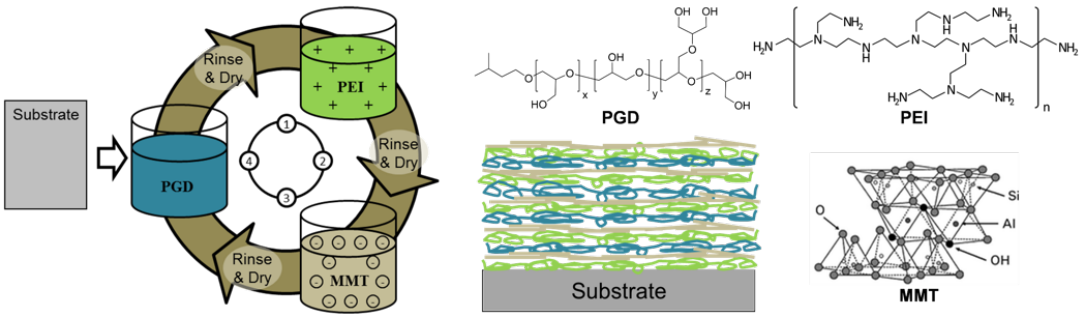

Figure A.1: Schematic representation of LbL trilayer assembly with PGD, PEI, and MMT onto a substrate.

A.2.3 Film Characterization

Film thickness was measured every five deposition cycles (on silicon wafers) using an α-SE ellipsometer (J. A. Woollam Co., Inc., Lincoln, NE) under ambient conditions. Oxygen transmission rate testing was performed by MOCON (Minneapolis, MN) using an Oxtran 2/21 ML instrument at 0% RH. An Instron model 4411 tensile tester (Instron, Norwood, MA) was used to apply 10% strain to the PET for 2 min before measuring the OTR and imaging with SEM. Films were imaged using a JEOL JSM-7500F SEM (JEOL Ltd., Tokyo, Japan). Prior to imaging, each film was coated with approximately 4 nm of platinum/palladium to reduce surface charging.

A.3 Results and Discussion

A.3.1 Film Growth

Trilayer assemblies were deposited with polyglycidol, polyethylenimine and montmorillonite clay in an effort to produce a partially hydrogen-bonded clay-containing assembly that is able to retain oxygen barrier following significant stretching ($\geq$ 10%). These thin films were compared to a bilayer control system deposited with PEI and MMT, which exhibits high oxygen barrier, but is very stiff (i.e., relatively unstretchable) [69]. Layer-by-layer assemblies are represented in the text and figures as xPGDTLy where x is the number of trilayers deposited and y is the pH of the aqueous solutions used to deposit the nanocoating. All control films were deposited with pH 10 PEI and pH 9.8 MMT (referred to as PEIMMT). Figure A.2 shows the linear growth of both the TL and BL systems. It is known that pH is a very important factor in the deposition of hydrogen-bonding systems [23, 208]. Lower pH values promote thicker growth in hydrogen-bonding systems because increased protonation of polyions allows for more hydrogen-bonding interactions with the neutral polymer [23]. The thickest growing trilayer film (at pH 3) was chosen to be the focus of this study because greater clay spacing is known to achieve better barrier for a given thickness [69, 198]. The PEIMMT control was grown to the same thickness (i.e., the 20PGDTL3 film was 125 nm and so was 31PEIMMT).

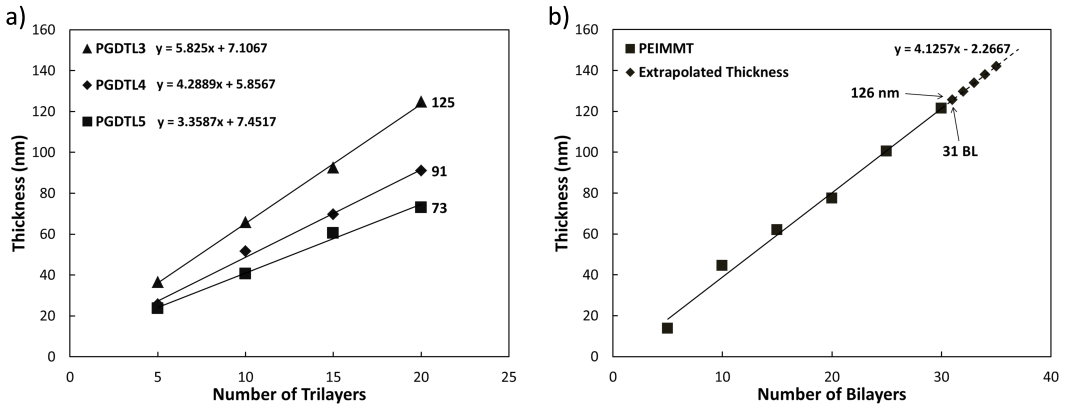

Figure A.2: (a) Thickness of PGDTL, at varying pH, as a function of trilayers deposited. (b) Thickness of PEIMMT as a function of bilayers deposited, with data extrapolated to 35 BL using the linear fit trend line ($R^2 = 0.9914$).

A.3.2 Influence of Strain on Oxygen Barrier

A common method to improve polymer gas barrier performance is the addition of clay [209, 210, 211, 212, 213]. Inorganic clay platelets are impermeable to oxygen and therefore increase the diffusion path of oxygen through the film. Layer-by-layer assembly results in high orientation of these nanoplatelets perpendicular to the diffusion path, which maximizes the tortuous path that oxygen molecules must travel [214]. Oxygen molecules are confined between the clay layers and must wiggle down a clay-walled corridor until a gap between clay platelets is found and the molecule enters a new corridor. Figure A.3 shows the oxygen transmission rate for uncoated 179 μm PET, 20PGDTL3 and 31PEIMMT (deposited on the PET) before and after a 10% strain was applied. It is important to note that even though the PET substrate is plastically deformed during stretching, its barrier remains unaffected. This counter-intuitive result is attributed to the alignment of polymer chains within the substrate that result in a slightly thinner, yet slightly denser material [215]. The 31PEIMMT

film performed as expected, exhibiting brittle behavior by cracking and exhibiting an OTR nearly 45 times greater after stretching (increasing from 0.14 to 6.00 cc/(m^2 · day · atm)). Although starting with a much larger OTR, the 20PGDTL3 nanocoating largely maintained its barrier, increasing only 17% after stretching (from 2.09 to 2.45 cc/(m^2 · day · atm)). By successfully maintaining barrier after exposure to 10% strain, the hydrogen-bonded film ended up with a significantly lower OTR than the PEIMMT control. The final post-strain oxygen barrier of 20PGDTL3 is more than three times better than the uncoated PET substrate.

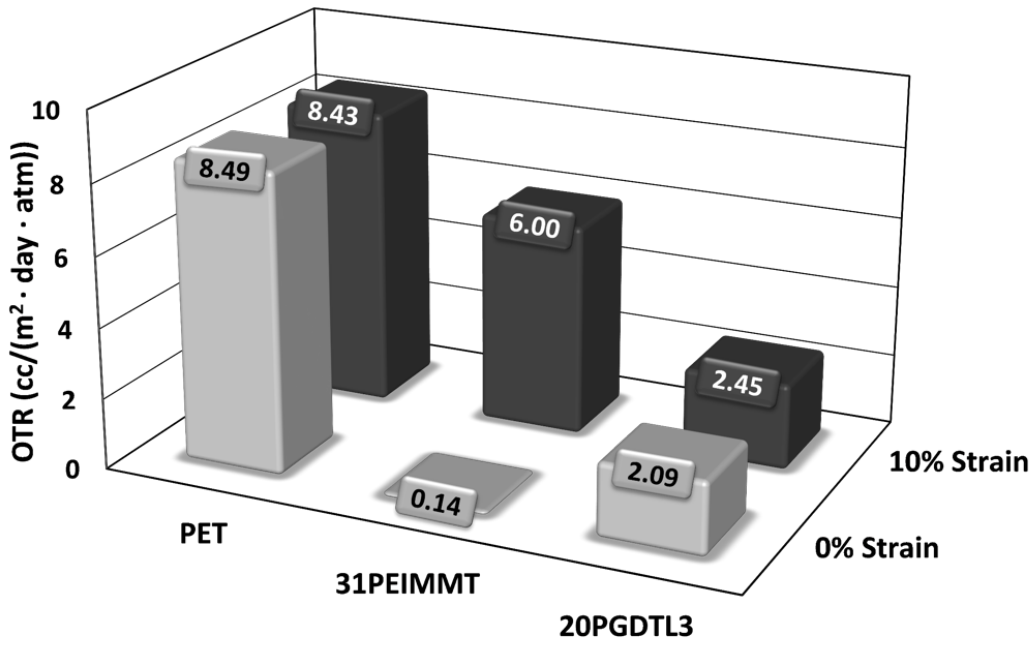

Figure A.3: Oxygen transmission rates of neat PET and PET coated with 31PEIMMT or 20PGDTL3, before and after the various films were subjected to a 10% strain.

SEM was used to image surface cracking in the 20PGDTL3 and the 31PEIMMT nanocoatings. Figure A.4 shows that there are no discernable cracks in either system prior to stretching. Both films look similarly cracked after being stretched, but these are only surface images and the appearance of cracks on the surface does not mean the cracks propagate through the entire film thickness. The significant increase in OTR of 31PEIMMT post-stretch suggests its cracks extend through the film. In the case of 20PGDTL3, the outermost two layers are PEI and MMT, which could result in more superficial cracking that does not significantly increase OTR. It has been reported that hydrogen-bonds along the basal planes of clay sheets allow for a somewhat fluidic motion of alcohol molecules between them [203]. This motion could be attributed to the hydrogen-bonding within these stretchy films. If through-thickness cracks had been created upon stretching, it is possible that the hydrogen-bonding layers (and their associated elasticity) facilitated self-healing. What appear to be cracks in Figure A.4(d) could be more like scars created upon healing. Qualitatively, there are fewer cracks per unit area in this partially hydrogen-bonded assembly.

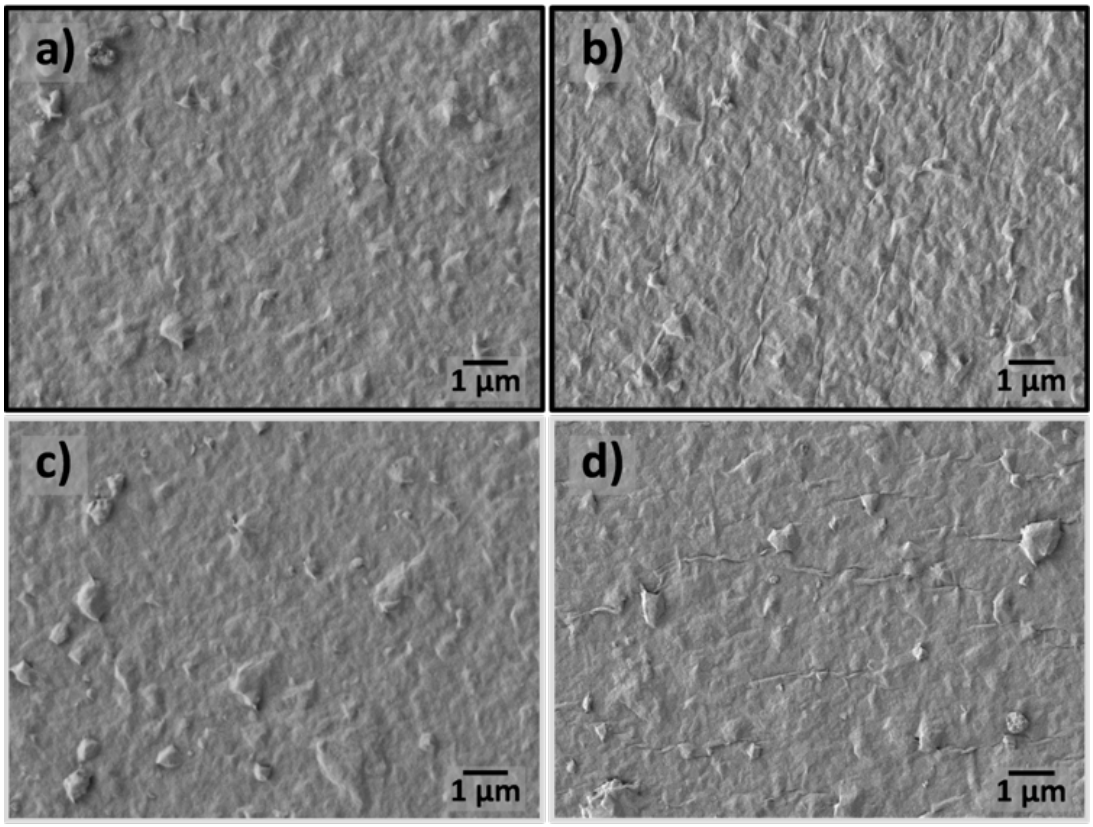

Figure A.4: Scanning electron micrographs of unstrained (a) 31PEIMMT and (b) 31PEIMMT after 10% strain. Images of (c) 20PGDTL3 and (d) 20PGDTL3 after 10% strain are also shown.

A.4 Conclusion

The layer-by-layer assembly of polyethylenimine and montmorillonite clay, with hydrogen-bonding polyglycidol, was used to generate the first reported stretchable thin film gas barrier. It was shown that adding a hydrogen-bonding polymer layer, between electrostatically-bonded PEIMMT layers, allows this multilayer assembly to maintain its oxygen barrier after being stretched 10%. The considerable post-strain barrier loss of 4350% displayed by the brittle PEIMMT thin film was reduced to a nominal 17% barrier loss in the stretchable thin film. This study establishes an

important proof of concept that is a first step toward very stretchable films with much lower gas transmission rates (i.e., better barrier). Future studies will investigate cyclic loading on an elastic substrate to assess durability. The ability to impart stretchiness to thin film gas barriers will make layer-by-layer deposition a viable approach for fabricating flexible and stretchable barrier films for pressurized elastomer systems, food packaging, and stretchable electronics applications.